Supplementary information for *"Modeling regulatory network topology improves genome-wide analyses of complex human traits"*

Xiang Zhu

The Pennsylvania State University, University Park, PA 16802, USA

E-mail: xiangzhu@psu.edu

Summary. This document contains Supplementary Notes, Figures 1-19 and Tables 1-21 associated with the manuscript entitled *"Modeling regulatory network topology improves genome-wide analyses of complex human traits"* (last edited on 2020-12-08).

Supplementary Notes

Computations underlying RSS-NET

RSS-NET is given by the following Bayesian model:

$$\begin{aligned}
\widehat{\boldsymbol{\beta}} &\sim \mathcal{N}(\widehat{\mathbf{S}}\widehat{\mathbf{R}}\widehat{\mathbf{S}}^{-1}\boldsymbol{\beta},\ \widehat{\mathbf{S}}\widehat{\mathbf{R}}\widehat{\mathbf{S}}), && (1)\\
\beta_j &\sim \pi_j\cdot\mathcal{N}(\mu_j,\ \sigma_0^2)+(1-\pi_j)\cdot\delta_0, && (2)\\
\pi_j &= 1\,/\,[1+10^{-(\theta_0+a_j\cdot\theta)}], && (3)\\
\mu_j &= \textstyle\sum_{g\in\mathbf{O}_j} w_{jg}\cdot\gamma_{jg}, && (4)\\
\gamma_{jg} &\sim \mathcal{N}(0,\ \sigma^2), && (5)
\end{aligned}$$

where $\mathcal{N}(\boldsymbol{\mu},\ \boldsymbol{\Sigma})$ denotes a normal distribution with mean vector $\boldsymbol{\mu}$ and covariance matrix $\boldsymbol{\Sigma}$, $\widehat{\boldsymbol{\beta}} := (\hat{\beta}_1,\ldots,\hat{\beta}_p)'$ is a $p\times 1$ vector, $\widehat{\mathbf{S}} := \text{diag}\{(\hat{s}_1,\ldots,\hat{s}_p)'\}$ is a $p\times p$ diagonal matrix, $\{\hat{\beta}_j,\hat{s}_j\}$ are single-SNP effect estimate and its standard error for each SNP j in a GWAS, $\widehat{\mathbf{R}}$ is a $p\times p$ LD matrix estimated from a reference panel with ancestry matching the GWAS, $\boldsymbol{\beta} := (\beta_1,\ldots,\beta_p)'$ is a $p\times 1$ vector, β_j is the true effect of each SNP j, π_j denotes the prior probability that $\beta_j\neq 0$, μ_j denotes the prior expected value of β_j conditioning on $\beta_j\neq 0$, δ_0 denotes point mass at zero, $\{a_j,\mathbf{O}_j,w_{jg}\}$ are known annotations derived from a given regulatory network (see main text Equations 3-5), γ_{jg} denotes the random effect of SNP j due to gene g, and $\{\theta_0,\theta,\sigma_0,\sigma\}$ are hyper-parameters.

To fit the RSS-NET model, we first integrate out γ_{jg}:

$$\begin{aligned}
\widehat{\boldsymbol{\beta}} &\sim \mathcal{N}(\widehat{\mathbf{S}}\widehat{\mathbf{R}}\widehat{\mathbf{S}}^{-1}\boldsymbol{\beta},\ \widehat{\mathbf{S}}\widehat{\mathbf{R}}\widehat{\mathbf{S}}), && (6)\\
\beta_j &\sim \pi_j\cdot\mathcal{N}(0,\ \sigma_j^2)+(1-\pi_j)\cdot\delta_0, && (7)\\
\pi_j &= 1\,/\,[1+10^{-(\theta_0+a_j\theta)}], && (8)\\
\sigma_j^2 &= \sigma_0^2+\sigma^2\cdot\textstyle\sum_{g\in\mathbf{O}_j} w_{jg}^2. && (9)
\end{aligned}$$

We then write the posterior distribution of $\boldsymbol{\beta}$ as

$$p(\boldsymbol{\beta}\mid\mathbf{D}) = \int p(\boldsymbol{\beta}\mid\mathbf{D},\theta_0,\theta,\sigma_0,\sigma)p(\theta_0,\theta,\sigma_0,\sigma\mid\mathbf{D})\mathrm{d}\theta_0\mathrm{d}\theta\mathrm{d}\sigma_0\mathrm{d}\sigma, \quad (10)$$

where $\mathbf{D}$ is a shorthand for the input data of RSS-NET including GWAS summary statistics $\{\widehat{\boldsymbol{\beta}},\widehat{\mathbf{S}}\}$, LD estimates $\widehat{\mathbf{R}}$ and network annotations $\{\mathbf{a},\mathbf{O},\mathbf{W}\}$ (see main text Equations 3-5). For a given set of $\{\theta_0,\theta,\sigma_0,\sigma\}$, we use the mean-field variational approximation algorithm from RSS-E (Zhu and Stephens 2018) to estimate $p(\boldsymbol{\beta} \mid \mathbf{D},\theta_0,\theta,\sigma_0,\sigma)$:

$$p(\boldsymbol{\beta} \mid \mathbf{D},\theta_0,\theta,\sigma_0,\sigma) \approx \prod_{j=1}^{p} q_j^\star(\beta_j \mid \mathbf{D},\theta_0,\theta,\sigma_0,\sigma), \tag{11}$$

$$q_j^\star(\beta_j \mid \mathbf{D},\theta_0,\theta,\sigma_0,\sigma) = \alpha_j^\star \cdot \mathcal{N}(\beta_j;\, \nu_j^\star,(\tau_j^\star)^2) + (1-\alpha_j^\star)\cdot\delta_0(\beta_j), \tag{12}$$

where the optimal variational parameters $\{\alpha_j^\star,\nu_j^\star,\tau_j^\star\}$ are given by:

$$(\tau_j^\star)^2 = \frac{1}{\hat{s}_j^{-2}+\sigma_j^{-2}}, \tag{13}$$

$$\nu_j^\star = (\tau_j^\star)^2\cdot\left(\frac{\hat{\beta}_j}{\hat{s}_j^2} - \sum_{i\neq j}\frac{\widehat{\mathbf{R}}_{ij}\alpha_i^\star\nu_i^\star}{\hat{s}_i\hat{s}_j}\right), \tag{14}$$

$$\frac{\alpha_j^\star}{1-\alpha_j^\star} = \frac{\pi_j}{1-\pi_j}\cdot\frac{\tau_j^\star}{\sigma_j}\cdot\exp\left\{\frac{(\nu_j^\star)^2}{2(\tau_j^\star)^2}\right\}. \tag{15}$$

The per-iteration complexity of the coordinate descent algorithm (13)-(15) is linear with p, the number of genome-wide SNPs analyzed.

We use $F^\star(\mathbf{D},\theta_0,\theta,\sigma_0,\sigma)$, the variational lower bound corresponding to the optimal variational parameters $\{\alpha_j^\star,\nu_j^\star,\tau_j^\star\}$ in (13)-(15) to approximate the log marginal likelihood $\log p(\widehat{\boldsymbol{\beta}} \mid \widehat{\mathbf{S}},\widehat{\mathbf{R}},\mathbf{a},\mathbf{O},\mathbf{W},\theta_0,\theta,\sigma_0,\sigma)$:

$$\begin{aligned}F^\star(\mathbf{D},\theta_0,\theta,\sigma_0,\sigma) =& F_0(\mathbf{D}) + \widehat{\boldsymbol{\beta}}'\widehat{\mathbf{S}}^{-2}\mathrm{E}_{q^\star}(\boldsymbol{\beta}) - \frac{1}{2}\mathrm{E}'_{q^\star}(\boldsymbol{\beta})\widehat{\mathbf{S}}^{-1}\widehat{\mathbf{R}}\widehat{\mathbf{S}}^{-1}\mathrm{E}_{q^\star}(\boldsymbol{\beta}) - \frac{1}{2}\sum_{j=1}^{p}\frac{\mathrm{Var}_{q^\star}(\beta_j)}{\hat{s}_j^2}\\ &- \sum_{j=1}^{p}\alpha_j^\star\log\left(\frac{\alpha_j^\star}{\pi_j}\right) - \sum_{j=1}^{p}(1-\alpha_j^\star)\log\left(\frac{1-\alpha_j^\star}{1-\pi_j}\right)\\ &+ \sum_{j=1}^{p}\frac{\alpha_j^\star}{2}\left\{1+\log\left[\frac{(\tau_j^\star)^2}{\sigma_j^2}\right] - \frac{(\tau_j^\star)^2+(\nu_j^\star)^2}{\sigma_j^2}\right\},\end{aligned}$$

$F_0(\mathbf{D}) = -[\log|2\pi\cdot\widehat{\mathbf{S}}\widehat{\mathbf{R}}\widehat{\mathbf{S}}| + \widehat{\boldsymbol{\beta}}'(\widehat{\mathbf{S}}\widehat{\mathbf{R}}\widehat{\mathbf{S}})^{-1}\widehat{\boldsymbol{\beta}}]\,/\,2$, $\mathrm{E}_{q^\star}(\boldsymbol{\beta}) = (\mathrm{E}_{q^\star}(\beta_1),\ldots,\mathrm{E}_{q^\star}(\beta_p))'$, $\mathrm{E}_{q^\star}(\beta_j) = \alpha_j^\star\nu_j^\star$ and $\mathrm{Var}_{q^\star}(\beta_j) = \alpha_j^\star[(\tau_j^\star)^2+(\nu_j^\star)^2] - (\alpha_j^\star\nu_j^\star)^2$. Of note, RSS-NET and RSS-E have the same posterior computation scheme if we set $\sigma_j^2 = \sigma_\beta^2$ for all $j=1,\ldots,p$ in (13)-(15) and $F^\star$.

Finally, we approximate the joint posterior of hyper-parameters $p(\theta_0,\theta,\sigma_0,\sigma \mid \mathbf{D})$ as:

$$p(\theta_0,\theta,\sigma_0,\sigma \mid \mathbf{D}) \approx \omega^\star(\theta_0,\theta,\sigma_0,\sigma) \propto \exp\{F^\star(\mathbf{D},\theta_0,\theta,\sigma_0,\sigma)\}, \tag{16}$$

since we use independent uniform grid hyper-priors (**Supplementary Table 19**).

Bayes factor for network enrichments

To assess whether a regulatory network is enriched for genetic associations with a trait, we evaluate the following Bayes factor (BF):

$$\mathrm{BF} = \frac{p(\widehat{\boldsymbol{\beta}} \mid \widehat{\mathbf{S}},\widehat{\mathbf{R}},\mathbf{a},\mathbf{O},\mathbf{W},M_1)}{p(\widehat{\boldsymbol{\beta}} \mid \widehat{\mathbf{S}},\widehat{\mathbf{R}},\mathbf{a},\mathbf{O},\mathbf{W},M_0)}, \tag{17}$$

where M_1 denotes the enrichment model where $\theta > 0$ or $\sigma^2 > 0$, and M_0 denotes the baseline model where $\theta = 0$ and $\sigma^2 = 0$. To compute BF (17), we approximate intractable marginal likelihoods by corresponding variational lower bounds $F^\star$:

$$\begin{aligned} \text{BF} &= \frac{\int p(\widehat{\boldsymbol{\beta}} \mid \widehat{\mathbf{S}}, \widehat{\mathbf{R}}, \mathbf{a}, \mathbf{O}, \mathbf{W}, \theta_0, \theta, \sigma_0, \sigma) p(\theta_0) p(\theta) p(\sigma_0) p(\sigma) \mathrm{d}\theta \mathrm{d}\theta_0 \mathrm{d}\sigma_0 \mathrm{d}\sigma}{\int p(\widehat{\boldsymbol{\beta}} \mid \widehat{\mathbf{S}}, \widehat{\mathbf{R}}, \mathbf{a}, \mathbf{O}, \mathbf{W}, \theta_0, \theta = 0, \sigma_0, \sigma = 0) p(\theta_0) p(\sigma_0) \mathrm{d}\theta_0 \mathrm{d}\sigma_0} \\ &\approx \frac{n_1^{-1} \sum_{s=1}^{n_1} \exp\{F^\star(\mathbf{D}, \theta_0^{(s)}, \theta^{(s)}, \sigma_0^{(s)}, \sigma^{(s)})\}}{n_0^{-1} \sum_{t=1}^{n_0} \exp\{F^\star(\mathbf{D}, \theta_0^{(t)}, \theta = 0, \sigma_0^{(t)}, \sigma = 0)\}}, \end{aligned} \tag{18}$$

where $\{\theta_0^{(s)}, \theta^{(s)}, \sigma_0^{(s)}, \sigma^{(s)}\}$ and $\{\theta_0^{(t)}, \sigma_0^{(t)}\}$ are pre-defined grids (**Supplementary Table 19**).

Posterior probability for genetic associations

To identify association between a locus and a trait, we compute P_1, the posterior probability that at least one SNP in the locus is associated with the trait:

$$P_1 = 1 - \Pr(\beta_j = 0, \forall j \in \text{locus} \mid \mathbf{D}, \text{model}), \tag{19}$$

where the "model" here can be the baseline model M_0 (yielding P_1^{base}), the enrichment model M_1 for the near-gene control network (yielding P_1^{near}) and a given network (yielding P_1^{net}). Given a grid $\{\theta_0^{(s)}, \theta^{(s)}, \sigma_0^{(s)}, \sigma^{(s)}\}$, P_1 is estimated as

$$\begin{aligned} P_1 &= 1 - \int \Pr(\beta_j = 0,\ \forall j \in \text{locus} \mid \mathbf{D}, \theta_0, \theta, \sigma_0, \sigma) p(\theta_0, \theta, \sigma_0, \sigma \mid \mathbf{D}) \mathrm{d}\theta \mathrm{d}\theta_0 \mathrm{d}\sigma_0 \mathrm{d}\sigma \\ &\approx 1 - \sum_{s=1}^{n_1} \prod_{j \in \text{locus}} \left[1 - \alpha_j^\star(\theta_0^{(s)}, \theta^{(s)}, \sigma_0^{(s)}, \sigma^{(s)})\right] \cdot \omega^\star(\theta_0^{(s)}, \theta^{(s)}, \sigma_0^{(s)}, \sigma^{(s)}). \end{aligned} \tag{20}$$

Regulatory network as a bipartite graph

In this study a regulatory network is a directed bipartite graph $\{\mathbf{V}_{\text{TF}}, \mathbf{V}_{\text{TG}}, \mathbf{E}_{\text{TF}\to\text{TG}}\}$, where $\mathbf{V}_{\text{TF}}$ denotes the node set of transcription factors (TFs), $\mathbf{V}_{\text{TG}}$ denotes the node set of target genes (TGs), and $\mathbf{E}_{\text{TF}\to\text{TG}}$ denotes the set of directed TF-to-TG edges, summarizing how TFs regulate TGs through regulatory elements (REs). Each edge has a weight between 0 and 1, measuring the relative regulation strength of a TF on a TG.

Below is a small subset of B cell regulatory network (https://github.com/suwonglab/rss-net/tree/master/data). In this example, $\mathbf{V}_{\text{TF}}$ corresponds to the column `TF`, $\mathbf{V}_{\text{TG}}$ corresponds to the column `TG`, $\mathbf{E}_{\text{TF}\to\text{TG}}$ corresponds to all rows of `TF` and `TG`, and the edge weights are specified by the column `Score`.

```
       TF      TG    Score
1:   RARG EEF1A1 0.723037
2:   SOX9   CD74 0.690921
3:   EBF1  FXYD5 0.659009
4:   PAX5   CD44 0.704366
5: TRIM28   GSAP 0.629798
6: POU6F1  RPS3A 0.632690
```

In this study, for a given TF, we only consider the downstream effects of all genes that are **directly** regulated by this TF (see main text Figure 1c and Equation 5). For example, it is

biologically possible that a TF 1 regulates a target gene which is also a TF, say TF 2; when specifying the RSS-NET SNP-level effect size distribution, we only incorporate the direct downstream effect of TF 1 on TF 2, and ignore all other indirect downstream effect of TF 1 on genes that are only directly regulated by TF 2.

Quantify *cis* impact of a SNP on a gene

To specify c_{jg}, the relative impact of a *cis* SNP j on a gene g (main text Equation 5), we use a simple approach based on published *cis* expression quantitative trait loci (eQTL). Specifically, if a pair of SNP j and gene g is available in an eQTL database, we define

$$c_{jg} = 1 + \sqrt{z_{jg}^2 / (z_{jg}^2 + n_{jg})}, \tag{21}$$

where n_{jg} is the number of individuals with both genotype of SNP j and expression of gene g available and z_{jg} is the single-SNP z-score measuring the marginal association between genotype of SNP j and expression of gene g across n_{jg} individuals; if the pair does not have eQTL association data available, we set $c_{jg} = 1$. When deriving c_{jg} from *cis*-eQTL data, we consider all available SNP-gene pairs, not just the significant ones.

In this study we specify c_{jg} in a context-matched manner. For example, if we analyze the regulatory network derived from liver samples, we also use *cis*-eQTL data from liver samples to define c_{jg}. For networks of 5 brain regions and 27 non-brain tissues, we use the tissue-matched *cis*-eQTL data from GTEx (https://storage.googleapis.com/gtex_analysis_v7/single_tissue_eqtl_data/GTEx_Analysis_v7_eQTL_all_associations.tar.gz, accessed April 7, 2019). For networks of 5 immune cells, we use the cell-type-matched *cis*-eQTL data from DICE (http://downloads.dice-database.org/downloads/DICE_DB_1/eqtl/unfiltered/, accessed July 3, 2019). For the "omnibus" network, we use the *cis*-eQTL data of blood samples from the eQTLGen Consortium (http://www.eqtlgen.org/cis-eqtls.html, accessed May 17, 2019). Summary statistics of c_{jg} are provided in **Supplementary Tables 17-18**.

The small sample sizes of eQTL studies make it hard to produce reliable model-based estimates of c_{jg}. Hence, we keep our specification of c_{jg} deliberately simple. We acknowledge that (21) could be potentially improved, although we have not fully investigated it here. Due to the modular design of RSS-NET, once improved estimates of c_{jg} become available, they can be incorporated into RSS-NET in a straightforward manner.

Explain SNP-level subscript j in γ_{jg}

In this work we model γ_{jg}, the random effect of SNP j due to gene g as

$$\gamma_{jg} \overset{\text{i.i.d.}}{\sim} \mathcal{N}(0,\ \sigma^2).$$

We emphasize that the SNP-level subscript j in γ_{jg} ensures the exchangeability of β_j required by (2), as shown in the following example. Suppose there are two nearby SNPs 1 and 2, and their effects are sums of random effects of genes 1 and 2. If we ignore the SNP-level subscript j and use the γ_g notation, then

$$\begin{aligned}
\beta_1 &= 0.18 \cdot \gamma_1 + 0.36 \cdot \gamma_2, \\
\beta_2 &= 0.36 \cdot \gamma_1 + 0.72 \cdot \gamma_2, \\
\gamma_g &\overset{\text{i.i.d.}}{\sim} \mathcal{N}(0,\ \sigma^2),\ g = 1, 2.
\end{aligned}$$

This is inconsistent with the independent prior (2) placed on β_j, because under this notation, $\beta_2 = 2\beta_1$ and the correlation of β_1 and β_2 is exactly 1. In contrast, this inconsistency disappears if we use the γ_{jg} notation:

$$\begin{aligned}\beta_1 &= 0.18 \cdot \gamma_{11} + 0.36 \cdot \gamma_{12},\\ \beta_2 &= 0.36 \cdot \gamma_{21} + 0.72 \cdot \gamma_{22},\\ \gamma_{jg} &\overset{\text{i.i.d.}}{\sim} \mathcal{N}(0,\ \sigma^2),\ j = 1,2,\ g = 1,2.\end{aligned}$$

Now β_1 and β_2 are independent, because γ_{jg}'s are all i.i.d for $j = 1,2$ and $g = 1,2$.

Induced prior distribution for σ_0^2 and σ^2

Here we assume a multiple regression model for the phenotype-genotype relationship:

$$\mathbf{y} = \mathbf{X}\boldsymbol{\beta} + \boldsymbol{\epsilon}, \tag{22}$$

where $\mathbf{y}$ is an $n \times 1$ centered vector of phenotype, $\mathbf{X}$ is an $n \times p$ column-centered matrix of genotype, $\boldsymbol{\beta}$ is a $p \times 1$ vector of multiple regression coefficients (i.e. SNP-level effect sizes), and $\boldsymbol{\epsilon}$ is an independent error term. Let $\sigma_{x,j}^2$ denote the population variance of genotype for SNP j, $j = 1,\ldots,p$, and let σ_y^2 denote the population variance of phenotype.

PROPOSITION 1. If SNP-level effect sizes $\boldsymbol{\beta}$ follow the prior distribution specified in RSS-NET (2), (4) and (5), then, for all $i, j = 1,\ldots,p$,

$$\mathrm{E}(\beta_j) = 0,\ \ \mathrm{Var}(\beta_j) = \pi_j\left(\sigma_0^2 + \sigma^2 \cdot \textstyle\sum_{g \in \mathbf{O}_j} w_{jg}^2\right),\ \ \mathrm{Cov}(\beta_i,\ \beta_j) = 0. \tag{23}$$

PROOF. This is a direct application of the law of total expectation. ■

PROPOSITION 2. $\mathrm{E}[V(\mathbf{X}\boldsymbol{\beta})] = \mathrm{E}^{\text{base}}[V(\mathbf{X}\boldsymbol{\beta})] + \mathrm{E}^{\text{net}}[V(\mathbf{X}\boldsymbol{\beta})]$, where

$$\mathrm{E}^{\text{base}}[V(\mathbf{X}\boldsymbol{\beta})] = \sigma_0^2 \cdot \sum_{j=1}^{p} \pi_j \cdot \mathrm{E}[V(\mathbf{X}_j)], \tag{24}$$

$$\mathrm{E}^{\text{net}}[V(\mathbf{X}\boldsymbol{\beta})] = \sigma^2 \cdot \sum_{j=1}^{p} \pi_j \cdot \left(\textstyle\sum_{g \in \mathbf{O}_j} w_{jg}^2\right) \cdot \mathrm{E}[V(\mathbf{X}_j)], \tag{25}$$

$\mathbf{X}_j$ is the jth column of $\mathbf{X}$, $j = 1,\ldots,p$, and $V(\mathbf{d})$ denotes the sample variance of a vector $\mathbf{d}$.

PROOF. Define a $p \times p$ diagonal matrix $\boldsymbol{\Sigma}_\beta$ where the jth diagonal entry is $\mathrm{Var}(\beta_j)$ in PROPOSITION 1. It suffices to notice that $V(\mathbf{X}\boldsymbol{\beta}) = n^{-1}\boldsymbol{\beta}'\mathbf{X}'\mathbf{X}\boldsymbol{\beta}$, and,

$$\begin{aligned}\mathrm{E}[V(\mathbf{X}\boldsymbol{\beta})] &= \mathrm{E}\{\mathrm{E}[V(\mathbf{X}\boldsymbol{\beta}) \mid \mathbf{X}]\} = \mathrm{E}[\mathrm{trace}(n^{-1}\mathbf{X}'\mathbf{X} \cdot \boldsymbol{\Sigma}_\beta)],\\ &= \mathrm{E}\left[\sum_{j=1}^{p} n^{-1}\mathbf{X}_j'\mathbf{X}_j \cdot \mathrm{Var}(\beta_j)\right] = \sum_{j=1}^{p} \mathrm{Var}(\beta_j) \cdot \mathrm{E}[V(\mathbf{X}_j)].\end{aligned} \tag{26}$$

Use PROPOSITION 1 to complete the proof. ■

REMARK 1. PROPOSITION 2 shows that the total genetic variation $\mathrm{E}[V(\mathbf{X}\boldsymbol{\beta})]$ can be decomposed into a component (24) that is shared by all p SNPs and a component (25) that is due to network annotations $\{\mathbf{O}_j, w_{jg}\}$.

PROPOSITION 3. Let $ns_j^2 = \sigma_y^2/\sigma_{x,j}^2$, for $j = 1,\ldots,p$. If $\{\sigma_0^2, \sigma^2\}$ are re-parameterized as

$$\sigma_0^2 = \eta\cdot(1-\rho)\cdot\left(\sum_{j=1}^{p}\frac{\pi_j}{ns_j^2}\right)^{-1},\quad \sigma^2 = \eta\cdot\rho\cdot\left(\sum_{j=1}^{p}\frac{\pi_j\cdot\sum_{g\in\mathbf{O}_j}w_{jg}^2}{ns_j^2}\right)^{-1}, \tag{27}$$

then

$$\eta = \frac{\mathrm{E}[V(\mathbf{X}\boldsymbol{\beta})]}{\mathrm{E}[V(\mathbf{y})]},\quad \rho = \frac{\mathrm{E}^{\mathrm{net}}[V(\mathbf{X}\boldsymbol{\beta})]}{\mathrm{E}[V(\mathbf{X}\boldsymbol{\beta})]}. \tag{28}$$

PROOF. It suffices to show that, for all $j = 1,\ldots,p$,

$$ns_j^2 = \frac{\sigma_y^2}{\sigma_{x,j}^2} = \frac{\mathrm{E}[V(\mathbf{y})]}{\mathrm{E}[V(\mathbf{X}_j)]}. \tag{29}$$

Use PROPOSITION 2 to complete the proof. ■

REMARK 2. PROPOSITION 3 provides the mathematical basis to interpret $\{\eta,\rho\}$. Specifically, η represents the proportion of the total phenotypic variation explained by p SNPs, and ρ represents the proportion of total genetic variation explained by network annotations $\{\mathbf{O}_j, w_{jg}\}$.

REMARK 3. Since $ns_j^2 = \sigma_y^2/\sigma_{x,j}^2$, where σ_y^2 is the population variance of phenotype and $\sigma_{x,j}^2$ is the population variance of genotype at SNP j, this re-parameterization based on $\{\eta,\rho\}$ ensures that the induced-prior (27) of $\{\sigma_0^2,\sigma^2\}$ does not depend on GWAS sample size n, and the resulting genetic effect sizes ($\boldsymbol{\beta}$) have the same measurement unit as the phenotype.

REMARK 4. The induced prior (27) of $\{\sigma_0^2,\sigma^2\}$ contains a quantity $ns_j^2 = \sigma_y^2/\sigma_{x,j}^2$ that depends on unknown population parameters $\{\sigma_y^2,\sigma_{x,j}^2\}$. As shown in Zhu and Stephens (2017), ns_j^2 can be reliably estimated from GWAS summary data: $ns_j^2 \approx n\hat{s}_j^2$. In practice, we replace the unknown ns_j^2 in (27) with known $n\hat{s}_j^2$ (see main text Equation 9).

Acknowledgments and data sources

This study uses data generated by the Wellcome Trust Case Control Consortium, 1000 Genomes Project, ENCODE Consortium, GTEx Project, DICE Project, eQTLGen Consortium, and multiple GWAS consortia. We thank them for making their data publicly available. Detailed acknowledgments and data sources are listed below.

- **Wellcome Trust Case Control Consortium (WTCCC).** This study use individual-level genotype data generated by WTCCC to design simulations. A full list of the investigators who contributed to the generation of the data is available from https://www.wtccc.org.uk/. The WTCCC data are available at the European Genome-phenome Archive (https://www.ebi.ac.uk/ega/).
- **1000 Genomes Project.** This study uses haplotypes of individuals with European ancestry from the 1000 Genomes Project Phase 3 to estimate LD. The 1000 Genomes Phase 3 haplotype data have been contributed by 1000 Genomes investigators and have been downloaded from ftp://ftp.1000genomes.ebi.ac.uk/vol1/ftp/release/20130502/.
- **Encyclopedia of DNA Elements (ENCODE) Consortium.** This study uses gene expression and chromatin accessibility data generated by the ENCODE Consortium

and the ENCODE production laboratories. The ENCODE data are available at the ENCODE portal (https://www.encodeproject.org/).

- **Genotype-Tissue Expression (GTEx) Project.** This study uses *cis*-eQTL data generated by the GTEx Project. The GTEx Project was supported by the Common Fund of the Office of the Director of the National Institutes of Health, and by NCI, NHGRI, NHLBI, NIDA, NIMH, and NINDS. The GTEx data are available at the GTEx Portal (https://gtexportal.org/home/).
- **Database of Immune Cell Expression, Expression quantitative trait loci and Epigenomics (DICE) Project.** This study uses *cis*-eQTL data generated by the DICE Project. The DICE Project was supported by NIH R24AI108564. The DICE data are available at https://dice-database.org/.
- **eQTLGen Consortium.** This study uses *cis*-eQTL data generated by the eQTLGen Consortium. The eQTLGen data are available at http://www.eqtlgen.org/.
- **Genetic Investigation of ANthropometric Traits (GIANT) Consortium.** GWAS summary statistics on adult human height (Wood et al. 2014), body mass index (Locke et al. 2015) and body fat distribution (Shungin et al. 2015) have been contributed by GIANT investigators and have been downloaded from http://portals.broadinstitute.org/collaboration/giant.
- **Psychiatric Genomics Consortium (PGC).** GWAS summary statistics on schizophrenia (Ripke et al. 2014) have been contributed by PGC investigators and have been downloaded from http://www.med.unc.edu/pgc.
- **International Inflammatory Bowel Disease Genetics Consortium (IIBDGC).** GWAS summary statistics on inflammatory bowel disease, Crohn's disease and ulcerative colitis (Liu et al. 2015) have been contributed by IIBDGC investigators and have been downloaded from https://www.ibdgenetics.org.
- **Coronary ARtery DIsease Genome wide Replication and Meta-analysis (CARDIoGRAM) plus The Coronary Artery Disease (C4D) Genetics (CARDIoGRAMplusC4D) Consortium.** GWAS summary statistics on coronary artery disease and myocardial infarction (Nikpay et al. 2015) have been contributed by CARDIoGRAMplusC4D investigators and downloaded from http://www.cardiogramplusc4d.org/.
- **GWAS summary statistics of heart rate.** GWAS summary statistics on heart rate have been contributed by authors of Den Hoed et al. (2013) and have been downloaded from https://walker05.u.hpc.mssm.edu/.
- **International Genomics of Alzheimer's Project (IGAP).** GWAS summary statistics on Alzheimer's disease (Lambert et al. 2013) have been contributed by IGAP investigators and have been downloaded from http://web.pasteur-lille.fr/en/recherche/u744/igap/igap_download.php. We thank the International Genomics of Alzheimer's Project (IGAP) for providing summary results data for these analyses. The investigators within IGAP contributed to the design and implementation of IGAP and/or provided data but did not participate in analysis or writing of this report. IGAP was made possible by the generous participation of the control subjects, the patients, and their families. The i-Select chips was funded by the French National Foundation on Alzheimer's disease and related disorders. EADI was supported by the LABEX (laboratory of excellence program investment for the future)

DISTALZ grant, Inserm, Institut Pasteur de Lille, Universite de Lille 2 and the Lille University Hospital. GERAD was supported by the Medical Research Council (Grant no. 503480), Alzheimer's Research UK (Grant no. 503176), the Wellcome Trust (Grant no. 082604/2/07/Z) and German Federal Ministry of Education and Research (BMBF): Competence Network Dementia (CND) grant no. 01GI0102, 01GI0711, 01GI0420. CHARGE was partly supported by the NIH/NIA grant R01 AG033193 and the NIA AG081220 and AGES contract N01-AG-12100, the NHLBI grant R01 HL105756, the Icelandic Heart Association, and the Erasmus Medical Center and Erasmus University. ADGC was supported by the NIH/NIA grants: U01 AG032984, U24 AG021886, U01 AG016976, and the Alzheimer's Association grant ADGC-10-196728.

- **Social Science Genetic Association Consortium (SSGAC).** GWAS summary statistics on neuroticism (Okbay et al. 2016) have been contributed by SSGAC investigators and have been downloaded from https://www.thessgac.org. For financial support, the SSGAC thanks the U.S. National Science Foundation, the U.S. National Institutes of Health (National Institute on Aging, and the Office for Behavioral and Social Science Research), the Ragnar Soderberg Foundation, the Swedish Research Council, The Jan Wallander and Tom Hedelius Foundation, the European Research Council, and the Pershing Square Fund of the Foundations of Human Behavior.

- **GWAS summary statistics of rheumatoid arthritis.** GWAS summary statistics on rheumatoid arthritis have been contributed by authors of Okada et al. (2014) and have been downloaded from http://plaza.umin.ac.jp/yokada/datasource/software.htm.

- **DIAbetes Genetics Replication And Meta-analysis (DIAGRAM) Consortium.** GWAS summary statistics on type 2 diabetes (Morris et al. 2012) have been contributed by DIAGRAM investigators and have been downloaded from http://www.diagram-consortium.org.

- **Global Lipids Genetics Consortium (GLGC).** GWAS summary statistics on low-density and high-density lipoprotein cholesterol (Teslovich et al. 2010) have been contributed by GLGC investigators and have been downloaded from http://csg.sph.umich.edu//abecasis/public/lipids2010.

- **GWAS summary statistics of atrial fibrillation.** GWAS summary statistics on atrial fibrillation have been contributed by authors of Christophersen et al. (2017) and are available from the corresponding author on reasonable request; see "Data availability" section of Christophersen et al. (2017).

- **Genetic Associations and Mechanisms in Oncology (GAME-ON), Discovery, Biology, and Risk of Inherited Variants in Breast Cancer (DRIVE) Project.** GWAS summary statistics on breast cancer have been contributed by the GAME-ON/DRIVE Project and have been downloaded from http://gameon.dfci.harvard.edu. The DRIVE project acknowledges the following GWASs and investigators that shared genome-wide summary data as part of the breast-cancer GWAS meta-analysis: the Australian Breast Cancer Family Study (ABCFS) (John L. Hopper, Melissa C. Southey, Enes Makalic, Daniel F. Schmidt), the British Breast Cancer Study (BBCS) (Olivia Fletcher, Julian Peto, Lorna Gibson, Isabel dos Santos Silva), the Breast and Prostate Cancer Cohort Consortium (BPC3) (David J. Hunter, Sara Lindstrom, Peter Kraft), the Breast Cancer Family Registries (BCFR) (Habib Ahsan, Alice Whitte-

more), the Dutch Familial Bilateral Breast Cancer Study (DFBBCS) (Quinten Waisfisz, Hanne Meijers-Heijboer, Muriel Adank, Rob B. van der Luijt, Andre G. Uitterlinden, Albert Hofman), German Consortium for Hereditary Breast and Ovarian Cancer (GC-HBOC) (Alfons Meindl, Rita K. Schmutzler, Bertram Muller-Myhsok, Peter Lichtner), the Helsinki Breast Cancer Study (HEBCS) (Heli Nevanlinna, Taru A. Muranen, Kristiina Aittomaki, Carl Blomqvist), the Mammary Carcinoma Risk Factor Investigation (MARIE) (Jenny Chang-Claude, Rebecca Hein, Norbert Dahmen, Lars Beckman), SardiNIA (Laura Crisponi), the Singapore and Sweden Breast Cancer Study (SASBAC) (Per Hall, Kamila Czene, Astrid Irwanto, Jianjun Liu), and the UK2 (Douglas F. Easton, Clare Turnbull, Nazneen Rahman).

Supplementary Figures

Supplementary Figure 1

Simulation details and additional results of Figure 2. We use real genotypes of 348,965 genome-wide SNPs on chromosomes 1-22 from 1,458 individuals in the UK Blood Service Control Group (Wellcome Trust Case Control Consortium 2007) to simulate phenotype data, and then compute single-SNP association summary statistics. On these summary data, we compare RSS-NET with existing enrichment methods.

We infer a B cell regulatory network from the paired gene expression and chromatin accessibility data of primary B cells from peripheral blood (Duren et al. 2017; Luo et al. 2020). We use the B cell network to create SNP-level annotation for 348,965 SNPs. Specifically, we let $a_j = 1$ if SNP j is within 100 kb of either a regulatory element or the transcribed region of a member gene in the B cell network, and let $a_j = 0$ otherwise. There are 121,308 SNPs mapped to the B cell network with annotation $a_j = 1$.

To ensure that simulated datasets have roughly the same proportion of true genetic signals, we simulate causal indicators for negative and positive datasets in a paired way. We first simulate the causal indicator ζ_j of each SNP j in a positive dataset as:

$$\zeta_j \sim \text{Bernoulli}(\pi_j), \quad \pi_j = 1 / [1 + 10^{-(\theta_0 + a_j \theta)}],$$

where θ_0 and θ are the baseline and enrichment proportion parameters respectively. We then count the number of causal SNPs in this positive dataset as $n_c := \sum_j \zeta_j$, and randomly choose n_c SNPs as causal SNPs for the corresponding negative dataset.

For positive datasets, we simulate the true effect β_j of each SNP j as

$$\begin{aligned} \beta_j \mid \zeta_j = 0 &\sim \delta_0, \\ \beta_j \mid \zeta_j = 1 &\sim \mathcal{N}(0,\ \sigma_0^2 + \sigma^2 \cdot \textstyle\sum_{g \in \mathbf{O}_j} w_{jg}^2), \end{aligned}$$

where δ_0 denotes point mass at zero, σ_0^2 and σ^2 are the baseline and enrichment magnitude parameter respectively, $\{\mathbf{O}_j, w_{jg}\}$ are network annotations (see main text Equations 4-5). For negative datasets, we simulate β_j from the same model above with $\sigma^2 = 0$.

To ensure that negative and positive datasets have roughly the same magnitude of total genetic signals, we simulate phenotypes by matching signal-to-noise ratios. Specifically, we simulate phenotype y_i of individual i as follows:

$$y_i = \textstyle\sum_{j=1}^{p} x_{ij} \cdot \beta_j + \epsilon_i, \quad \epsilon_i \sim \mathcal{N}(0, \tau^{-1}),$$

where p is 348,965, x_{ij} is the genotype of SNP j for individual i. The true value of residual variance τ^{-1} is determined by the total proportion of variance in phenotype $\mathbf{y}$ explained by effects of all available SNPs in $\mathbf{X}$: PVE = $V(\mathbf{X}\boldsymbol{\beta}) / [\tau^{-1} + V(\mathbf{X}\boldsymbol{\beta})]$, where $V(\mathbf{X}\boldsymbol{\beta})$ is the sample variance of $\mathbf{X}\boldsymbol{\beta}$.

We set the true values of hyper-parameter as follows: baseline proportion parameter $\theta_0 \in \{-2,-3,-4\}$, enrichment proportion parameter $\theta \in \{0,2\}$, baseline magnitude parameter $\sigma_0 = 1$, enrichment magnitude parameter $\sigma \in \{0, 0.5, 2\}$, and PVE $\in \{0.2, 0.6\}$. For each combination of $\{\theta_0, \theta, \sigma_0, \sigma, \text{PVE}\}$ (excluding negative cases where $\theta = \sigma = 0$), we simulate 200 negative and 200 positive independent datasets. The caption of each panel in this supplementary figure shows the true hyper-parameter values of positive datasets. The table below lists true values of positive datasets for each panel in **Figure 2** ($\sigma_0 = 1$).

	a	b	c	d
sparse: $\theta_0 = -4$	$\theta = 2, \sigma = 0, \text{PVE} = 0.6$	$\theta = 0, \sigma = 0.5, \text{PVE} = 0.6$	$\theta = 2, \sigma = 0.5, \text{PVE} = 0.6$	$\theta = 2, \sigma = 0, \text{PVE} = 0.2$
polygenic: $\theta_0 = -2$	$\theta = 2, \sigma = 0, \text{PVE} = 0.6$	$\theta = 0, \sigma = 0.5, \text{PVE} = 0.6$	$\theta = 2, \sigma = 0.5, \text{PVE} = 0.6$	$\theta = 2, \sigma = 0, \text{PVE} = 0.2$

We apply RSS-NET to simulated datasets with the following hyper-parameter grids. The baseline parameters θ_0 and σ_0 are set as their true values. The grids on the enrichment parameters θ and σ are `(0:0.25:1)` if their true values are zero; otherwise they are `[0 ((truth-0.5):0.25:(truth+0.5))]`. For the same simulation scenario, we use the same hyper-parameter grid in RSS-NET analyses of all negative and positive datasets.

For all datasets the target of enrichment testing is the B cell network. A false positive occurs if a method identifies enrichment in a negative dataset. A true positive occurs if a method identifies enrichment in a positive dataset. We evaluate the performance of enrichment methods by plotting the receiver operating characteristic (ROC) curve and computing the area under the ROC curve (AUROC) for each method. Both metrics are implemented in the R package `plotROC` (Sachs 2017).

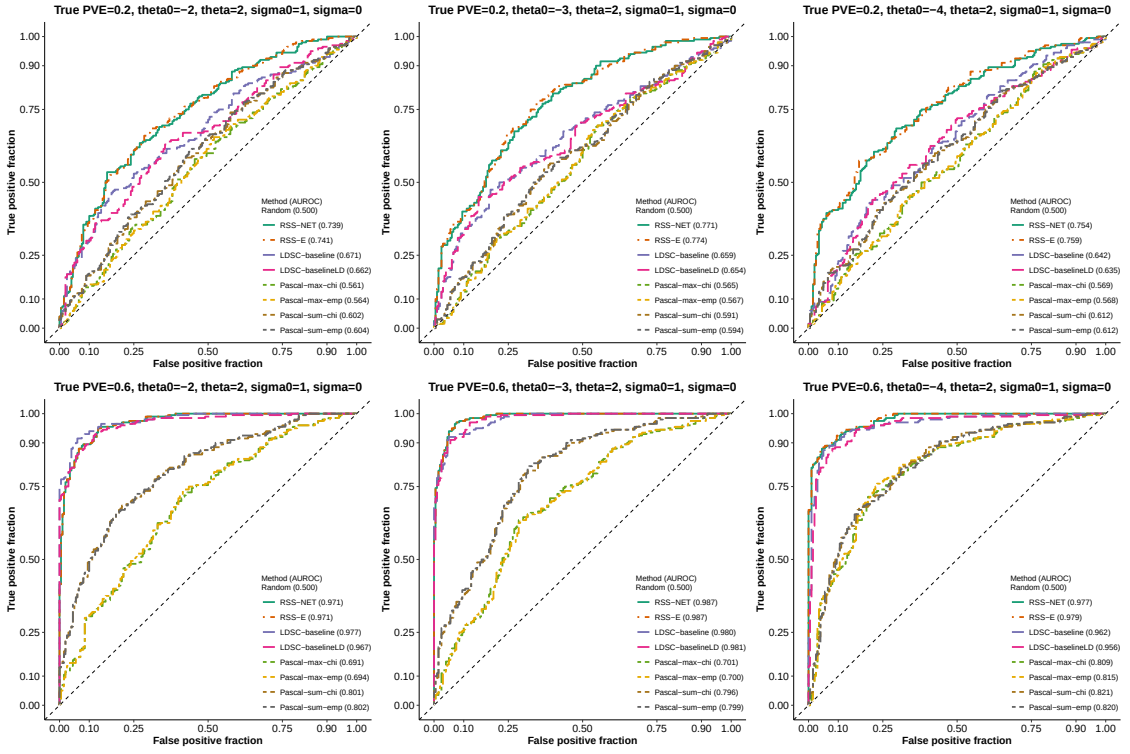

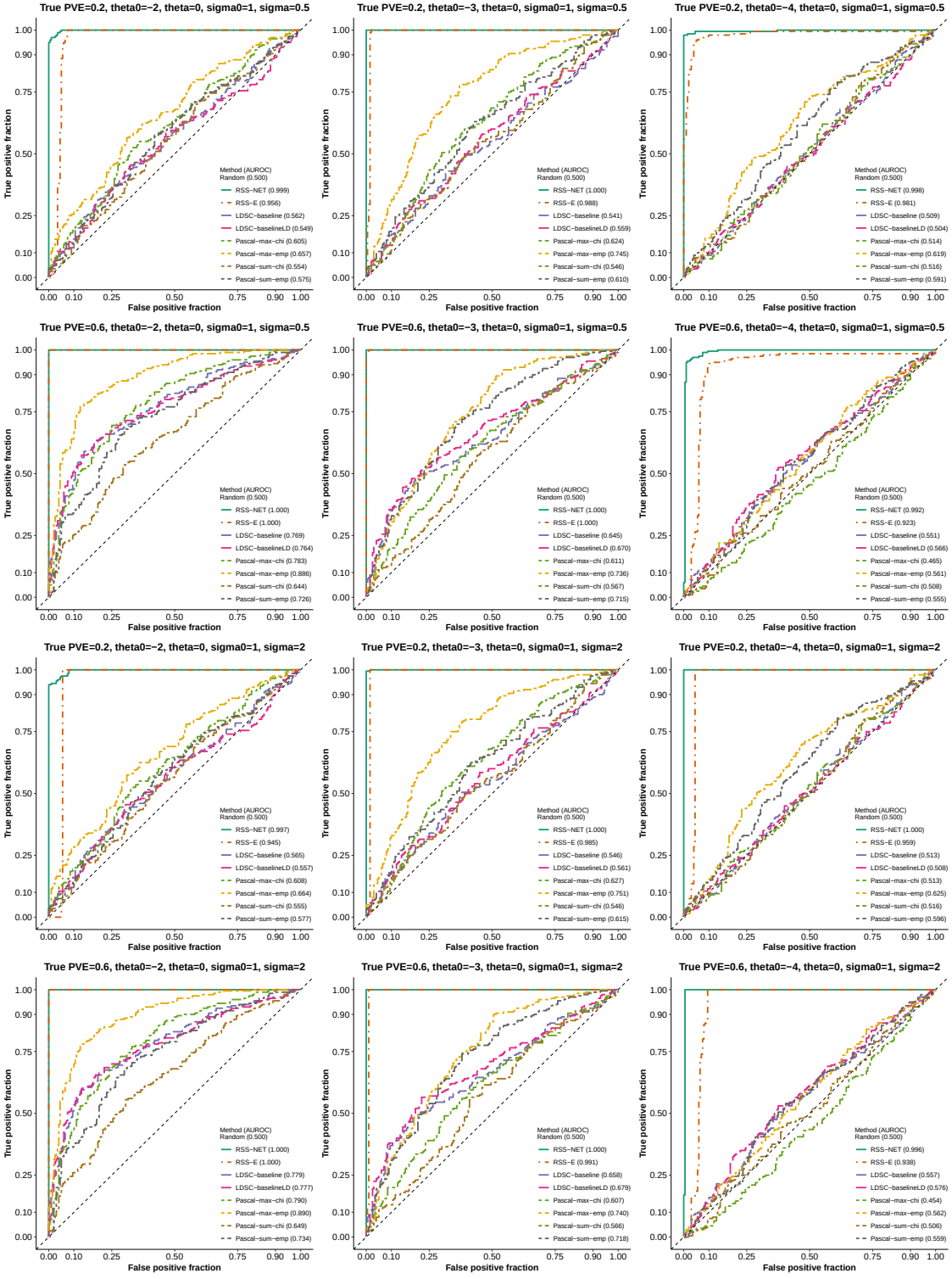
True PVE=0.2, theta0=−2, theta=0, sigma0=1, sigma=0.5
Method (AUROC)
Random (0.500)
RSS−NET (0.999)
RSS−E (0.956)
LDSC−baseline (0.562)
LDSC−baselineLD (0.549)
Pascal−max−chi (0.605)
Pascal−max−emp (0.657)
Pascal−sum−chi (0.554)
Pascal−sum−emp (0.575)
True PVE=0.2, theta0=−3, theta=0, sigma0=1, sigma=0.5
Method (AUROC)
Random (0.500)
RSS−NET (1.000)
RSS−E (0.988)
LDSC−baseline (0.541)
LDSC−baselineLD (0.559)
Pascal−max−chi (0.624)
Pascal−max−emp (0.745)
Pascal−sum−chi (0.546)
Pascal−sum−emp (0.610)
True PVE=0.2, theta0=−4, theta=0, sigma0=1, sigma=0.5
Method (AUROC)
Random (0.500)
RSS−NET (0.998)
RSS−E (0.981)
LDSC−baseline (0.509)
LDSC−baselineLD (0.504)
Pascal−max−chi (0.514)
Pascal−max−emp (0.619)
Pascal−sum−chi (0.516)
Pascal−sum−emp (0.591)
True PVE=0.6, theta0=−2, theta=0, sigma0=1, sigma=0.5
Method (AUROC)
Random (0.500)
RSS−NET (1.000)
RSS−E (1.000)
LDSC−baseline (0.769)
LDSC−baselineLD (0.764)
Pascal−max−chi (0.783)
Pascal−max−emp (0.886)
Pascal−sum−chi (0.644)
Pascal−sum−emp (0.726)
True PVE=0.6, theta0=−3, theta=0, sigma0=1, sigma=0.5
Method (AUROC)
Random (0.500)
RSS−NET (1.000)
RSS−E (1.000)
LDSC−baseline (0.645)
LDSC−baselineLD (0.670)
Pascal−max−chi (0.611)
Pascal−max−emp (0.736)
Pascal−sum−chi (0.567)
Pascal−sum−emp (0.715)
True PVE=0.6, theta0=−4, theta=0, sigma0=1, sigma=0.5
Method (AUROC)
Random (0.500)
RSS−NET (0.992)
RSS−E (0.923)
LDSC−baseline (0.551)
LDSC−baselineLD (0.566)
Pascal−max−chi (0.465)
Pascal−max−emp (0.561)
Pascal−sum−chi (0.508)
Pascal−sum−emp (0.555)
True PVE=0.2, theta0=−2, theta=0, sigma0=1, sigma=2
Method (AUROC)
Random (0.500)
RSS−NET (0.997)
RSS−E (0.945)
LDSC−baseline (0.565)
LDSC−baselineLD (0.557)
Pascal−max−chi (0.608)
Pascal−max−emp (0.664)
Pascal−sum−chi (0.555)
Pascal−sum−emp (0.577)
True PVE=0.2, theta0=−3, theta=0, sigma0=1, sigma=2
Method (AUROC)
Random (0.500)
RSS−NET (1.000)
RSS−E (0.985)
LDSC−baseline (0.546)
LDSC−baselineLD (0.561)
Pascal−max−chi (0.627)
Pascal−max−emp (0.751)
Pascal−sum−chi (0.546)
Pascal−sum−emp (0.615)
True PVE=0.2, theta0=−4, theta=0, sigma0=1, sigma=2
Method (AUROC)
Random (0.500)
RSS−NET (1.000)
RSS−E (0.959)
LDSC−baseline (0.513)
LDSC−baselineLD (0.508)
Pascal−max−chi (0.513)
Pascal−max−emp (0.625)
Pascal−sum−chi (0.516)
Pascal−sum−emp (0.596)
True PVE=0.6, theta0=−2, theta=0, sigma0=1, sigma=2
Method (AUROC)
Random (0.500)
RSS−NET (1.000)
RSS−E (1.000)
LDSC−baseline (0.779)
LDSC−baselineLD (0.777)
Pascal−max−chi (0.790)
Pascal−max−emp (0.890)
Pascal−sum−chi (0.649)
Pascal−sum−emp (0.734)
True PVE=0.6, theta0=−3, theta=0, sigma0=1, sigma=2
Method (AUROC)
Random (0.500)
RSS−NET (1.000)
RSS−E (0.991)
LDSC−baseline (0.658)
LDSC−baselineLD (0.679)
Pascal−max−chi (0.607)
Pascal−max−emp (0.740)
Pascal−sum−chi (0.566)
Pascal−sum−emp (0.718)
True PVE=0.6, theta0=−4, theta=0, sigma0=1, sigma=2
Method (AUROC)
Random (0.500)
RSS−NET (0.996)
RSS−E (0.938)
LDSC−baseline (0.557)
LDSC−baselineLD (0.576)
Pascal−max−chi (0.454)
Pascal−max−emp (0.562)
Pascal−sum−chi (0.506)
Pascal−sum−emp (0.559)
True positive fraction
False positive fraction
0.00
0.10
0.25
0.50
0.75
0.90
1.00

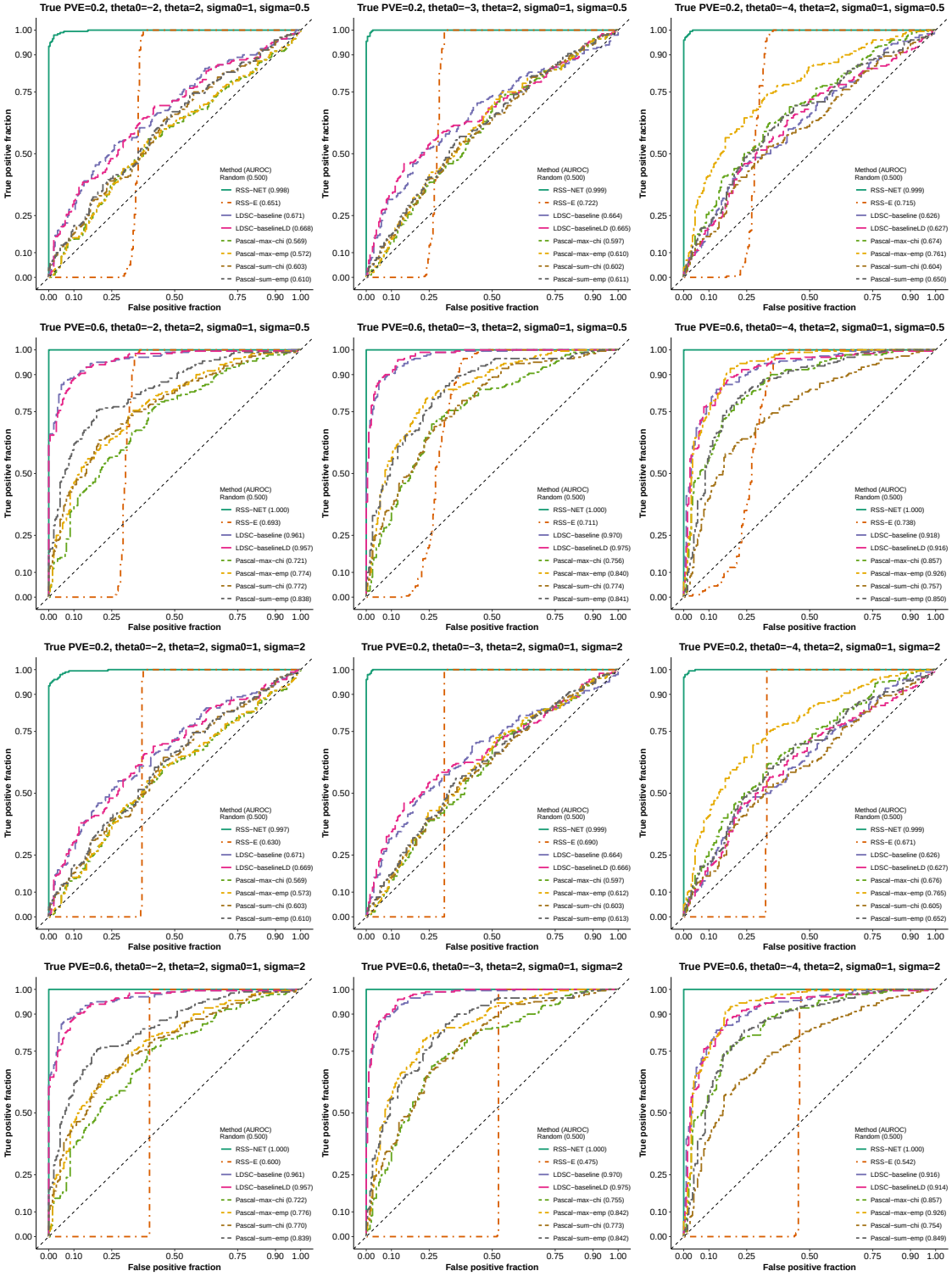
True PVE=0.2, theta0=−2, theta=2, sigma0=1, sigma=0.5
Method (AUROC)
Random (0.500)
RSS−NET (0.998)
RSS−E (0.651)
LDSC−baseline (0.671)
LDSC−baselineLD (0.668)
Pascal−max−chi (0.569)
Pascal−max−emp (0.572)
Pascal−sum−chi (0.603)
Pascal−sum−emp (0.610)
True PVE=0.2, theta0=−3, theta=2, sigma0=1, sigma=0.5
Method (AUROC)
Random (0.500)
RSS−NET (0.999)
RSS−E (0.722)
LDSC−baseline (0.664)
LDSC−baselineLD (0.665)
Pascal−max−chi (0.597)
Pascal−max−emp (0.610)
Pascal−sum−chi (0.602)
Pascal−sum−emp (0.611)
True PVE=0.2, theta0=−4, theta=2, sigma0=1, sigma=0.5
Method (AUROC)
Random (0.500)
RSS−NET (0.999)
RSS−E (0.715)
LDSC−baseline (0.626)
LDSC−baselineLD (0.627)
Pascal−max−chi (0.674)
Pascal−max−emp (0.761)
Pascal−sum−chi (0.604)
Pascal−sum−emp (0.650)
True PVE=0.6, theta0=−2, theta=2, sigma0=1, sigma=0.5
Method (AUROC)
Random (0.500)
RSS−NET (1.000)
RSS−E (0.693)
LDSC−baseline (0.961)
LDSC−baselineLD (0.957)
Pascal−max−chi (0.721)
Pascal−max−emp (0.774)
Pascal−sum−chi (0.772)
Pascal−sum−emp (0.838)
True PVE=0.6, theta0=−3, theta=2, sigma0=1, sigma=0.5
Method (AUROC)
Random (0.500)
RSS−NET (1.000)
RSS−E (0.711)
LDSC−baseline (0.970)
LDSC−baselineLD (0.975)
Pascal−max−chi (0.756)
Pascal−max−emp (0.840)
Pascal−sum−chi (0.774)
Pascal−sum−emp (0.841)
True PVE=0.6, theta0=−4, theta=2, sigma0=1, sigma=0.5
Method (AUROC)
Random (0.500)
RSS−NET (1.000)
RSS−E (0.738)
LDSC−baseline (0.918)
LDSC−baselineLD (0.916)
Pascal−max−chi (0.857)
Pascal−max−emp (0.926)
Pascal−sum−chi (0.757)
Pascal−sum−emp (0.850)
True PVE=0.2, theta0=−2, theta=2, sigma0=1, sigma=2
Method (AUROC)
Random (0.500)
RSS−NET (0.997)
RSS−E (0.630)
LDSC−baseline (0.671)
LDSC−baselineLD (0.669)
Pascal−max−chi (0.569)
Pascal−max−emp (0.573)
Pascal−sum−chi (0.603)
Pascal−sum−emp (0.610)
True PVE=0.2, theta0=−3, theta=2, sigma0=1, sigma=2
Method (AUROC)
Random (0.500)
RSS−NET (0.999)
RSS−E (0.690)
LDSC−baseline (0.664)
LDSC−baselineLD (0.666)
Pascal−max−chi (0.597)
Pascal−max−emp (0.612)
Pascal−sum−chi (0.603)
Pascal−sum−emp (0.613)
True PVE=0.2, theta0=−4, theta=2, sigma0=1, sigma=2
Method (AUROC)
Random (0.500)
RSS−NET (0.999)
RSS−E (0.671)
LDSC−baseline (0.626)
LDSC−baselineLD (0.627)
Pascal−max−chi (0.676)
Pascal−max−emp (0.765)
Pascal−sum−chi (0.605)
Pascal−sum−emp (0.652)
True PVE=0.6, theta0=−2, theta=2, sigma0=1, sigma=2
Method (AUROC)
Random (0.500)
RSS−NET (1.000)
RSS−E (0.600)
LDSC−baseline (0.961)
LDSC−baselineLD (0.957)
Pascal−max−chi (0.722)
Pascal−max−emp (0.776)
Pascal−sum−chi (0.770)
Pascal−sum−emp (0.839)
True PVE=0.6, theta0=−3, theta=2, sigma0=1, sigma=2
Method (AUROC)
Random (0.500)
RSS−NET (1.000)
RSS−E (0.475)
LDSC−baseline (0.970)
LDSC−baselineLD (0.975)
Pascal−max−chi (0.755)
Pascal−max−emp (0.842)
Pascal−sum−chi (0.773)
Pascal−sum−emp (0.842)
True PVE=0.6, theta0=−4, theta=2, sigma0=1, sigma=2
Method (AUROC)
Random (0.500)
RSS−NET (1.000)
RSS−E (0.542)
LDSC−baseline (0.916)
LDSC−baselineLD (0.914)
Pascal−max−chi (0.857)
Pascal−max−emp (0.926)
Pascal−sum−chi (0.754)
Pascal−sum−emp (0.849)
True positive fraction
False positive fraction
0.00
0.10
0.25
0.50
0.75
0.90
1.00

Supplementary Figure 2

We repeat the simulations in **Supplementary Figure 1** on a different network based on data from vagina (https://github.com/suwonglab/rss-net/tree/master/data/).

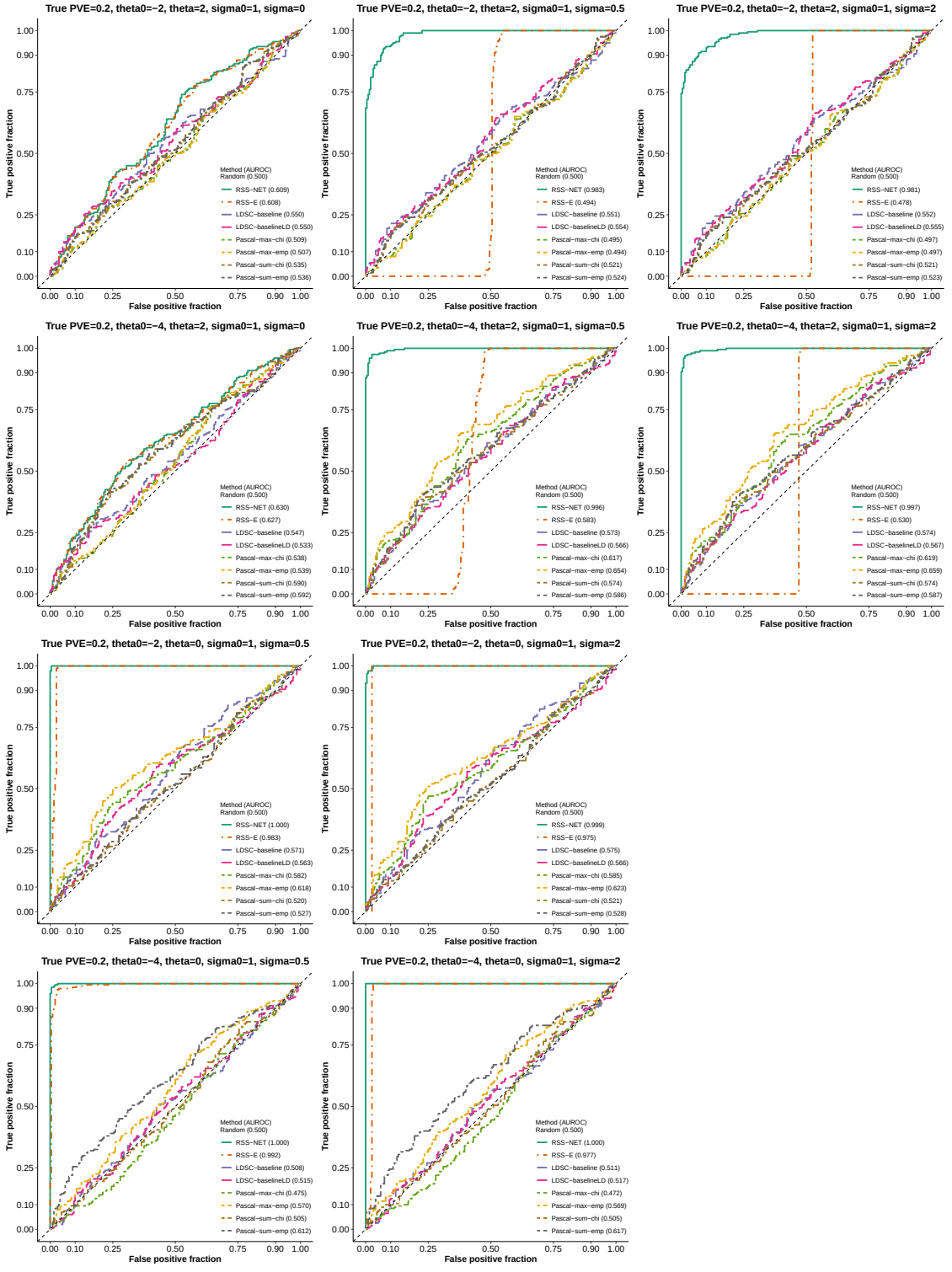

Supplementary Figure 3

Simulation details and additional results of Figure 3(a). This part aims to assess the robustness of RSS-NET to model mis-specification where a random set of "near-gene" SNPs is enriched for association in negative datasets. Details of this part are almost identical to those in **Supplementary Figure 1**. Here we only highlight the differences.

We define a SNP as "near-gene" if this SNP is within 100 kb of the transcribed region of any autosomal protein-coding gene. In total, there are 254,296 near-gene SNPs among 348,965 genome-wide SNPs from Wellcome Trust Case Control Consortium (2007).

Here we simulate negative and positive datasets in a paired way. We first simulate a positive dataset as in **Supplementary Figure 1**. For this positive dataset, we count the total number of causal SNPs as $n_c = \sum_j \zeta_j$, and count the number of causal SNPs in the target network as $n_p = \sum_j \zeta_j a_j$ (recall that $a_j = 1$ if SNP j is in the network). We then randomly choose n_p SNPs from the 254,296 near-gene SNPs and $(n_c - n_p)$ SNPs from the remaining SNPs, and use them as causal SNPs for the corresponding negative dataset. With causal indicators $\{\zeta_j\}$ in place, we simulate the true genetic effects $\boldsymbol{\beta}$ in a negative dataset as follows

$$\begin{aligned} \beta_j \mid \zeta_j = 0 &\sim \delta_0, \\ \beta_j \mid \zeta_j = 1,\ \alpha_j = 0 &\sim \mathcal{N}(0,\ \sigma_0^2), \\ \beta_j \mid \zeta_j = 1,\ \alpha_j = 1 &\sim \mathcal{N}(0,\ (2 \cdot \sigma_0)^2), \end{aligned}$$

where $\zeta_j = 1$ if SNP j is causal and 0 otherwise, $\alpha_j = 1$ if SNP j is near-gene and 0 otherwise. The rest of simulations is the same as **Supplementary Figure 1**.

The caption of each panel in this supplementary figure shows the true hyper-parameter values of positive datasets. The sparse scenario in **Figure 3(a)** corresponds to simulations with true hyper-parameter values of positive datasets being $\theta_0 = -4$, $\theta = 2$, $\sigma_0 = 1$, $\sigma = 0.5$ and PVE = 0.6. The polygenic scenario in **Figure 3(a)** corresponds to simulations with true hyper-parameter values of positive datasets being $\theta_0 = -2$, $\theta = 2$, $\sigma_0 = 1$, $\sigma = 0.5$ and PVE = 0.6.

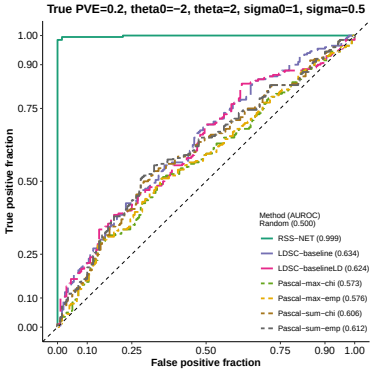
True PVE=0.2, theta0=−2, theta=2, sigma0=1, sigma=0.5
True positive fraction
False positive fraction
Method (AUROC)
Random (0.500)
RSS−NET (0.999)
LDSC−baseline (0.634)
LDSC−baselineLD (0.624)
Pascal−max−chi (0.573)
Pascal−max−emp (0.576)
Pascal−sum−chi (0.606)
Pascal−sum−emp (0.612)

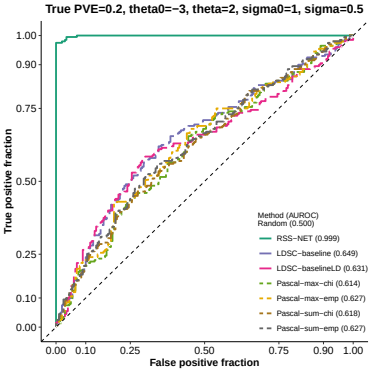
True PVE=0.2, theta0=−3, theta=2, sigma0=1, sigma=0.5
True positive fraction
False positive fraction
Method (AUROC)
Random (0.500)
RSS−NET (0.999)
LDSC−baseline (0.649)
LDSC−baselineLD (0.631)
Pascal−max−chi (0.614)
Pascal−max−emp (0.627)
Pascal−sum−chi (0.618)
Pascal−sum−emp (0.627)

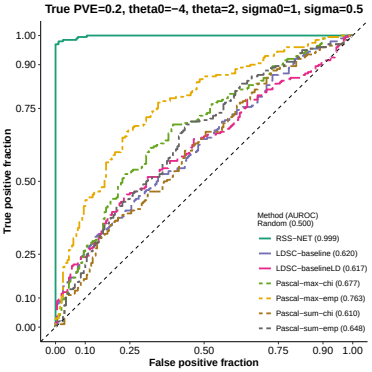
True PVE=0.2, theta0=−4, theta=2, sigma0=1, sigma=0.5
True positive fraction
False positive fraction
Method (AUROC)
Random (0.500)
RSS−NET (0.999)
LDSC−baseline (0.620)
LDSC−baselineLD (0.617)
Pascal−max−chi (0.677)
Pascal−max−emp (0.763)
Pascal−sum−chi (0.610)
Pascal−sum−emp (0.648)

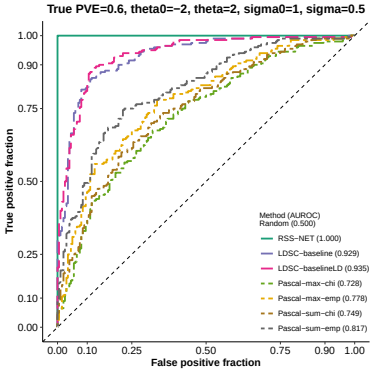
True PVE=0.6, theta0=−2, theta=2, sigma0=1, sigma=0.5
True positive fraction
False positive fraction
Method (AUROC)
Random (0.500)
RSS−NET (1.000)
LDSC−baseline (0.929)
LDSC−baselineLD (0.935)
Pascal−max−chi (0.728)
Pascal−max−emp (0.778)
Pascal−sum−chi (0.749)
Pascal−sum−emp (0.817)

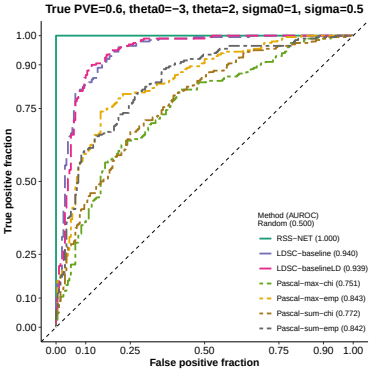
True PVE=0.6, theta0=−3, theta=2, sigma0=1, sigma=0.5
True positive fraction
False positive fraction
Method (AUROC)
Random (0.500)
RSS−NET (1.000)
LDSC−baseline (0.940)
LDSC−baselineLD (0.939)
Pascal−max−chi (0.751)
Pascal−max−emp (0.843)
Pascal−sum−chi (0.772)
Pascal−sum−emp (0.842)

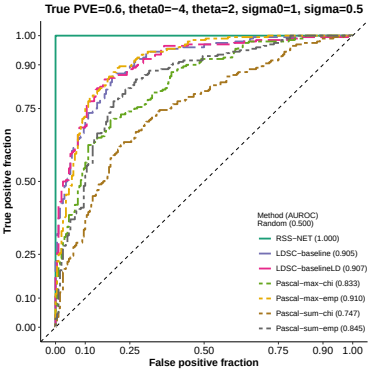
True PVE=0.6, theta0=−4, theta=2, sigma0=1, sigma=0.5
True positive fraction
False positive fraction
Method (AUROC)
Random (0.500)
RSS−NET (1.000)
LDSC−baseline (0.905)
LDSC−baselineLD (0.907)
Pascal−max−chi (0.833)
Pascal−max−emp (0.910)
Pascal−sum−chi (0.747)
Pascal−sum−emp (0.845)

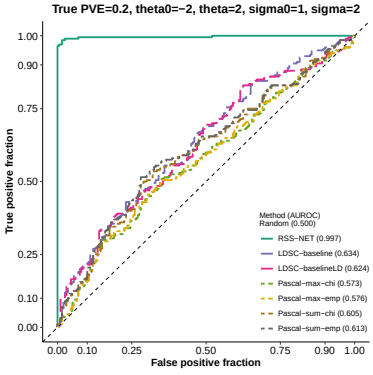
True PVE=0.2, theta0=−2, theta=2, sigma0=1, sigma=2
True positive fraction
False positive fraction
Method (AUROC)
Random (0.500)
RSS−NET (0.997)
LDSC−baseline (0.634)
LDSC−baselineLD (0.624)
Pascal−max−chi (0.573)
Pascal−max−emp (0.576)
Pascal−sum−chi (0.605)
Pascal−sum−emp (0.613)

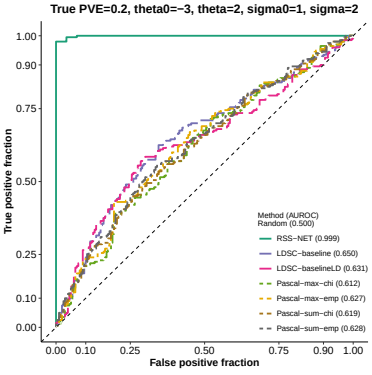
True PVE=0.2, theta0=−3, theta=2, sigma0=1, sigma=2
True positive fraction
False positive fraction
Method (AUROC)
Random (0.500)
RSS−NET (0.999)
LDSC−baseline (0.650)
LDSC−baselineLD (0.631)
Pascal−max−chi (0.612)
Pascal−max−emp (0.627)
Pascal−sum−chi (0.619)
Pascal−sum−emp (0.628)

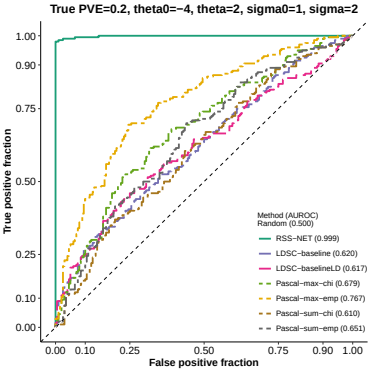
True PVE=0.2, theta0=−4, theta=2, sigma0=1, sigma=2
True positive fraction
False positive fraction
Method (AUROC)
Random (0.500)
RSS−NET (0.999)
LDSC−baseline (0.620)
LDSC−baselineLD (0.617)
Pascal−max−chi (0.679)
Pascal−max−emp (0.767)
Pascal−sum−chi (0.610)
Pascal−sum−emp (0.651)

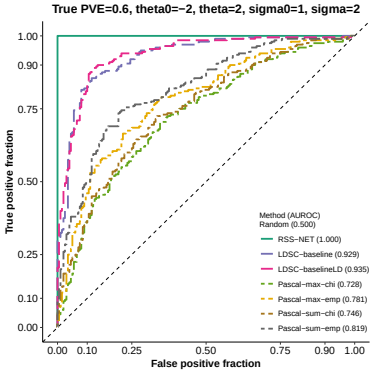
True PVE=0.6, theta0=−2, theta=2, sigma0=1, sigma=2
True positive fraction
False positive fraction
Method (AUROC)
Random (0.500)
RSS−NET (1.000)
LDSC−baseline (0.929)
LDSC−baselineLD (0.935)
Pascal−max−chi (0.728)
Pascal−max−emp (0.781)
Pascal−sum−chi (0.746)
Pascal−sum−emp (0.819)

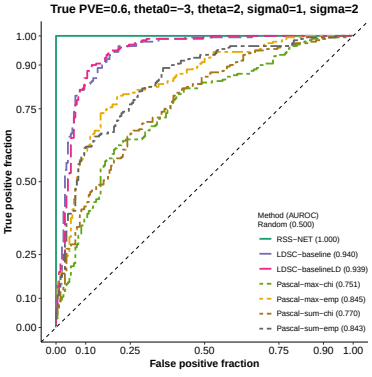
True PVE=0.6, theta0=−3, theta=2, sigma0=1, sigma=2
True positive fraction
False positive fraction
Method (AUROC)
Random (0.500)
RSS−NET (1.000)
LDSC−baseline (0.940)
LDSC−baselineLD (0.939)
Pascal−max−chi (0.751)
Pascal−max−emp (0.845)
Pascal−sum−chi (0.770)
Pascal−sum−emp (0.843)

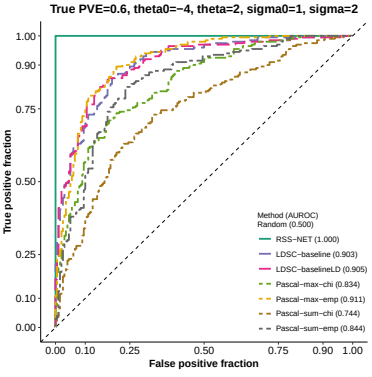
True PVE=0.6, theta0=−4, theta=2, sigma0=1, sigma=2
True positive fraction
False positive fraction
Method (AUROC)
Random (0.500)
RSS−NET (1.000)
LDSC−baseline (0.903)
LDSC−baselineLD (0.905)
Pascal−max−chi (0.834)
Pascal−max−emp (0.911)
Pascal−sum−chi (0.744)
Pascal−sum−emp (0.844)

Supplementary Figure 4

Simulation details and additional results of Figure 3(b). This part aims to assess the robustness of RSS-NET to model mis-specification where a random set of "near-RE" SNPs is enriched for association in negative datasets. Details of this part are almost identical to those in **Supplementary Figure 1**. Here we only highlight the differences.

We define a SNP as "near-RE" if this SNP is within 10 kb of any RE. There are 3,895,021 unique autosomal REs associated with 38 regulatory networks analyzed in this study. In total, there are 169,100 near-RE SNPs among 348,965 genome-wide SNPs from Wellcome Trust Case Control Consortium (2007).

Here we simulate negative and positive datasets in a paired way. We first simulate a positive dataset as in **Supplementary Figure 1**. For this positive dataset, we count the total number of causal SNPs as $n_c = \sum_j \zeta_j$, and count the number of causal SNPs in the target network as $n_p = \sum_j \zeta_j a_j$ (recall that $a_j = 1$ if SNP j is in the network). We then randomly choose n_p SNPs from the 169,100 near-RE SNPs and $(n_c - n_p)$ SNPs from the remaining SNPs, and use them as causal SNPs for the corresponding negative dataset. With causal indicators $\{\zeta_j\}$ in place, we simulate the true genetic effects $\boldsymbol{\beta}$ in a negative dataset as follows

$$\begin{aligned} \beta_j \mid \zeta_j = 0 &\sim \delta_0, \\ \beta_j \mid \zeta_j = 1,\ \alpha_j = 0 &\sim \mathcal{N}(0,\ \sigma_0^2), \\ \beta_j \mid \zeta_j = 1,\ \alpha_j = 1 &\sim \mathcal{N}(0,\ (2 \cdot \sigma_0)^2), \end{aligned}$$

where $\zeta_j = 1$ if SNP j is causal and 0 otherwise, $\alpha_j = 1$ if SNP j is near-RE and 0 otherwise. The rest of simulations is the same as **Supplementary Figure 1**

The caption of each panel in this supplementary figure shows the true hyper-parameter values of positive datasets. The sparse scenario in **Figure 3(b)** corresponds to simulations with true hyper-parameter values of positive datasets being $\theta_0 = -4$, $\theta = 2$, $\sigma_0 = 1$, $\sigma = 0.5$ and PVE = 0.6. The polygenic scenario in **Figure 3(b)** corresponds to simulations with true hyper-parameter values of positive datasets being $\theta_0 = -2$, $\theta = 2$, $\sigma_0 = 1$, $\sigma = 0.5$ and PVE = 0.6.

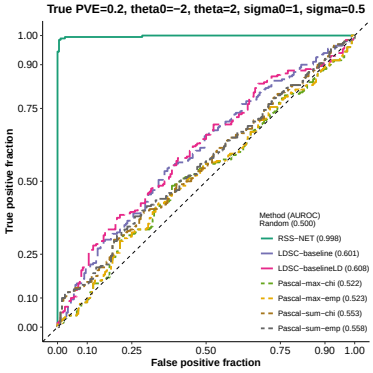
True PVE=0.2, theta0=−2, theta=2, sigma0=1, sigma=0.5
True positive fraction
False positive fraction
Method (AUROC)
Random (0.500)
RSS−NET (0.998)
LDSC−baseline (0.601)
LDSC−baselineLD (0.608)
Pascal−max−chi (0.522)
Pascal−max−emp (0.523)
Pascal−sum−chi (0.553)
Pascal−sum−emp (0.558)

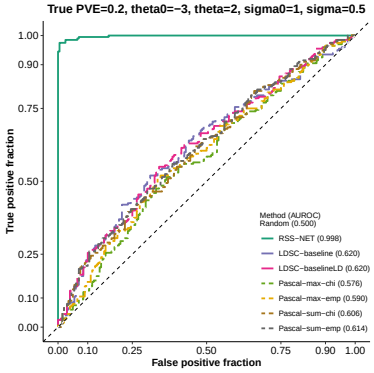
True PVE=0.2, theta0=−3, theta=2, sigma0=1, sigma=0.5
True positive fraction
False positive fraction
Method (AUROC)
Random (0.500)
RSS−NET (0.998)
LDSC−baseline (0.620)
LDSC−baselineLD (0.620)
Pascal−max−chi (0.576)
Pascal−max−emp (0.590)
Pascal−sum−chi (0.606)
Pascal−sum−emp (0.614)

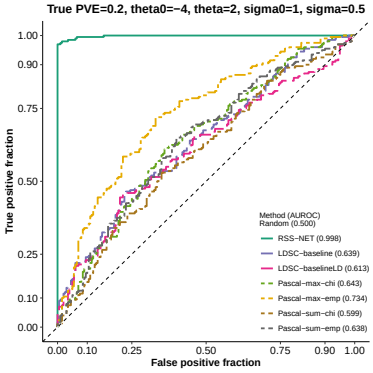
True PVE=0.2, theta0=−4, theta=2, sigma0=1, sigma=0.5
True positive fraction
False positive fraction
Method (AUROC)
Random (0.500)
RSS−NET (0.998)
LDSC−baseline (0.639)
LDSC−baselineLD (0.613)
Pascal−max−chi (0.643)
Pascal−max−emp (0.734)
Pascal−sum−chi (0.599)
Pascal−sum−emp (0.638)

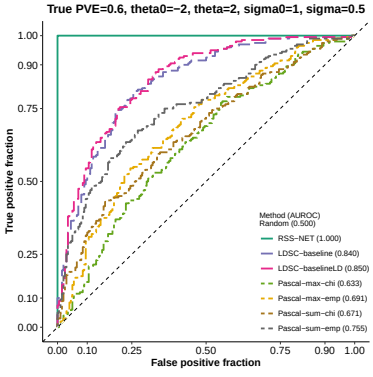
True PVE=0.6, theta0=−2, theta=2, sigma0=1, sigma=0.5
True positive fraction
False positive fraction
Method (AUROC)
Random (0.500)
RSS−NET (1.000)
LDSC−baseline (0.840)
LDSC−baselineLD (0.850)
Pascal−max−chi (0.633)
Pascal−max−emp (0.691)
Pascal−sum−chi (0.671)
Pascal−sum−emp (0.755)

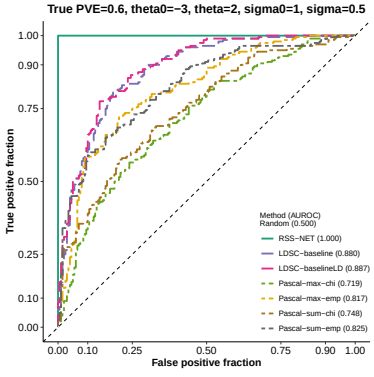
True PVE=0.6, theta0=−3, theta=2, sigma0=1, sigma=0.5
True positive fraction
False positive fraction
Method (AUROC)
Random (0.500)
RSS−NET (1.000)
LDSC−baseline (0.880)
LDSC−baselineLD (0.887)
Pascal−max−chi (0.719)
Pascal−max−emp (0.817)
Pascal−sum−chi (0.748)
Pascal−sum−emp (0.825)

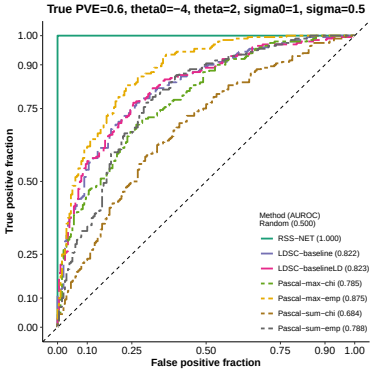
True PVE=0.6, theta0=−4, theta=2, sigma0=1, sigma=0.5
True positive fraction
False positive fraction
Method (AUROC)
Random (0.500)
RSS−NET (1.000)
LDSC−baseline (0.822)
LDSC−baselineLD (0.823)
Pascal−max−chi (0.785)
Pascal−max−emp (0.875)
Pascal−sum−chi (0.684)
Pascal−sum−emp (0.788)

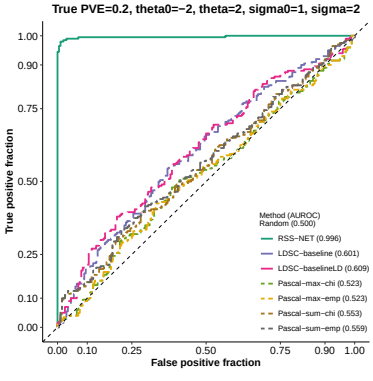
True PVE=0.2, theta0=−2, theta=2, sigma0=1, sigma=2
True positive fraction
False positive fraction
Method (AUROC)
Random (0.500)
RSS−NET (0.996)
LDSC−baseline (0.601)
LDSC−baselineLD (0.609)
Pascal−max−chi (0.523)
Pascal−max−emp (0.523)
Pascal−sum−chi (0.553)
Pascal−sum−emp (0.559)

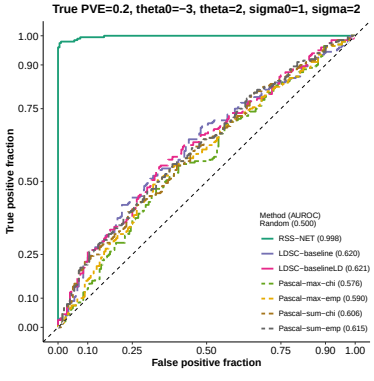
True PVE=0.2, theta0=−3, theta=2, sigma0=1, sigma=2
True positive fraction
False positive fraction
Method (AUROC)
Random (0.500)
RSS−NET (0.998)
LDSC−baseline (0.620)
LDSC−baselineLD (0.621)
Pascal−max−chi (0.576)
Pascal−max−emp (0.590)
Pascal−sum−chi (0.606)
Pascal−sum−emp (0.615)

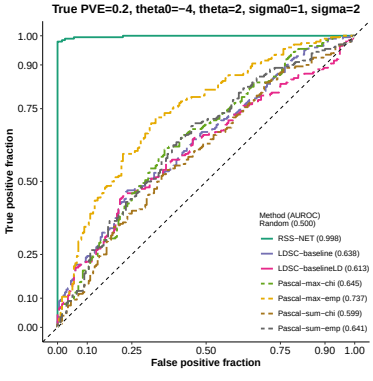
True PVE=0.2, theta0=−4, theta=2, sigma0=1, sigma=2
True positive fraction
False positive fraction
Method (AUROC)
Random (0.500)
RSS−NET (0.998)
LDSC−baseline (0.638)
LDSC−baselineLD (0.613)
Pascal−max−chi (0.645)
Pascal−max−emp (0.737)
Pascal−sum−chi (0.599)
Pascal−sum−emp (0.641)

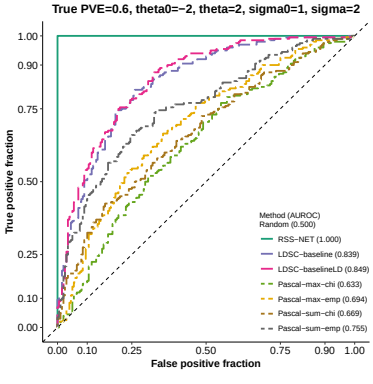
True PVE=0.6, theta0=−2, theta=2, sigma0=1, sigma=2
True positive fraction
False positive fraction
Method (AUROC)
Random (0.500)
RSS−NET (1.000)
LDSC−baseline (0.839)
LDSC−baselineLD (0.849)
Pascal−max−chi (0.633)
Pascal−max−emp (0.694)
Pascal−sum−chi (0.669)
Pascal−sum−emp (0.755)

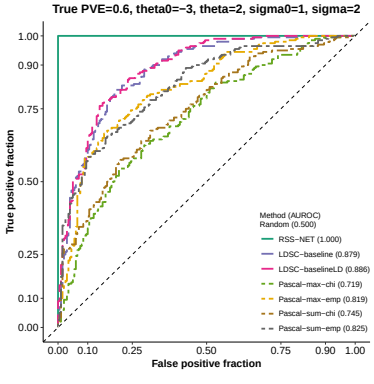
True PVE=0.6, theta0=−3, theta=2, sigma0=1, sigma=2
True positive fraction
False positive fraction
Method (AUROC)
Random (0.500)
RSS−NET (1.000)
LDSC−baseline (0.879)
LDSC−baselineLD (0.886)
Pascal−max−chi (0.719)
Pascal−max−emp (0.819)
Pascal−sum−chi (0.745)
Pascal−sum−emp (0.825)

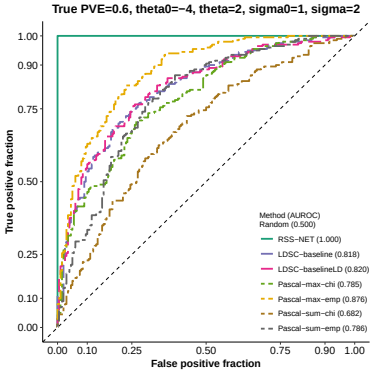
True PVE=0.6, theta0=−4, theta=2, sigma0=1, sigma=2
True positive fraction
False positive fraction
Method (AUROC)
Random (0.500)
RSS−NET (1.000)
LDSC−baseline (0.818)
LDSC−baselineLD (0.820)
Pascal−max−chi (0.785)
Pascal−max−emp (0.876)
Pascal−sum−chi (0.682)
Pascal−sum−emp (0.786)

Supplementary Figure 5

Simulation details and additional results of Figure 3(c). This part aims to assess the robustness of RSS-NET to model mis-specification where true genetic effects are MAF- and LD-dependent in negative datasets. Details of this part are almost identical to those in **Supplementary Figure 1**. Here we only highlight the differences.

Here we simulate negative and positive datasets in a paired way. We first simulate a positive dataset as in **Supplementary Figure 1**. For this positive dataset, we count the total number of causal SNPs as $n_c = \sum_j \zeta_j$. We then randomly choose n_c genome-wide SNPs as causal SNPs for the corresponding negative dataset. With causal indicators $\{\zeta_j\}$ in place, we simulate the true genetic effects $\boldsymbol{\beta}$ in a negative dataset as follows

$$\begin{aligned} \beta_j \mid \zeta_j = 0 &\sim \delta_0, \\ \beta_j \mid \zeta_j = 1 &\sim \mathcal{N}(0,\, \sigma_0^2 + \textstyle\sum_{k=1}^{16} a_{jk} \cdot \tau_k), \\ \tau_k &\sim \mathcal{N}(\hat{\mu}_k,\, \hat{\sigma}_k^2), \end{aligned}$$

where $\zeta_j = 1$ if SNP j is causal and 0 otherwise, a_{jk} is the value of annotation k at SNP j, the 16 annotations include 10 MAF bins and 6 LD-related annotations defined in Gazal et al. (2017), $\{\hat{\mu}_k, \hat{\sigma}_k\}$ are meta-analyzed mean and standard error estimates for τ_k across 31 independent human traits, which are provided in the Supplementary Table 9 of Gazal et al. (2017). The rest of simulations is the same as **Supplementary Figure 1**

The caption of each panel in this supplementary figure shows the true hyper-parameter values of positive datasets. The sparse scenario in **Figure 3(c)** corresponds to simulations with true hyper-parameter values of positive datasets being $\theta_0 = -4$, $\theta = 2$, $\sigma_0 = 1$, $\sigma = 0.5$ and PVE = 0.6. The polygenic scenario in **Figure 3(c)** corresponds to simulations with true hyper-parameter values of positive datasets being $\theta_0 = -2$, $\theta = 2$, $\sigma_0 = 1$, $\sigma = 0.5$ and PVE = 0.6.

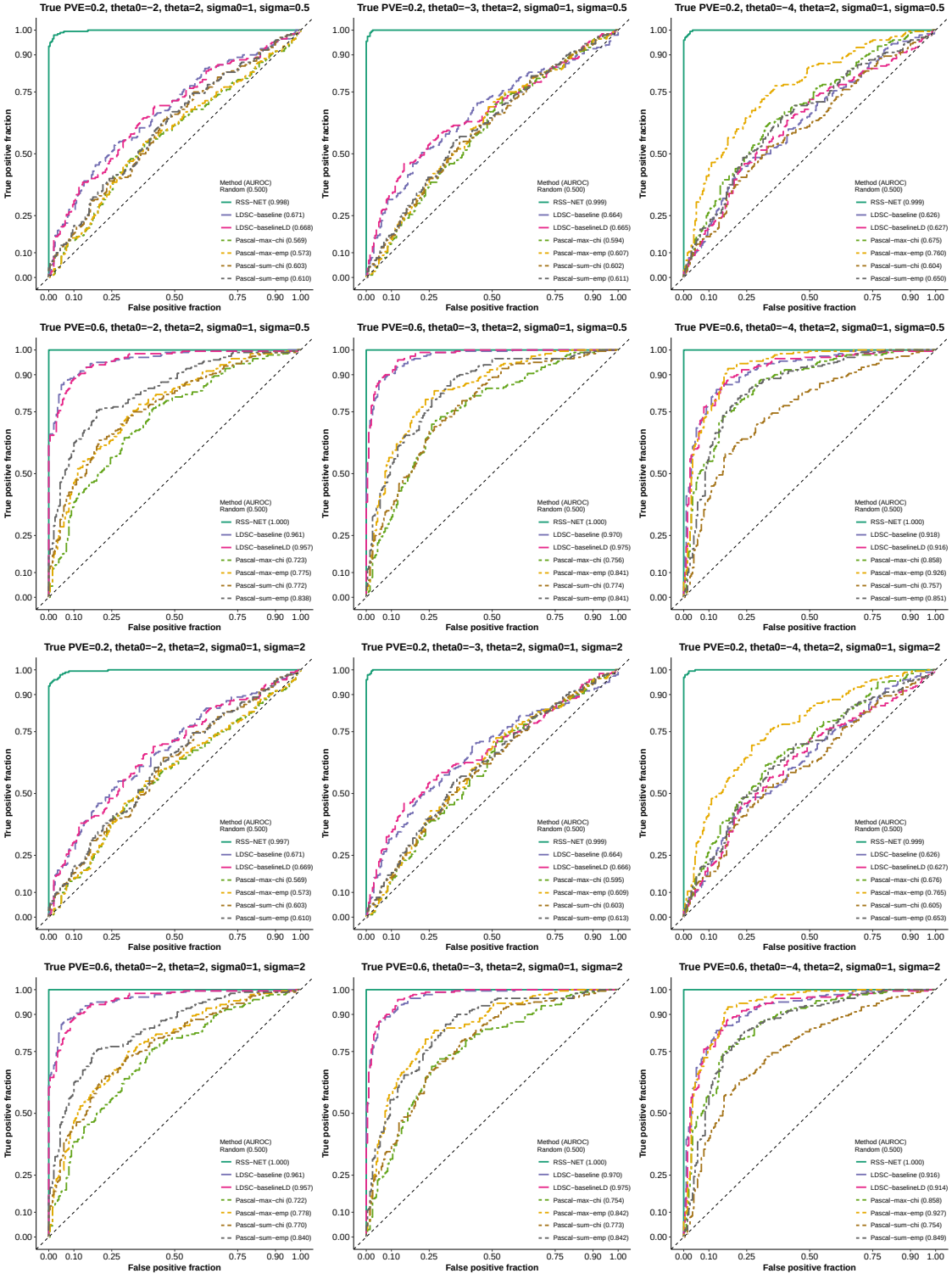
True PVE=0.2, theta0=−2, theta=2, sigma0=1, sigma=0.5
Method (AUROC)
Random (0.500)
RSS−NET (0.998)
LDSC−baseline (0.671)
LDSC−baselineLD (0.668)
Pascal−max−chi (0.569)
Pascal−max−emp (0.573)
Pascal−sum−chi (0.603)
Pascal−sum−emp (0.610)
True PVE=0.2, theta0=−3, theta=2, sigma0=1, sigma=0.5
Method (AUROC)
Random (0.500)
RSS−NET (0.999)
LDSC−baseline (0.664)
LDSC−baselineLD (0.665)
Pascal−max−chi (0.594)
Pascal−max−emp (0.607)
Pascal−sum−chi (0.602)
Pascal−sum−emp (0.611)
True PVE=0.2, theta0=−4, theta=2, sigma0=1, sigma=0.5
Method (AUROC)
Random (0.500)
RSS−NET (0.999)
LDSC−baseline (0.626)
LDSC−baselineLD (0.627)
Pascal−max−chi (0.675)
Pascal−max−emp (0.760)
Pascal−sum−chi (0.604)
Pascal−sum−emp (0.650)
True PVE=0.6, theta0=−2, theta=2, sigma0=1, sigma=0.5
Method (AUROC)
Random (0.500)
RSS−NET (1.000)
LDSC−baseline (0.961)
LDSC−baselineLD (0.957)
Pascal−max−chi (0.723)
Pascal−max−emp (0.775)
Pascal−sum−chi (0.772)
Pascal−sum−emp (0.838)
True PVE=0.6, theta0=−3, theta=2, sigma0=1, sigma=0.5
Method (AUROC)
Random (0.500)
RSS−NET (1.000)
LDSC−baseline (0.970)
LDSC−baselineLD (0.975)
Pascal−max−chi (0.756)
Pascal−max−emp (0.841)
Pascal−sum−chi (0.774)
Pascal−sum−emp (0.841)
True PVE=0.6, theta0=−4, theta=2, sigma0=1, sigma=0.5
Method (AUROC)
Random (0.500)
RSS−NET (1.000)
LDSC−baseline (0.918)
LDSC−baselineLD (0.916)
Pascal−max−chi (0.858)
Pascal−max−emp (0.926)
Pascal−sum−chi (0.757)
Pascal−sum−emp (0.851)
True PVE=0.2, theta0=−2, theta=2, sigma0=1, sigma=2
Method (AUROC)
Random (0.500)
RSS−NET (0.997)
LDSC−baseline (0.671)
LDSC−baselineLD (0.669)
Pascal−max−chi (0.569)
Pascal−max−emp (0.573)
Pascal−sum−chi (0.603)
Pascal−sum−emp (0.610)
True PVE=0.2, theta0=−3, theta=2, sigma0=1, sigma=2
Method (AUROC)
Random (0.500)
RSS−NET (0.999)
LDSC−baseline (0.664)
LDSC−baselineLD (0.666)
Pascal−max−chi (0.595)
Pascal−max−emp (0.609)
Pascal−sum−chi (0.603)
Pascal−sum−emp (0.613)
True PVE=0.2, theta0=−4, theta=2, sigma0=1, sigma=2
Method (AUROC)
Random (0.500)
RSS−NET (0.999)
LDSC−baseline (0.626)
LDSC−baselineLD (0.627)
Pascal−max−chi (0.676)
Pascal−max−emp (0.765)
Pascal−sum−chi (0.605)
Pascal−sum−emp (0.653)
True PVE=0.6, theta0=−2, theta=2, sigma0=1, sigma=2
Method (AUROC)
Random (0.500)
RSS−NET (1.000)
LDSC−baseline (0.961)
LDSC−baselineLD (0.957)
Pascal−max−chi (0.722)
Pascal−max−emp (0.778)
Pascal−sum−chi (0.770)
Pascal−sum−emp (0.840)
True PVE=0.6, theta0=−3, theta=2, sigma0=1, sigma=2
Method (AUROC)
Random (0.500)
RSS−NET (1.000)
LDSC−baseline (0.970)
LDSC−baselineLD (0.975)
Pascal−max−chi (0.754)
Pascal−max−emp (0.842)
Pascal−sum−chi (0.773)
Pascal−sum−emp (0.842)
True PVE=0.6, theta0=−4, theta=2, sigma0=1, sigma=2
Method (AUROC)
Random (0.500)
RSS−NET (1.000)
LDSC−baseline (0.916)
LDSC−baselineLD (0.914)
Pascal−max−chi (0.858)
Pascal−max−emp (0.927)
Pascal−sum−chi (0.754)
Pascal−sum−emp (0.849)
True positive fraction
False positive fraction
0.00
0.10
0.25
0.50
0.75
0.90
1.00

Supplementary Figure 6

Simulation details and additional results of Figure 3(d). This part aims to assess the robustness of RSS-NET to model mis-specification where an edge-altered version of the true network is enriched for genetic association in negative datasets. Details of this part are almost identical to those in **Supplementary Figure 1**. Here we only highlight the differences.

We simulate random edge-altered networks on the basis of the B cell regulatory network defined in **Supplementary Figure 1**. Specifically, we keep all associated REs and member genes of the B cell network, remove the actual connections between TFs and TGs, and then create fake edges by randomly connecting TFs to TGs with random edge weights. We ensure that the edge-altered network has the same number of edges as the actual B cell network, and their edge weights have the same distribution. For each negative dataset, we simulate a new edge-altered network.

We first simulate positive datasets as in **Supplementary Figure 1**. Since the true and edge-altered networks have the same associated REs and member genes, we let a negative dataset and its corresponding positive dataset have the same causal indicators $\{\zeta_j\}$. We then simulate true genetic effects $\boldsymbol{\beta}$ in a negative dataset as:

$$\begin{aligned} \beta_j \mid \zeta_j = 0 &\sim \delta_0, \\ \beta_j \mid \zeta_j = 1 &\sim \mathcal{N}(0,\ \sigma_0^2 + \sigma^2 \cdot \textstyle\sum_{g \in \mathbf{O}_j^\dagger} (w_{jg}^\dagger)^2), \end{aligned}$$

where $\{\mathbf{O}_j^\dagger, w_{jg}^\dagger\}$ are annotations of the random edge-altered network. For all datasets the target of enrichment testing is the actual B cell network.

The caption of each panel in this supplementary figure shows the true hyper-parameter values of positive datasets. The sparse scenario in **Figure 3(d)** corresponds to simulations with true hyper-parameter values of positive datasets being $\theta_0 = -4$, $\theta = 2$, $\sigma_0 = 1$, $\sigma = 0.5$ and PVE = 0.6. The polygenic scenario in **Figure 3(d)** corresponds to simulations with true hyper-parameter values of positive datasets being $\theta_0 = -2$, $\theta = 2$, $\sigma_0 = 1$, $\sigma = 0.5$ and PVE = 0.6.

The true and random edge-altered networks have the same associated REs and member genes but totally different topology (TF-TG edges and edge weights). Existing methods like LDSC and Pascal only exploits proximity between SNPs and network genes and/or REs, and thus they cannot distinguish the true and random edge-altered networks. In contrast, because of the edge-enrichment parameter σ^2, RSS-NET is able to capture the topological differences among networks, and thus it can reliably distinguish true enrichments of the B cell network from enrichments of its edge-altered counterparts.

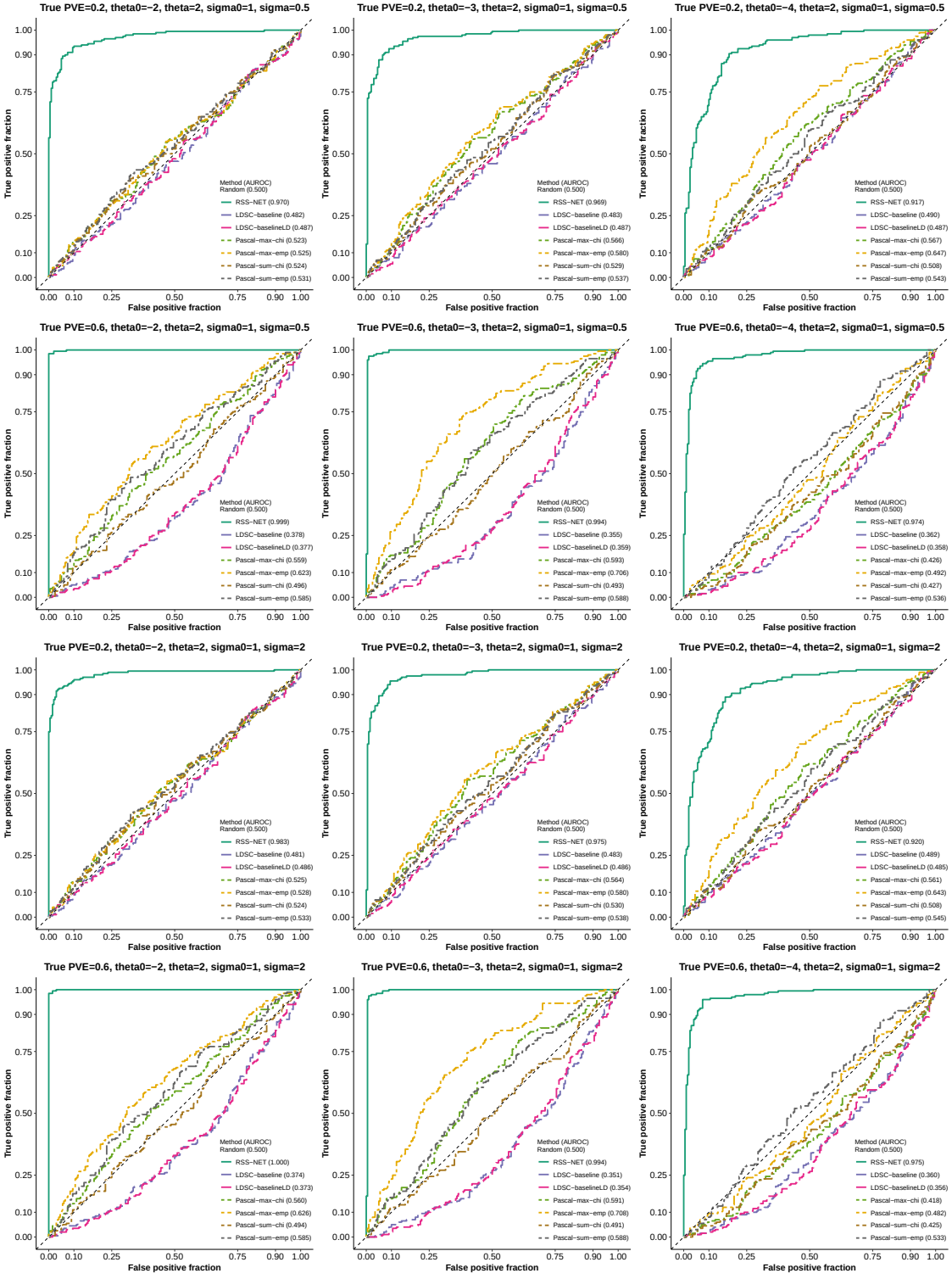
True PVE=0.2, theta0=−2, theta=2, sigma0=1, sigma=0.5
Method (AUROC)
Random (0.500)
RSS−NET (0.970)
LDSC−baseline (0.482)
LDSC−baselineLD (0.487)
Pascal−max−chi (0.523)
Pascal−max−emp (0.525)
Pascal−sum−chi (0.524)
Pascal−sum−emp (0.531)
True PVE=0.2, theta0=−3, theta=2, sigma0=1, sigma=0.5
Method (AUROC)
Random (0.500)
RSS−NET (0.969)
LDSC−baseline (0.483)
LDSC−baselineLD (0.487)
Pascal−max−chi (0.566)
Pascal−max−emp (0.580)
Pascal−sum−chi (0.529)
Pascal−sum−emp (0.537)
True PVE=0.2, theta0=−4, theta=2, sigma0=1, sigma=0.5
Method (AUROC)
Random (0.500)
RSS−NET (0.917)
LDSC−baseline (0.490)
LDSC−baselineLD (0.487)
Pascal−max−chi (0.567)
Pascal−max−emp (0.647)
Pascal−sum−chi (0.508)
Pascal−sum−emp (0.543)
True PVE=0.6, theta0=−2, theta=2, sigma0=1, sigma=0.5
Method (AUROC)
Random (0.500)
RSS−NET (0.999)
LDSC−baseline (0.378)
LDSC−baselineLD (0.377)
Pascal−max−chi (0.559)
Pascal−max−emp (0.623)
Pascal−sum−chi (0.496)
Pascal−sum−emp (0.585)
True PVE=0.6, theta0=−3, theta=2, sigma0=1, sigma=0.5
Method (AUROC)
Random (0.500)
RSS−NET (0.994)
LDSC−baseline (0.355)
LDSC−baselineLD (0.359)
Pascal−max−chi (0.593)
Pascal−max−emp (0.706)
Pascal−sum−chi (0.493)
Pascal−sum−emp (0.588)
True PVE=0.6, theta0=−4, theta=2, sigma0=1, sigma=0.5
Method (AUROC)
Random (0.500)
RSS−NET (0.974)
LDSC−baseline (0.362)
LDSC−baselineLD (0.358)
Pascal−max−chi (0.426)
Pascal−max−emp (0.492)
Pascal−sum−chi (0.427)
Pascal−sum−emp (0.536)
True PVE=0.2, theta0=−2, theta=2, sigma0=1, sigma=2
Method (AUROC)
Random (0.500)
RSS−NET (0.983)
LDSC−baseline (0.481)
LDSC−baselineLD (0.486)
Pascal−max−chi (0.525)
Pascal−max−emp (0.528)
Pascal−sum−chi (0.524)
Pascal−sum−emp (0.533)
True PVE=0.2, theta0=−3, theta=2, sigma0=1, sigma=2
Method (AUROC)
Random (0.500)
RSS−NET (0.975)
LDSC−baseline (0.483)
LDSC−baselineLD (0.486)
Pascal−max−chi (0.564)
Pascal−max−emp (0.580)
Pascal−sum−chi (0.530)
Pascal−sum−emp (0.538)
True PVE=0.2, theta0=−4, theta=2, sigma0=1, sigma=2
Method (AUROC)
Random (0.500)
RSS−NET (0.920)
LDSC−baseline (0.489)
LDSC−baselineLD (0.485)
Pascal−max−chi (0.561)
Pascal−max−emp (0.643)
Pascal−sum−chi (0.508)
Pascal−sum−emp (0.545)
True PVE=0.6, theta0=−2, theta=2, sigma0=1, sigma=2
Method (AUROC)
Random (0.500)
RSS−NET (1.000)
LDSC−baseline (0.374)
LDSC−baselineLD (0.373)
Pascal−max−chi (0.560)
Pascal−max−emp (0.626)
Pascal−sum−chi (0.494)
Pascal−sum−emp (0.585)
True PVE=0.6, theta0=−3, theta=2, sigma0=1, sigma=2
Method (AUROC)
Random (0.500)
RSS−NET (0.994)
LDSC−baseline (0.351)
LDSC−baselineLD (0.354)
Pascal−max−chi (0.591)
Pascal−max−emp (0.708)
Pascal−sum−chi (0.491)
Pascal−sum−emp (0.588)
True PVE=0.6, theta0=−4, theta=2, sigma0=1, sigma=2
Method (AUROC)
Random (0.500)
RSS−NET (0.975)
LDSC−baseline (0.360)
LDSC−baselineLD (0.356)
Pascal−max−chi (0.418)
Pascal−max−emp (0.482)
Pascal−sum−chi (0.425)
Pascal−sum−emp (0.533)
True positive fraction
False positive fraction
0.00
0.10
0.25
0.50
0.75
0.90
1.00

Supplementary Figure 7

Simulation details and additional results of Figure 4. Here we compare RSS-NET with existing gene-level association testing methods on the same simulated summary data used in **Supplementary Figure 1**. Details of this part are almost identical to those in **Supplementary Figure 1**. Here we only highlight the differences.

For each simulated dataset, we define a gene as "trait-associated" if at lease one SNP j within 100 kb of the transcribed region of this gene has non-zero effect ($\beta_j \neq 0$). For each gene in each simulated dataset, RSS-NET and RSS-E methods (Zhu and Stephens 2018) produce P_1, the posterior probability that the gene is trait-associated, whereas Pascal methods (Lamparter et al. 2016) produce P-value for the null hypothesis that the gene is not trait-associated; these statistics are used to rank the significance of gene-level associations. If a method identifies association between a non-trait-associated gene and the trait, then it is a "false positive". If a method identifies association between a trait-associated gene and the trait, then it is a "true positive".

Here the true values of baseline proportion parameter θ_0 are $\{-2,-3,-4\}$, the true values of enrichment proportion parameter θ are $\{0,2\}$, the true value of baseline magnitude parameter σ_0 is 1, the true values of enrichment magnitude parameter σ are $\{0,0.5,2\}$, and the true values of PVE are $\{0.2,0.6\}$. In total there are 36 ($= 3 \times 2 \times 3 \times 2$) simulation scenarios. Each scenario contains 200 independent datasets. For all datasets we test associations of 16,954 autosomal protein-coding genes that are available in Pascal-required database.

The caption of each panel in this supplementary figure shows the true hyper-parameter values of simulated datasets. All panels of **Figure 4** correspond to simulations with true $\theta_0 = -4$, $\sigma_0 = 1$ and PVE = 0.6. **Figure 4(a)** corresponds to simulations with true $\theta = 0$ and $\sigma = 0$. **Figure 4(b)** corresponds to simulations with true $\theta = 2$ and $\sigma = 0$. **Figure 4(c)** corresponds to simulations with true $\theta = 0$ and $\sigma = 2$. **Figure 4(d)** corresponds to simulations with true $\theta = 2$ and $\sigma = 2$.

We evaluate the performance of these gene-level association methods by plotting the receiver operating characteristic (ROC) curve and computing the area under the ROC curve (AUROC) for each method. Both metrics are implemented in the R package `plotROC` (Sachs 2017). Unlike the balanced enrichment simulations (200 positive and 200 negative datasets in each scenario), the numbers of trait-associated genes (true labels) and non-trait-associated genes (false labels) are often very different. Due to this imbalance nature, we also plot the precision-recall (PRC) curve and compute the area under the PRC curve (AUPRC) for each method. Both metrics are implemented in the R package `precrec` (Saito and Rehmsmeier 2017).

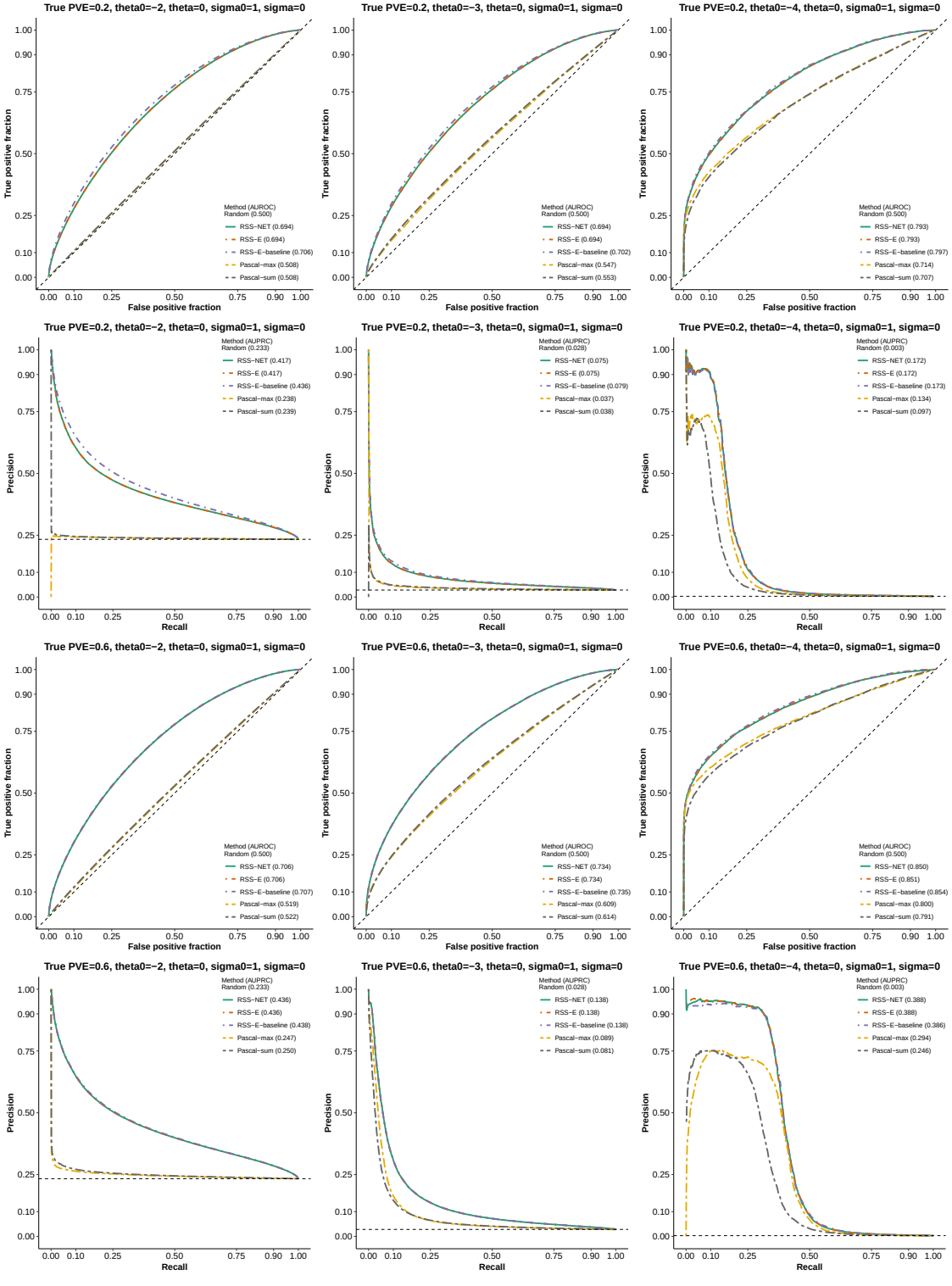
True PVE=0.2, theta0=−2, theta=0, sigma0=1, sigma=0
True positive fraction
False positive fraction
Method (AUROC)
Random (0.500)
RSS−NET (0.694)
RSS−E (0.694)
RSS−E−baseline (0.706)
Pascal−max (0.508)
Pascal−sum (0.508)
True PVE=0.2, theta0=−3, theta=0, sigma0=1, sigma=0
True positive fraction
False positive fraction
Method (AUROC)
Random (0.500)
RSS−NET (0.694)
RSS−E (0.694)
RSS−E−baseline (0.702)
Pascal−max (0.547)
Pascal−sum (0.553)
True PVE=0.2, theta0=−4, theta=0, sigma0=1, sigma=0
True positive fraction
False positive fraction
Method (AUROC)
Random (0.500)
RSS−NET (0.793)
RSS−E (0.793)
RSS−E−baseline (0.797)
Pascal−max (0.714)
Pascal−sum (0.707)
True PVE=0.2, theta0=−2, theta=0, sigma0=1, sigma=0
Precision
Recall
Method (AUPRC)
Random (0.233)
RSS−NET (0.417)
RSS−E (0.417)
RSS−E−baseline (0.436)
Pascal−max (0.238)
Pascal−sum (0.239)
True PVE=0.2, theta0=−3, theta=0, sigma0=1, sigma=0
Precision
Recall
Method (AUPRC)
Random (0.028)
RSS−NET (0.075)
RSS−E (0.075)
RSS−E−baseline (0.079)
Pascal−max (0.037)
Pascal−sum (0.038)
True PVE=0.2, theta0=−4, theta=0, sigma0=1, sigma=0
Precision
Recall
Method (AUPRC)
Random (0.003)
RSS−NET (0.172)
RSS−E (0.172)
RSS−E−baseline (0.173)
Pascal−max (0.134)
Pascal−sum (0.097)
True PVE=0.6, theta0=−2, theta=0, sigma0=1, sigma=0
True positive fraction
False positive fraction
Method (AUROC)
Random (0.500)
RSS−NET (0.706)
RSS−E (0.706)
RSS−E−baseline (0.707)
Pascal−max (0.519)
Pascal−sum (0.522)
True PVE=0.6, theta0=−3, theta=0, sigma0=1, sigma=0
True positive fraction
False positive fraction
Method (AUROC)
Random (0.500)
RSS−NET (0.734)
RSS−E (0.734)
RSS−E−baseline (0.735)
Pascal−max (0.609)
Pascal−sum (0.614)
True PVE=0.6, theta0=−4, theta=0, sigma0=1, sigma=0
True positive fraction
False positive fraction
Method (AUROC)
Random (0.500)
RSS−NET (0.850)
RSS−E (0.851)
RSS−E−baseline (0.854)
Pascal−max (0.800)
Pascal−sum (0.791)
True PVE=0.6, theta0=−2, theta=0, sigma0=1, sigma=0
Precision
Recall
Method (AUPRC)
Random (0.233)
RSS−NET (0.436)
RSS−E (0.436)
RSS−E−baseline (0.438)
Pascal−max (0.247)
Pascal−sum (0.250)
True PVE=0.6, theta0=−3, theta=0, sigma0=1, sigma=0
Precision
Recall
Method (AUPRC)
Random (0.028)
RSS−NET (0.138)
RSS−E (0.138)
RSS−E−baseline (0.138)
Pascal−max (0.089)
Pascal−sum (0.081)
True PVE=0.6, theta0=−4, theta=0, sigma0=1, sigma=0
Precision
Recall
Method (AUPRC)
Random (0.003)
RSS−NET (0.388)
RSS−E (0.388)
RSS−E−baseline (0.386)
Pascal−max (0.294)
Pascal−sum (0.246)

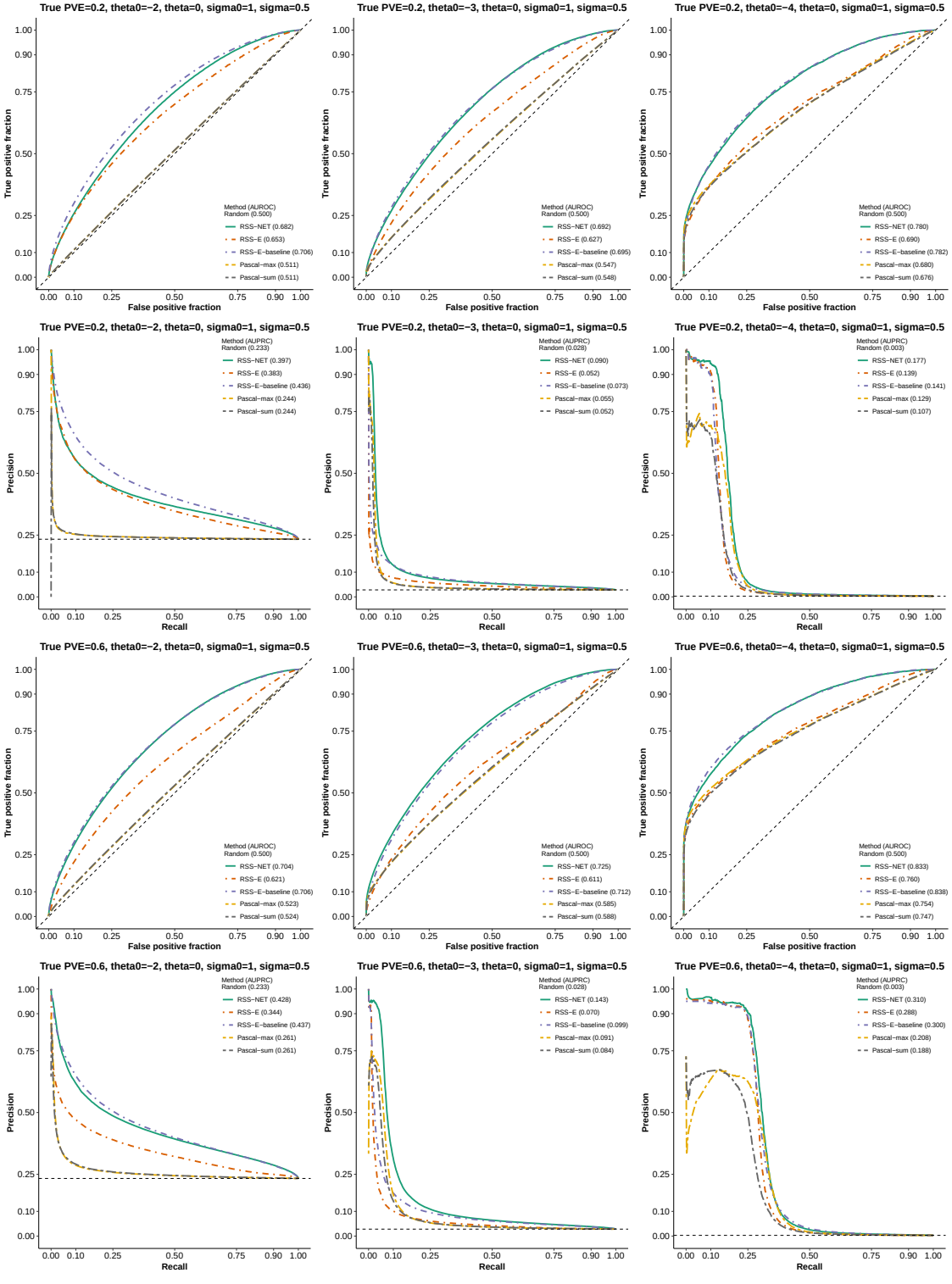
True PVE=0.2, theta0=−2, theta=0, sigma0=1, sigma=0.5
True positive fraction
False positive fraction
Method (AUROC)
Random (0.500)
RSS−NET (0.682)
RSS−E (0.653)
RSS−E−baseline (0.706)
Pascal−max (0.511)
Pascal−sum (0.511)
True PVE=0.2, theta0=−3, theta=0, sigma0=1, sigma=0.5
True positive fraction
False positive fraction
Method (AUROC)
Random (0.500)
RSS−NET (0.692)
RSS−E (0.627)
RSS−E−baseline (0.695)
Pascal−max (0.547)
Pascal−sum (0.548)
True PVE=0.2, theta0=−4, theta=0, sigma0=1, sigma=0.5
True positive fraction
False positive fraction
Method (AUROC)
Random (0.500)
RSS−NET (0.780)
RSS−E (0.690)
RSS−E−baseline (0.782)
Pascal−max (0.680)
Pascal−sum (0.676)
True PVE=0.2, theta0=−2, theta=0, sigma0=1, sigma=0.5
Precision
Recall
Method (AUPRC)
Random (0.233)
RSS−NET (0.397)
RSS−E (0.383)
RSS−E−baseline (0.436)
Pascal−max (0.244)
Pascal−sum (0.244)
True PVE=0.2, theta0=−3, theta=0, sigma0=1, sigma=0.5
Precision
Recall
Method (AUPRC)
Random (0.028)
RSS−NET (0.090)
RSS−E (0.052)
RSS−E−baseline (0.073)
Pascal−max (0.055)
Pascal−sum (0.052)
True PVE=0.2, theta0=−4, theta=0, sigma0=1, sigma=0.5
Precision
Recall
Method (AUPRC)
Random (0.003)
RSS−NET (0.177)
RSS−E (0.139)
RSS−E−baseline (0.141)
Pascal−max (0.129)
Pascal−sum (0.107)
True PVE=0.6, theta0=−2, theta=0, sigma0=1, sigma=0.5
True positive fraction
False positive fraction
Method (AUROC)
Random (0.500)
RSS−NET (0.704)
RSS−E (0.621)
RSS−E−baseline (0.706)
Pascal−max (0.523)
Pascal−sum (0.524)
True PVE=0.6, theta0=−3, theta=0, sigma0=1, sigma=0.5
True positive fraction
False positive fraction
Method (AUROC)
Random (0.500)
RSS−NET (0.725)
RSS−E (0.611)
RSS−E−baseline (0.712)
Pascal−max (0.585)
Pascal−sum (0.588)
True PVE=0.6, theta0=−4, theta=0, sigma0=1, sigma=0.5
True positive fraction
False positive fraction
Method (AUROC)
Random (0.500)
RSS−NET (0.833)
RSS−E (0.760)
RSS−E−baseline (0.838)
Pascal−max (0.754)
Pascal−sum (0.747)
True PVE=0.6, theta0=−2, theta=0, sigma0=1, sigma=0.5
Precision
Recall
Method (AUPRC)
Random (0.233)
RSS−NET (0.428)
RSS−E (0.344)
RSS−E−baseline (0.437)
Pascal−max (0.261)
Pascal−sum (0.261)
True PVE=0.6, theta0=−3, theta=0, sigma0=1, sigma=0.5
Precision
Recall
Method (AUPRC)
Random (0.028)
RSS−NET (0.143)
RSS−E (0.070)
RSS−E−baseline (0.099)
Pascal−max (0.091)
Pascal−sum (0.084)
True PVE=0.6, theta0=−4, theta=0, sigma0=1, sigma=0.5
Precision
Recall
Method (AUPRC)
Random (0.003)
RSS−NET (0.310)
RSS−E (0.288)
RSS−E−baseline (0.300)
Pascal−max (0.208)
Pascal−sum (0.188)

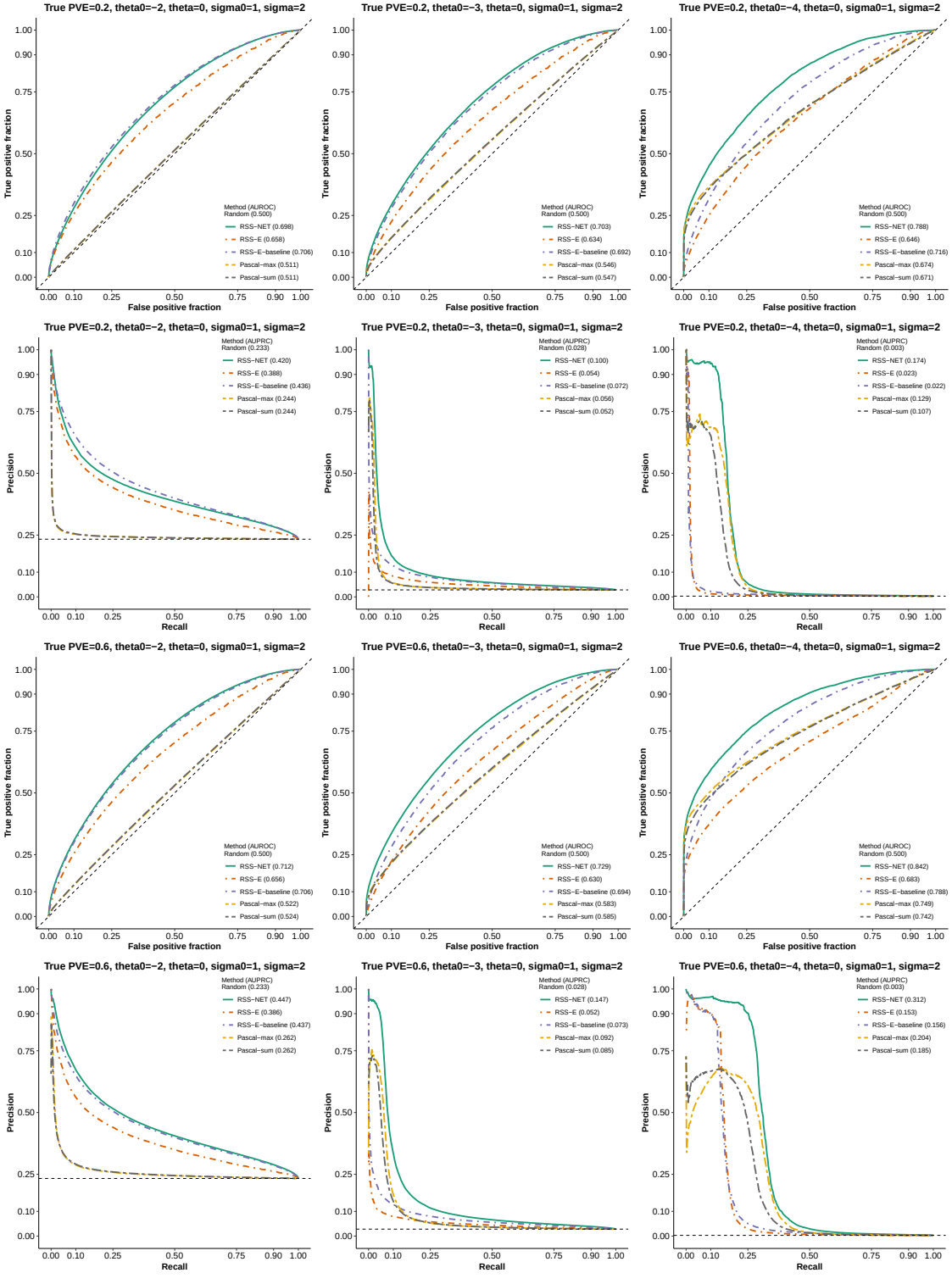
True PVE=0.2, theta0=−2, theta=0, sigma0=1, sigma=2
True positive fraction
False positive fraction
Method (AUROC)
Random (0.500)
RSS−NET (0.698)
RSS−E (0.658)
RSS−E−baseline (0.706)
Pascal−max (0.511)
Pascal−sum (0.511)
True PVE=0.2, theta0=−3, theta=0, sigma0=1, sigma=2
True positive fraction
False positive fraction
Method (AUROC)
Random (0.500)
RSS−NET (0.703)
RSS−E (0.634)
RSS−E−baseline (0.692)
Pascal−max (0.546)
Pascal−sum (0.547)
True PVE=0.2, theta0=−4, theta=0, sigma0=1, sigma=2
True positive fraction
False positive fraction
Method (AUROC)
Random (0.500)
RSS−NET (0.788)
RSS−E (0.646)
RSS−E−baseline (0.716)
Pascal−max (0.674)
Pascal−sum (0.671)
True PVE=0.2, theta0=−2, theta=0, sigma0=1, sigma=2
Precision
Recall
Method (AUPRC)
Random (0.233)
RSS−NET (0.420)
RSS−E (0.388)
RSS−E−baseline (0.436)
Pascal−max (0.244)
Pascal−sum (0.244)
True PVE=0.2, theta0=−3, theta=0, sigma0=1, sigma=2
Precision
Recall
Method (AUPRC)
Random (0.028)
RSS−NET (0.100)
RSS−E (0.054)
RSS−E−baseline (0.072)
Pascal−max (0.056)
Pascal−sum (0.052)
True PVE=0.2, theta0=−4, theta=0, sigma0=1, sigma=2
Precision
Recall
Method (AUPRC)
Random (0.003)
RSS−NET (0.174)
RSS−E (0.023)
RSS−E−baseline (0.022)
Pascal−max (0.129)
Pascal−sum (0.107)
True PVE=0.6, theta0=−2, theta=0, sigma0=1, sigma=2
True positive fraction
False positive fraction
Method (AUROC)
Random (0.500)
RSS−NET (0.712)
RSS−E (0.656)
RSS−E−baseline (0.706)
Pascal−max (0.522)
Pascal−sum (0.524)
True PVE=0.6, theta0=−3, theta=0, sigma0=1, sigma=2
True positive fraction
False positive fraction
Method (AUROC)
Random (0.500)
RSS−NET (0.729)
RSS−E (0.630)
RSS−E−baseline (0.694)
Pascal−max (0.583)
Pascal−sum (0.585)
True PVE=0.6, theta0=−4, theta=0, sigma0=1, sigma=2
True positive fraction
False positive fraction
Method (AUROC)
Random (0.500)
RSS−NET (0.842)
RSS−E (0.683)
RSS−E−baseline (0.788)
Pascal−max (0.749)
Pascal−sum (0.742)
True PVE=0.6, theta0=−2, theta=0, sigma0=1, sigma=2
Precision
Recall
Method (AUPRC)
Random (0.233)
RSS−NET (0.447)
RSS−E (0.386)
RSS−E−baseline (0.437)
Pascal−max (0.262)
Pascal−sum (0.262)
True PVE=0.6, theta0=−3, theta=0, sigma0=1, sigma=2
Precision
Recall
Method (AUPRC)
Random (0.028)
RSS−NET (0.147)
RSS−E (0.052)
RSS−E−baseline (0.073)
Pascal−max (0.092)
Pascal−sum (0.085)
True PVE=0.6, theta0=−4, theta=0, sigma0=1, sigma=2
Precision
Recall
Method (AUPRC)
Random (0.003)
RSS−NET (0.312)
RSS−E (0.153)
RSS−E−baseline (0.156)
Pascal−max (0.204)
Pascal−sum (0.185)

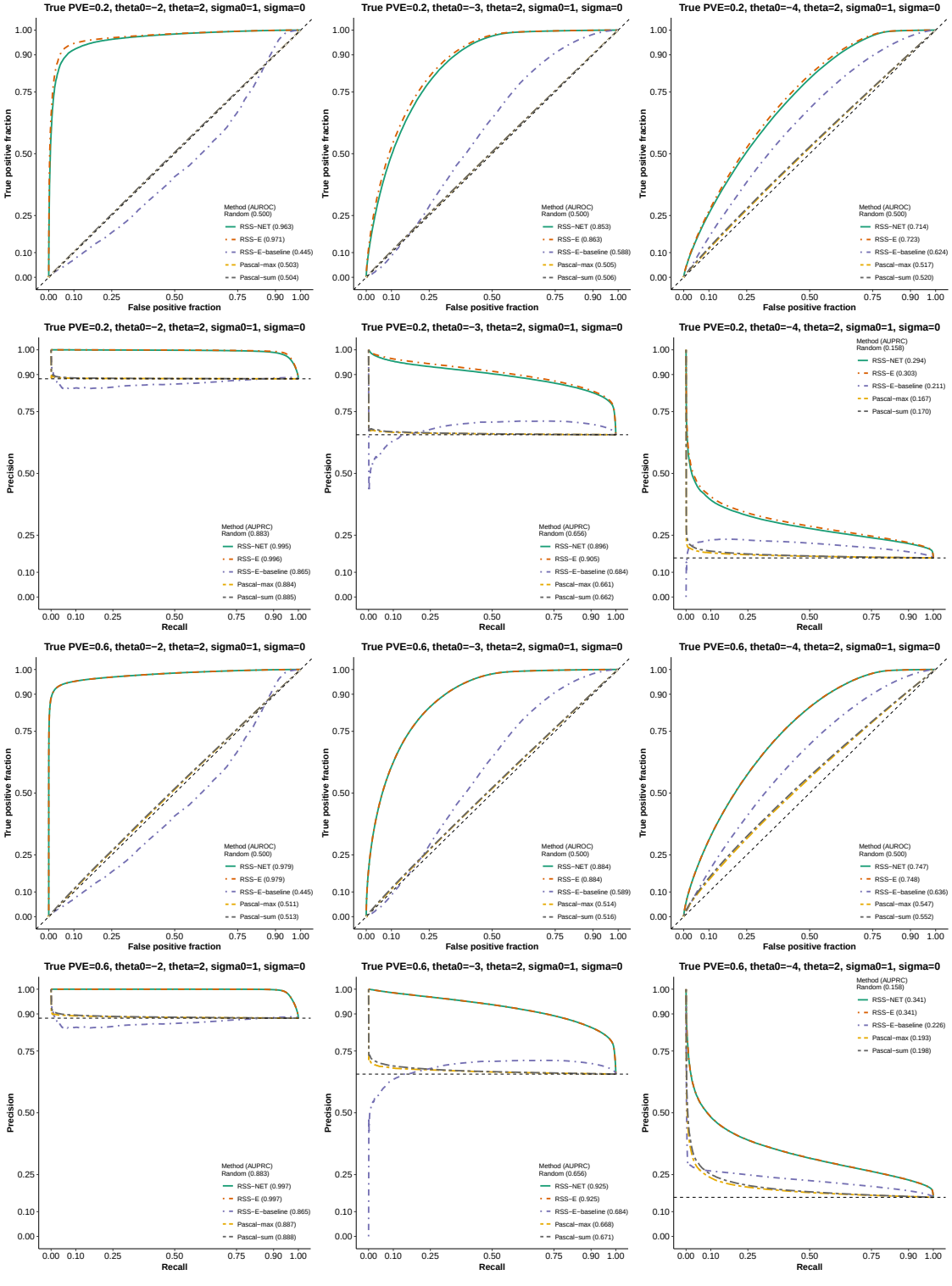
True PVE=0.2, theta0=−2, theta=2, sigma0=1, sigma=0
True positive fraction
False positive fraction
Method (AUROC)
Random (0.500)
RSS−NET (0.963)
RSS−E (0.971)
RSS−E−baseline (0.445)
Pascal−max (0.503)
Pascal−sum (0.504)
True PVE=0.2, theta0=−3, theta=2, sigma0=1, sigma=0
True positive fraction
False positive fraction
Method (AUROC)
Random (0.500)
RSS−NET (0.853)
RSS−E (0.863)
RSS−E−baseline (0.588)
Pascal−max (0.505)
Pascal−sum (0.506)
True PVE=0.2, theta0=−4, theta=2, sigma0=1, sigma=0
True positive fraction
False positive fraction
Method (AUROC)
Random (0.500)
RSS−NET (0.714)
RSS−E (0.723)
RSS−E−baseline (0.624)
Pascal−max (0.517)
Pascal−sum (0.520)
True PVE=0.2, theta0=−2, theta=2, sigma0=1, sigma=0
Precision
Recall
Method (AUPRC)
Random (0.883)
RSS−NET (0.995)
RSS−E (0.996)
RSS−E−baseline (0.865)
Pascal−max (0.884)
Pascal−sum (0.885)
True PVE=0.2, theta0=−3, theta=2, sigma0=1, sigma=0
Precision
Recall
Method (AUPRC)
Random (0.656)
RSS−NET (0.896)
RSS−E (0.905)
RSS−E−baseline (0.684)
Pascal−max (0.661)
Pascal−sum (0.662)
True PVE=0.2, theta0=−4, theta=2, sigma0=1, sigma=0
Precision
Recall
Method (AUPRC)
Random (0.158)
RSS−NET (0.294)
RSS−E (0.303)
RSS−E−baseline (0.211)
Pascal−max (0.167)
Pascal−sum (0.170)
True PVE=0.6, theta0=−2, theta=2, sigma0=1, sigma=0
True positive fraction
False positive fraction
Method (AUROC)
Random (0.500)
RSS−NET (0.979)
RSS−E (0.979)
RSS−E−baseline (0.445)
Pascal−max (0.511)
Pascal−sum (0.513)
True PVE=0.6, theta0=−3, theta=2, sigma0=1, sigma=0
True positive fraction
False positive fraction
Method (AUROC)
Random (0.500)
RSS−NET (0.884)
RSS−E (0.884)
RSS−E−baseline (0.589)
Pascal−max (0.514)
Pascal−sum (0.516)
True PVE=0.6, theta0=−4, theta=2, sigma0=1, sigma=0
True positive fraction
False positive fraction
Method (AUROC)
Random (0.500)
RSS−NET (0.747)
RSS−E (0.748)
RSS−E−baseline (0.636)
Pascal−max (0.547)
Pascal−sum (0.552)
True PVE=0.6, theta0=−2, theta=2, sigma0=1, sigma=0
Precision
Recall
Method (AUPRC)
Random (0.883)
RSS−NET (0.997)
RSS−E (0.997)
RSS−E−baseline (0.865)
Pascal−max (0.887)
Pascal−sum (0.888)
True PVE=0.6, theta0=−3, theta=2, sigma0=1, sigma=0
Precision
Recall
Method (AUPRC)
Random (0.656)
RSS−NET (0.925)
RSS−E (0.925)
RSS−E−baseline (0.684)
Pascal−max (0.668)
Pascal−sum (0.671)
True PVE=0.6, theta0=−4, theta=2, sigma0=1, sigma=0
Precision
Recall
Method (AUPRC)
Random (0.158)
RSS−NET (0.341)
RSS−E (0.341)
RSS−E−baseline (0.226)
Pascal−max (0.193)
Pascal−sum (0.198)

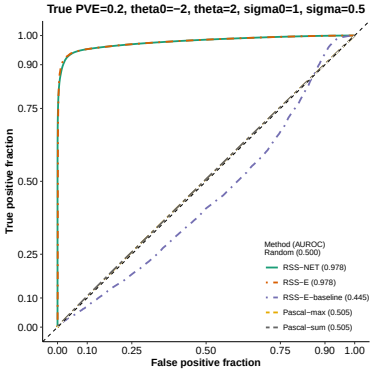
True PVE=0.2, theta0=−2, theta=2, sigma0=1, sigma=0.5
True positive fraction
False positive fraction
Method (AUROC)
Random (0.500)
RSS−NET (0.978)
RSS−E (0.978)
RSS−E−baseline (0.445)
Pascal−max (0.505)
Pascal−sum (0.505)

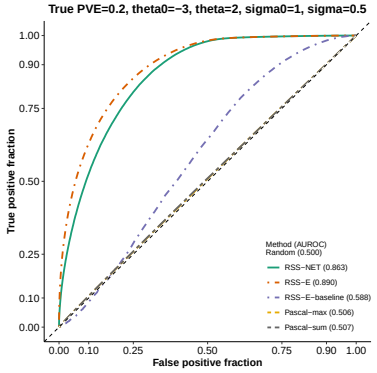
True PVE=0.2, theta0=−3, theta=2, sigma0=1, sigma=0.5
True positive fraction
False positive fraction
Method (AUROC)
Random (0.500)
RSS−NET (0.863)
RSS−E (0.890)
RSS−E−baseline (0.588)
Pascal−max (0.506)
Pascal−sum (0.507)

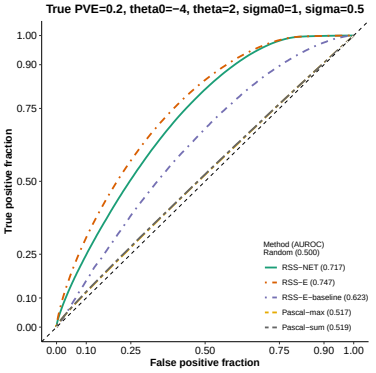
True PVE=0.2, theta0=−4, theta=2, sigma0=1, sigma=0.5
True positive fraction
False positive fraction
Method (AUROC)
Random (0.500)
RSS−NET (0.717)
RSS−E (0.747)
RSS−E−baseline (0.623)
Pascal−max (0.517)
Pascal−sum (0.519)

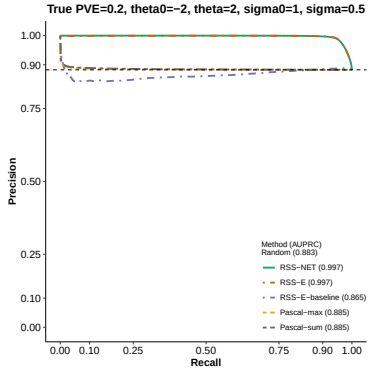
True PVE=0.2, theta0=−2, theta=2, sigma0=1, sigma=0.5
Precision
Recall
Method (AUPRC)
Random (0.883)
RSS−NET (0.997)
RSS−E (0.997)
RSS−E−baseline (0.865)
Pascal−max (0.885)
Pascal−sum (0.885)

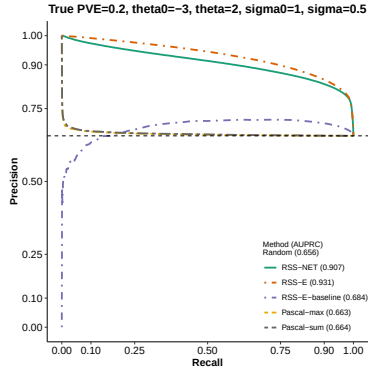
True PVE=0.2, theta0=−3, theta=2, sigma0=1, sigma=0.5
Precision
Recall
Method (AUPRC)
Random (0.656)
RSS−NET (0.907)
RSS−E (0.931)
RSS−E−baseline (0.684)
Pascal−max (0.663)
Pascal−sum (0.664)

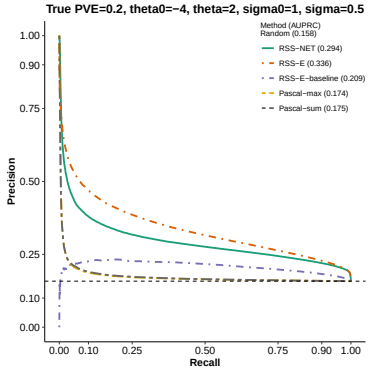
True PVE=0.2, theta0=−4, theta=2, sigma0=1, sigma=0.5
Precision
Recall
Method (AUPRC)
Random (0.158)
RSS−NET (0.294)
RSS−E (0.336)
RSS−E−baseline (0.209)
Pascal−max (0.174)
Pascal−sum (0.175)

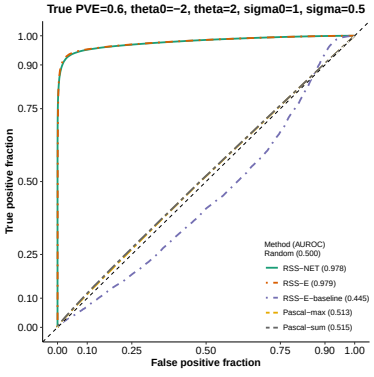
True PVE=0.6, theta0=−2, theta=2, sigma0=1, sigma=0.5
True positive fraction
False positive fraction
Method (AUROC)
Random (0.500)
RSS−NET (0.978)
RSS−E (0.979)
RSS−E−baseline (0.445)
Pascal−max (0.513)
Pascal−sum (0.515)

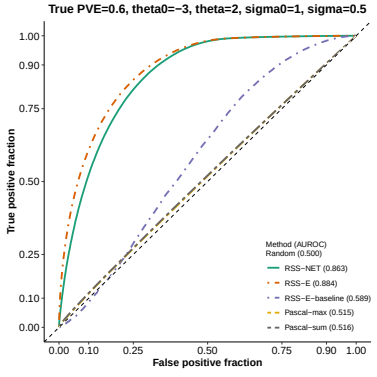
True PVE=0.6, theta0=−3, theta=2, sigma0=1, sigma=0.5
True positive fraction
False positive fraction
Method (AUROC)
Random (0.500)
RSS−NET (0.863)
RSS−E (0.884)
RSS−E−baseline (0.589)
Pascal−max (0.515)
Pascal−sum (0.516)

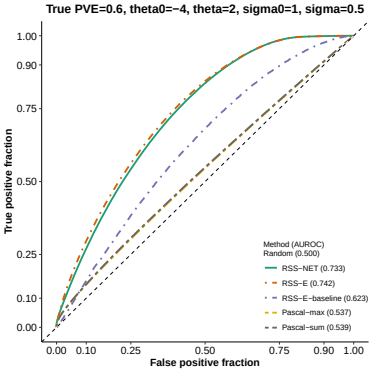
True PVE=0.6, theta0=−4, theta=2, sigma0=1, sigma=0.5
True positive fraction
False positive fraction
Method (AUROC)
Random (0.500)
RSS−NET (0.733)
RSS−E (0.742)
RSS−E−baseline (0.623)
Pascal−max (0.537)
Pascal−sum (0.539)

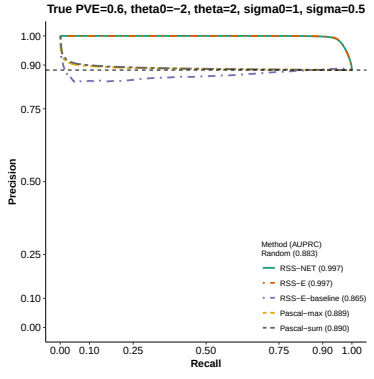
True PVE=0.6, theta0=−2, theta=2, sigma0=1, sigma=0.5
Precision
Recall
Method (AUPRC)
Random (0.883)
RSS−NET (0.997)
RSS−E (0.997)
RSS−E−baseline (0.865)
Pascal−max (0.889)
Pascal−sum (0.890)

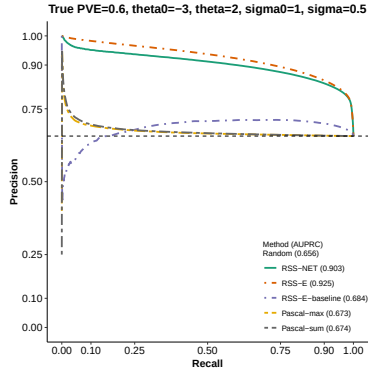
True PVE=0.6, theta0=−3, theta=2, sigma0=1, sigma=0.5
Precision
Recall
Method (AUPRC)
Random (0.656)
RSS−NET (0.903)
RSS−E (0.925)
RSS−E−baseline (0.684)
Pascal−max (0.673)
Pascal−sum (0.674)

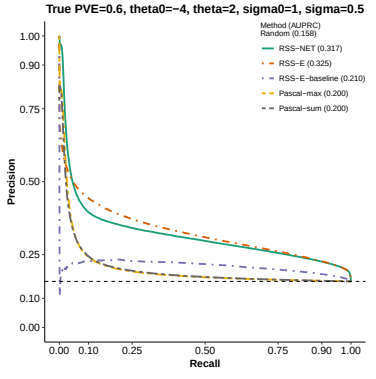
True PVE=0.6, theta0=−4, theta=2, sigma0=1, sigma=0.5
Precision
Recall
Method (AUPRC)
Random (0.158)
RSS−NET (0.317)
RSS−E (0.325)
RSS−E−baseline (0.210)
Pascal−max (0.200)
Pascal−sum (0.200)

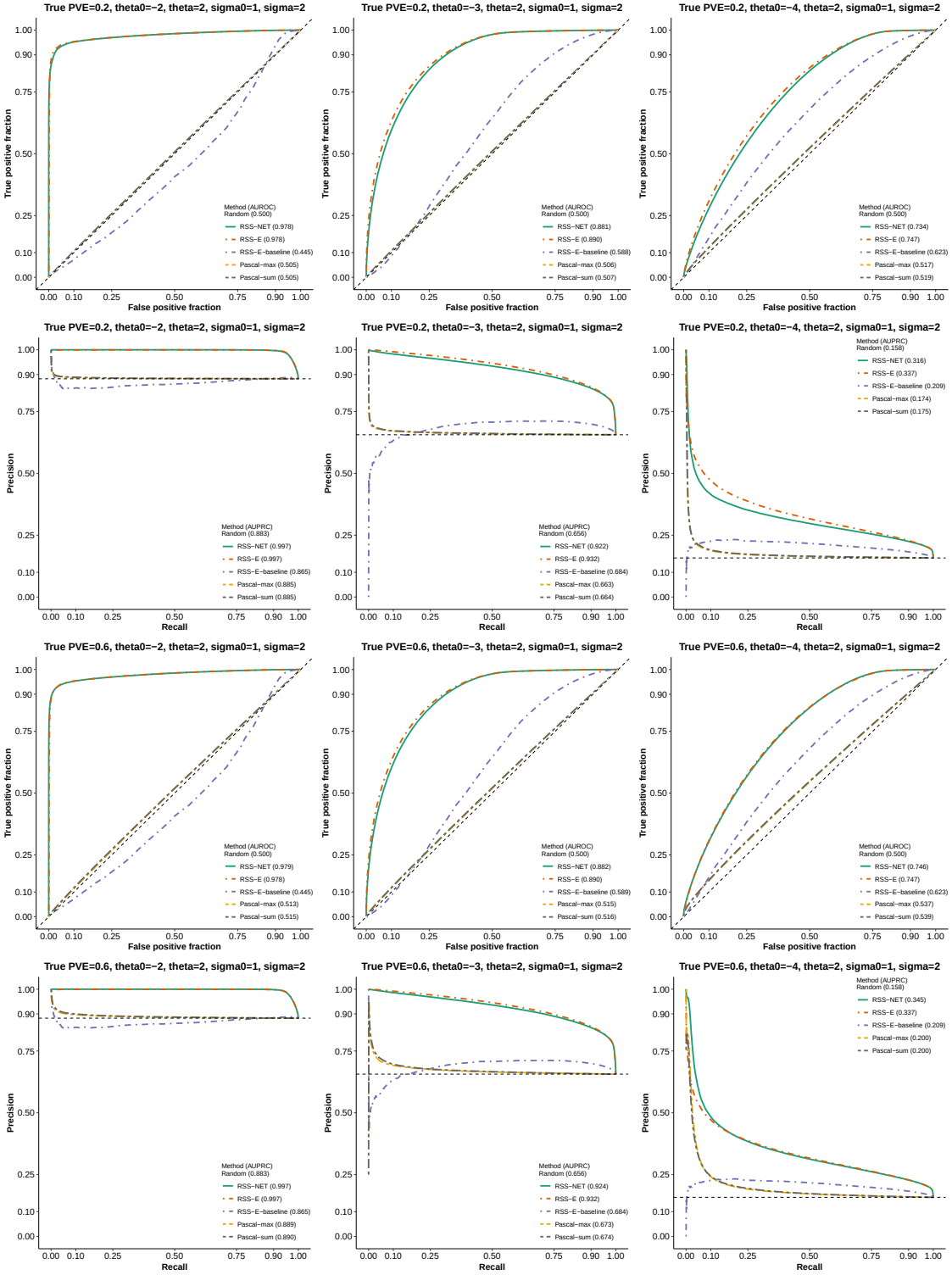
True PVE=0.2, theta0=−2, theta=2, sigma0=1, sigma=2
True positive fraction
False positive fraction
Method (AUROC)
Random (0.500)
RSS−NET (0.978)
RSS−E (0.978)
RSS−E−baseline (0.445)
Pascal−max (0.505)
Pascal−sum (0.505)
True PVE=0.2, theta0=−3, theta=2, sigma0=1, sigma=2
True positive fraction
False positive fraction
Method (AUROC)
Random (0.500)
RSS−NET (0.881)
RSS−E (0.890)
RSS−E−baseline (0.588)
Pascal−max (0.506)
Pascal−sum (0.507)
True PVE=0.2, theta0=−4, theta=2, sigma0=1, sigma=2
True positive fraction
False positive fraction
Method (AUROC)
Random (0.500)
RSS−NET (0.734)
RSS−E (0.747)
RSS−E−baseline (0.623)
Pascal−max (0.517)
Pascal−sum (0.519)
True PVE=0.2, theta0=−2, theta=2, sigma0=1, sigma=2
Precision
Recall
Method (AUPRC)
Random (0.883)
RSS−NET (0.997)
RSS−E (0.997)
RSS−E−baseline (0.865)
Pascal−max (0.885)
Pascal−sum (0.885)
True PVE=0.2, theta0=−3, theta=2, sigma0=1, sigma=2
Precision
Recall
Method (AUPRC)
Random (0.656)
RSS−NET (0.922)
RSS−E (0.932)
RSS−E−baseline (0.684)
Pascal−max (0.663)
Pascal−sum (0.664)
True PVE=0.2, theta0=−4, theta=2, sigma0=1, sigma=2
Precision
Recall
Method (AUPRC)
Random (0.158)
RSS−NET (0.316)
RSS−E (0.337)
RSS−E−baseline (0.209)
Pascal−max (0.174)
Pascal−sum (0.175)
True PVE=0.6, theta0=−2, theta=2, sigma0=1, sigma=2
True positive fraction
False positive fraction
Method (AUROC)
Random (0.500)
RSS−NET (0.979)
RSS−E (0.978)
RSS−E−baseline (0.445)
Pascal−max (0.513)
Pascal−sum (0.515)
True PVE=0.6, theta0=−3, theta=2, sigma0=1, sigma=2
True positive fraction
False positive fraction
Method (AUROC)
Random (0.500)
RSS−NET (0.882)
RSS−E (0.890)
RSS−E−baseline (0.589)
Pascal−max (0.515)
Pascal−sum (0.516)
True PVE=0.6, theta0=−4, theta=2, sigma0=1, sigma=2
True positive fraction
False positive fraction
Method (AUROC)
Random (0.500)
RSS−NET (0.746)
RSS−E (0.747)
RSS−E−baseline (0.623)
Pascal−max (0.537)
Pascal−sum (0.539)
True PVE=0.6, theta0=−2, theta=2, sigma0=1, sigma=2
Precision
Recall
Method (AUPRC)
Random (0.883)
RSS−NET (0.997)
RSS−E (0.997)
RSS−E−baseline (0.865)
Pascal−max (0.889)
Pascal−sum (0.890)
True PVE=0.6, theta0=−3, theta=2, sigma0=1, sigma=2
Precision
Recall
Method (AUPRC)
Random (0.656)
RSS−NET (0.924)
RSS−E (0.932)
RSS−E−baseline (0.684)
Pascal−max (0.673)
Pascal−sum (0.674)
True PVE=0.6, theta0=−4, theta=2, sigma0=1, sigma=2
Precision
Recall
Method (AUPRC)
Random (0.158)
RSS−NET (0.345)
RSS−E (0.337)
RSS−E−baseline (0.209)
Pascal−max (0.200)
Pascal−sum (0.200)

Supplementary Figure 8

We repeat the simulations in **Supplementary Figure 7** on GWAS summary statistics simulated in **Supplementary Figure 2** and the vagina regulatory network.

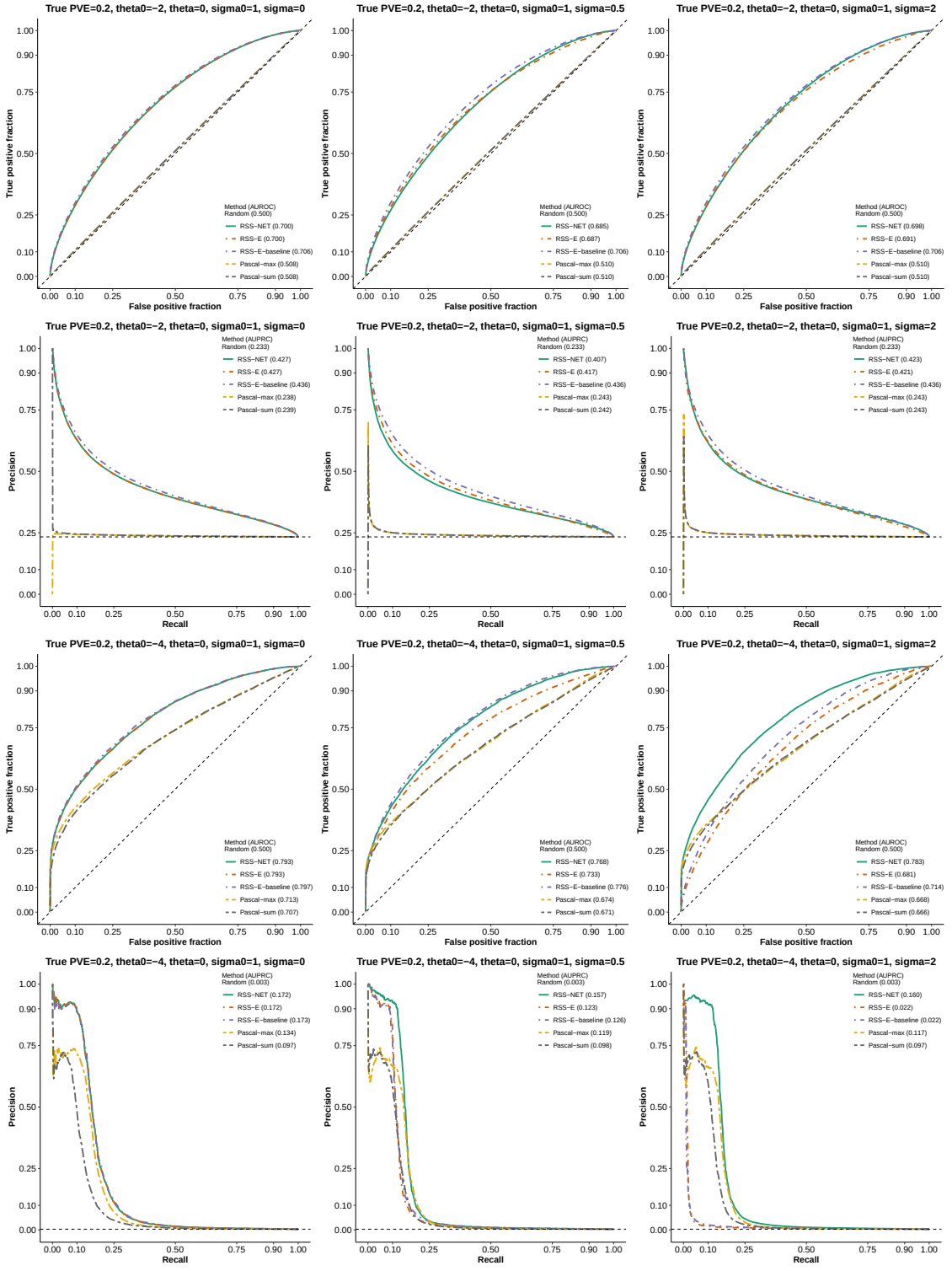

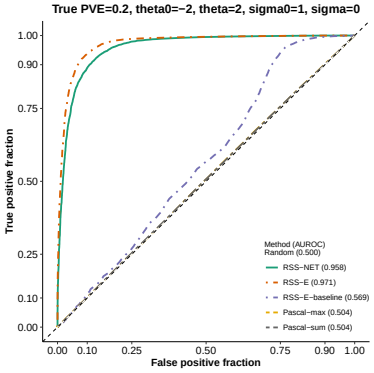
True PVE=0.2, theta0=−2, theta=2, sigma0=1, sigma=0
True positive fraction
False positive fraction
Method (AUROC)
Random (0.500)
RSS−NET (0.958)
RSS−E (0.971)
RSS−E−baseline (0.569)
Pascal−max (0.504)
Pascal−sum (0.504)

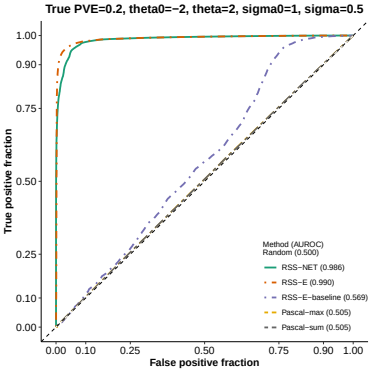
True PVE=0.2, theta0=−2, theta=2, sigma0=1, sigma=0.5
True positive fraction
False positive fraction
Method (AUROC)
Random (0.500)
RSS−NET (0.986)
RSS−E (0.990)
RSS−E−baseline (0.569)
Pascal−max (0.505)
Pascal−sum (0.505)

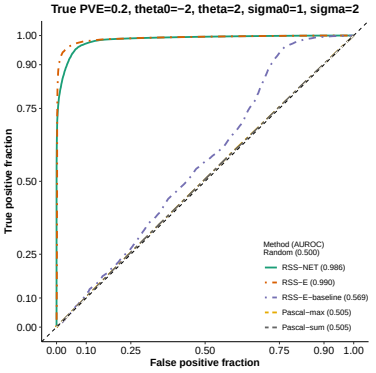
True PVE=0.2, theta0=−2, theta=2, sigma0=1, sigma=2
True positive fraction
False positive fraction
Method (AUROC)
Random (0.500)
RSS−NET (0.986)
RSS−E (0.990)
RSS−E−baseline (0.569)
Pascal−max (0.505)
Pascal−sum (0.505)

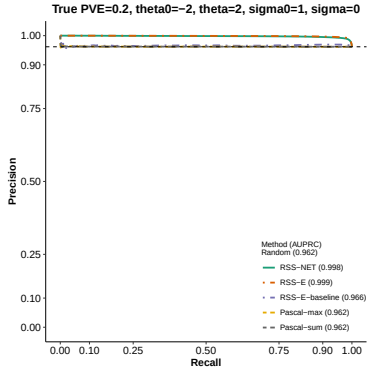
True PVE=0.2, theta0=−2, theta=2, sigma0=1, sigma=0
Precision
Recall
Method (AUPRC)
Random (0.962)
RSS−NET (0.998)
RSS−E (0.999)
RSS−E−baseline (0.966)
Pascal−max (0.962)
Pascal−sum (0.962)

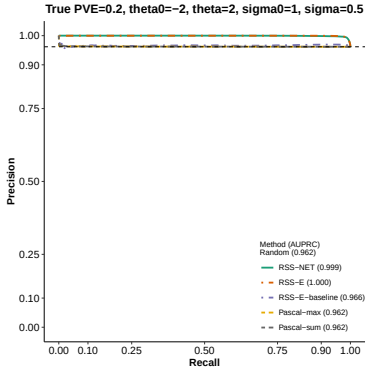
True PVE=0.2, theta0=−2, theta=2, sigma0=1, sigma=0.5
Precision
Recall
Method (AUPRC)
Random (0.962)
RSS−NET (0.999)
RSS−E (1.000)
RSS−E−baseline (0.966)
Pascal−max (0.962)
Pascal−sum (0.962)

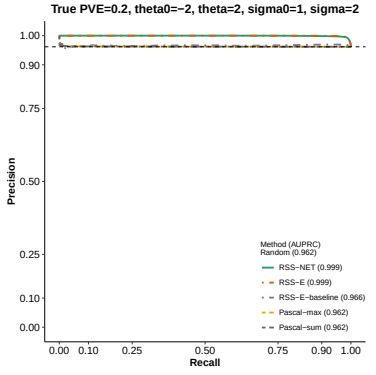
True PVE=0.2, theta0=−2, theta=2, sigma0=1, sigma=2
Precision
Recall
Method (AUPRC)
Random (0.962)
RSS−NET (0.999)
RSS−E (0.999)
RSS−E−baseline (0.966)
Pascal−max (0.962)
Pascal−sum (0.962)

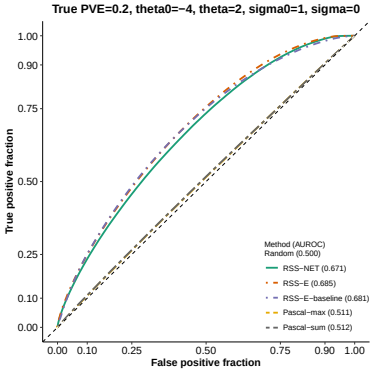
True PVE=0.2, theta0=−4, theta=2, sigma0=1, sigma=0
True positive fraction
False positive fraction
Method (AUROC)
Random (0.500)
RSS−NET (0.671)
RSS−E (0.685)
RSS−E−baseline (0.681)
Pascal−max (0.511)
Pascal−sum (0.512)

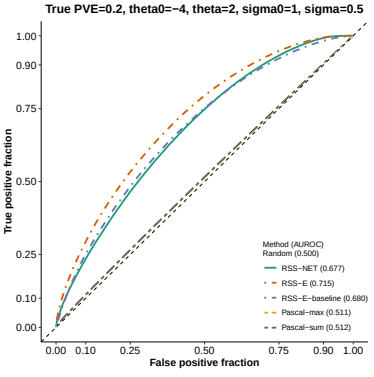
True PVE=0.2, theta0=−4, theta=2, sigma0=1, sigma=0.5
True positive fraction
False positive fraction
Method (AUROC)
Random (0.500)
RSS−NET (0.677)
RSS−E (0.715)
RSS−E−baseline (0.680)
Pascal−max (0.511)
Pascal−sum (0.512)

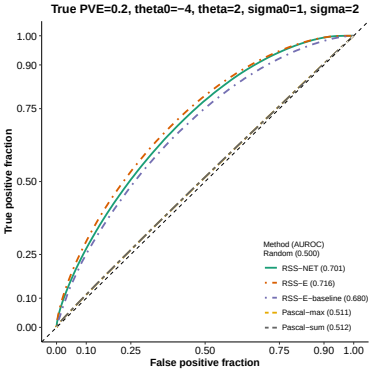
True PVE=0.2, theta0=−4, theta=2, sigma0=1, sigma=2
True positive fraction
False positive fraction
Method (AUROC)
Random (0.500)
RSS−NET (0.701)
RSS−E (0.716)
RSS−E−baseline (0.680)
Pascal−max (0.511)
Pascal−sum (0.512)

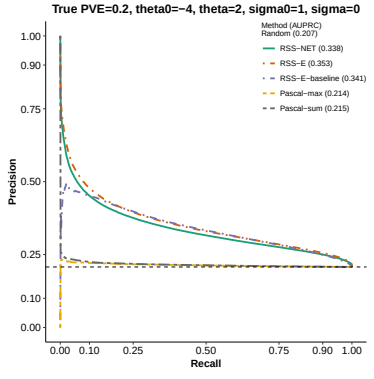
True PVE=0.2, theta0=−4, theta=2, sigma0=1, sigma=0
Precision
Recall
Method (AUPRC)
Random (0.207)
RSS−NET (0.338)
RSS−E (0.353)
RSS−E−baseline (0.341)
Pascal−max (0.214)
Pascal−sum (0.215)

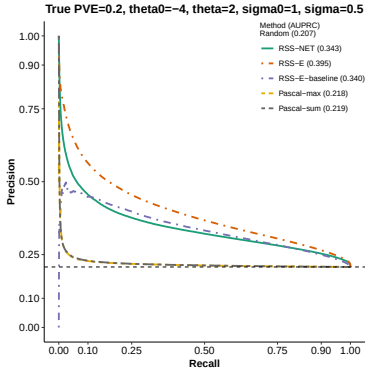
True PVE=0.2, theta0=−4, theta=2, sigma0=1, sigma=0.5
Precision
Recall
Method (AUPRC)
Random (0.207)
RSS−NET (0.343)
RSS−E (0.395)
RSS−E−baseline (0.340)
Pascal−max (0.218)
Pascal−sum (0.219)

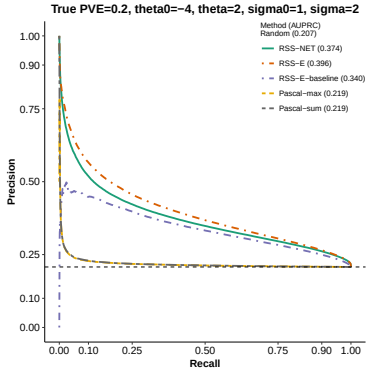
True PVE=0.2, theta0=−4, theta=2, sigma0=1, sigma=2
Precision
Recall
Method (AUPRC)
Random (0.207)
RSS−NET (0.374)
RSS−E (0.396)
RSS−E−baseline (0.340)
Pascal−max (0.219)
Pascal−sum (0.219)

Supplementary Figure 9

RSS-NET simulations based on 1 million common SNPs. This part is the same as **Supplementary Figure 1**, except that here we use the haplotype data of 503 European-ancestry individuals on 1,030,397 common SNPs (MAF ≥ 1%) from 1000 Genomes Project Consortium (2015) to specify the genotype matrix X. Results below (**a**: timing; **b**: network enrichment; **c**: gene-level association) correspond to simulations with true hyper-parameters of positive datasets being $\theta_0 = -4$, $\theta = 2$, $\sigma_0 = 1$, $\sigma = 2$ and PVE = 0.6.

As shown in Panel **a**, the computation time of RSS-NET increases as the number of genome-wide SNPs analyzed increases. On average, when the number of SNPs increases from 348,965 to 1,030,397, the total computation time per dataset is four times longer (one-sided Wilcoxon $P = 8.02 \times 10^{-132}$). Due to the large-scale simulations conducted in this study, we mostly use 348,965 genome-wide SNPs in order to reduce computation.

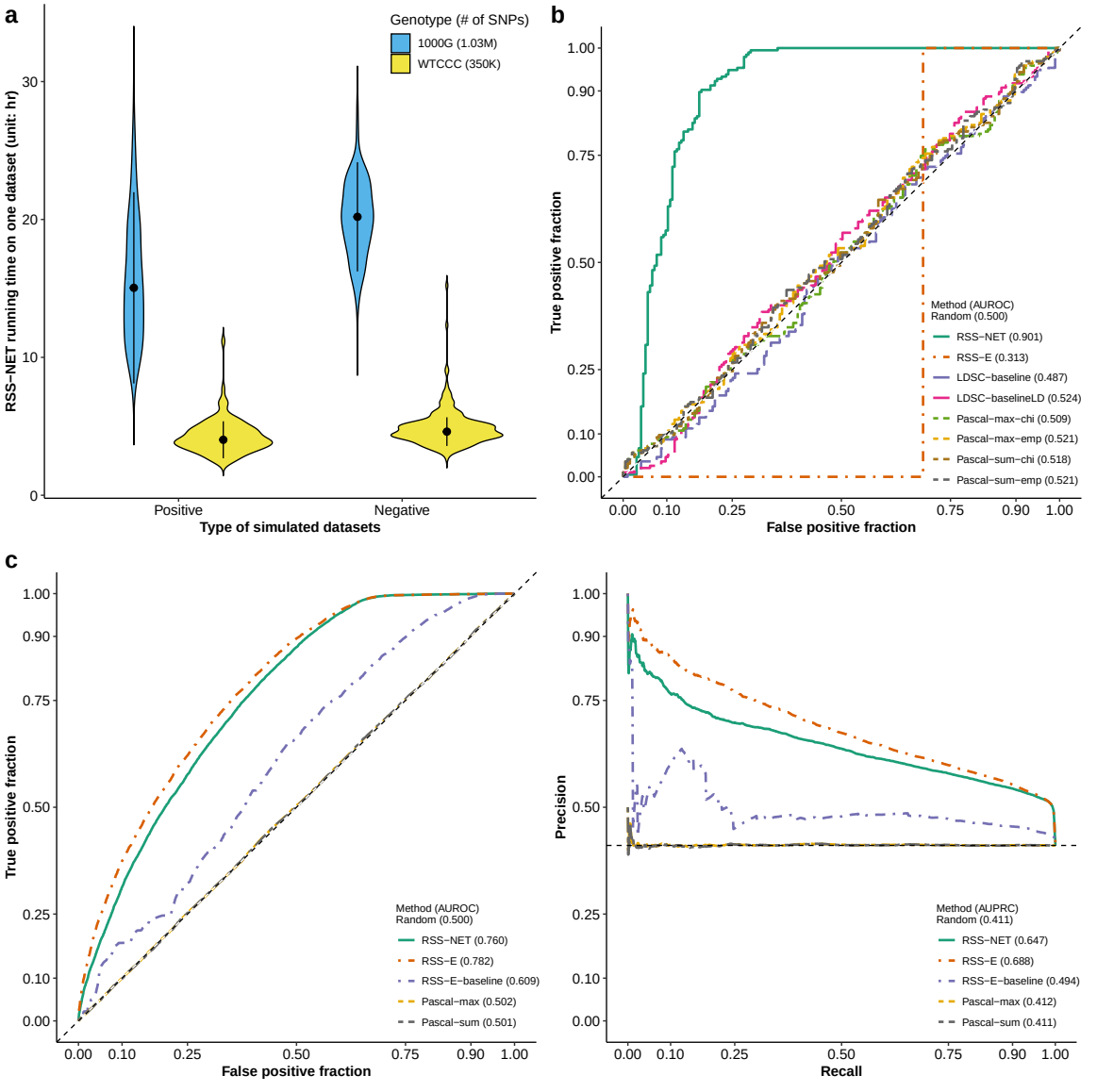

Supplementary Figure 10

Robustness of RSS-NET under noisy networks. This part aims to assess the robustness of RSS-NET to model mis-specification where the GWAS summary data are simulated from a real target network and the enrichment testing is performed on a noisy version of this real target. Details of this part are almost identical to those in **Supplementary Figure 1**. Here we only highlight the differences.

The real target network used to simulate GWAS summary data is the B cell regulatory network in **Supplementary Figure 1**. We create a noisy network for this target by randomly subsetting a given fraction of its TF-TG edges and the associated REs. Here the fraction of TF-TG edges to subset are $\{1\%, 5\%, 10\%, 50\%\}$. For each pair of negative and positive GWAS datasets, we simulate a new noisy network and use it in RSS-NET.

The GWAS summary data (both negative and positive) used here are the same as those used in **Supplementary Figure 1**, with true $\theta_0 = -4$, $\theta = 2$, $\sigma_0 = 1$, $\sigma = 2$ and PVE $= 0.2$. Unlike **Supplementary Figure 1**, here we do not test the enrichment of B cell network (i.e. the real target network), but test its random subsets instead.

Panels **a**-**c** Comparison of network enrichment results between using the real target network and using its noisy versions in RSS-NET.

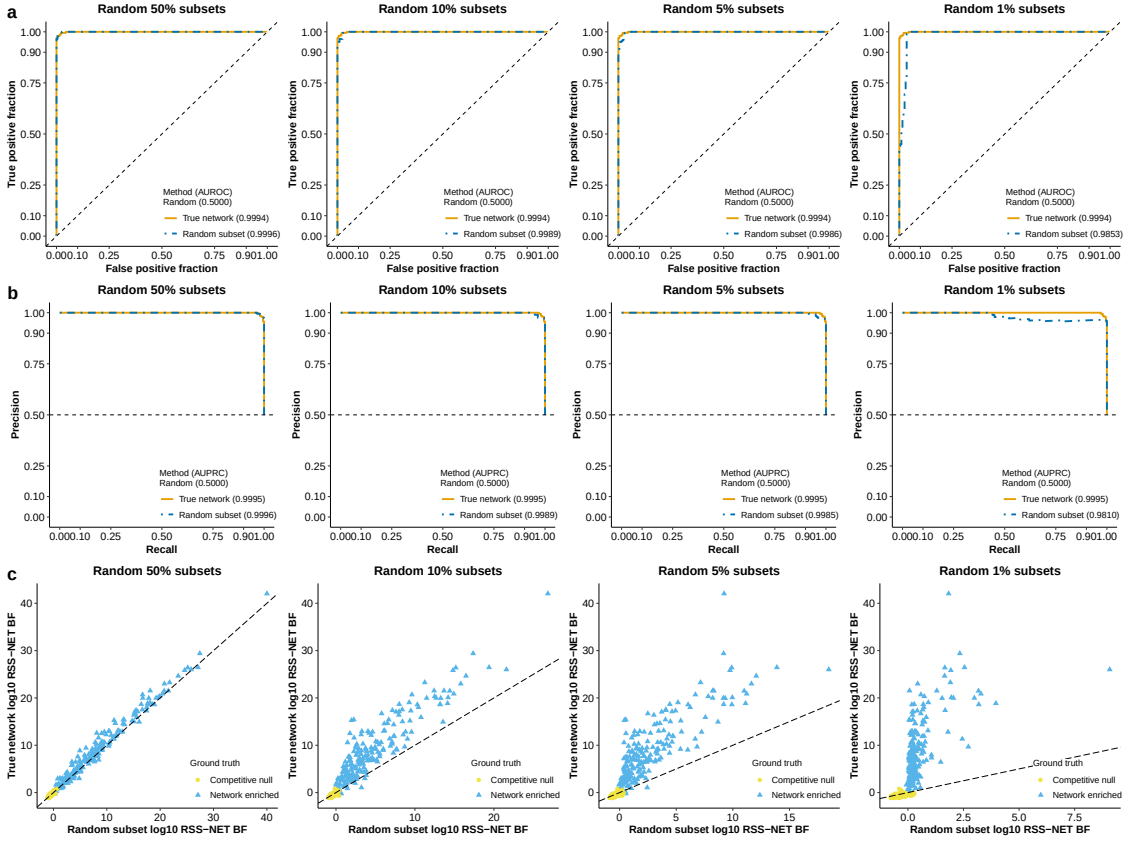

Panels **d-e** Comparison of gene-level association results between using the real target network and using its noisy versions in RSS-NET. Note that the AUROC based on true network shown below is slightly different from the AUROC shown in **Supplementary Figure 7**, although they are generated from the same simulated datasets. This is because AUROC shown in **Supplementary Figure 7** is evaluated based on 16,954 autosomal protein-coding genes that are available in Pascal-required database, and AUROC shown below is evaluated based on all available autosomal protein-coding genes.

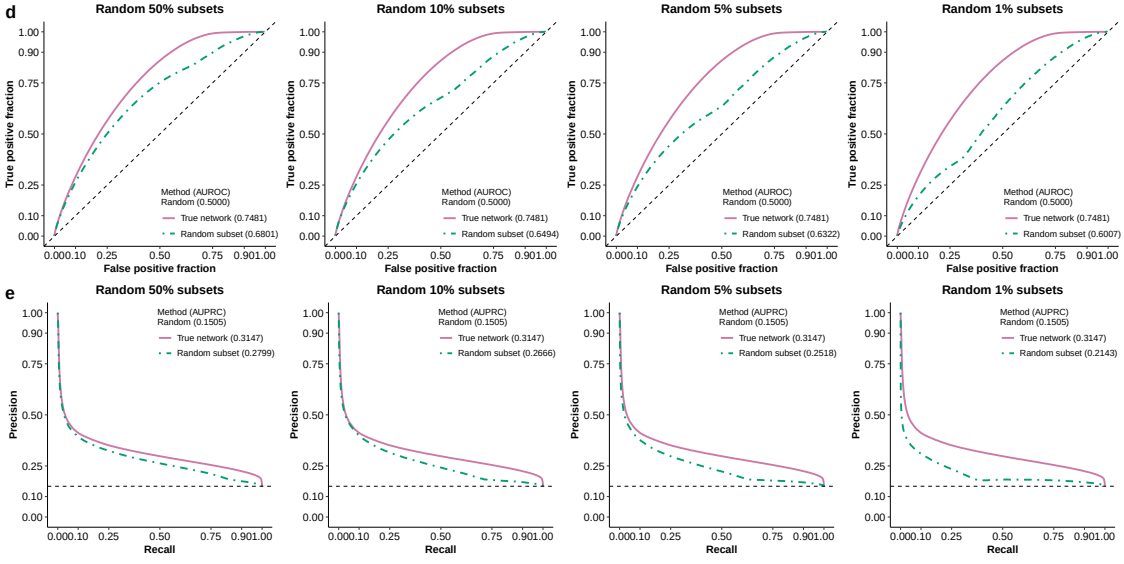

Panels **f-i** Descriptive statistics of noisy networks under different subsetting fractions. Each box plot below is based on 200 noisy networks.

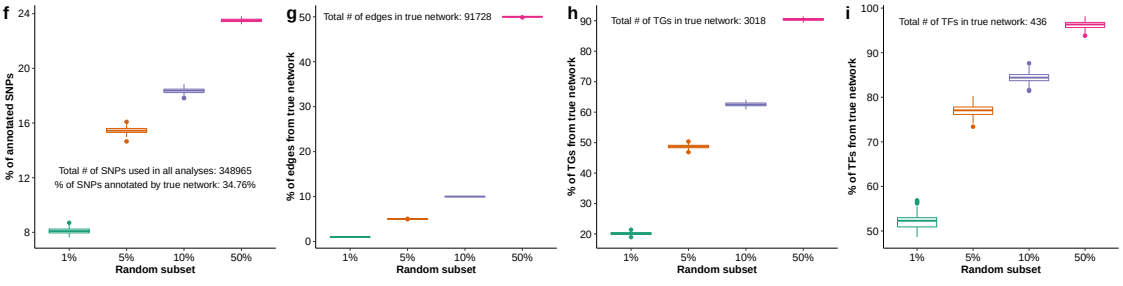

Supplementary Figure 11

Analysis details and additional results for Figure 5(a). Here we perform clustering analysis of 38 regulatory networks based on principal component analysis (PCA), *t*-distributed stochastic neighbor embedding (t-SNE), and hierarchical clustering. To perform PCA, we use the R built-in function `prcomp`. To perform t-SNE, we use the R package `Rtsne`. To perform hierarchical clustering, we use the R built-in function `hclust`, with distance = 1 – Pearson correlation, and average method. **Figure 5(a)** corresponds to the t-SNE plot in Panel **e**.

Panel **a** Here the input data matrix has 1,289,786 rows (SNPs) and 38 columns (networks), where the (i, j)-th entry is 1 if SNP i is within 100 kb of any associated RE or transcribed region of any member gene of network j, and it is 0 otherwise.

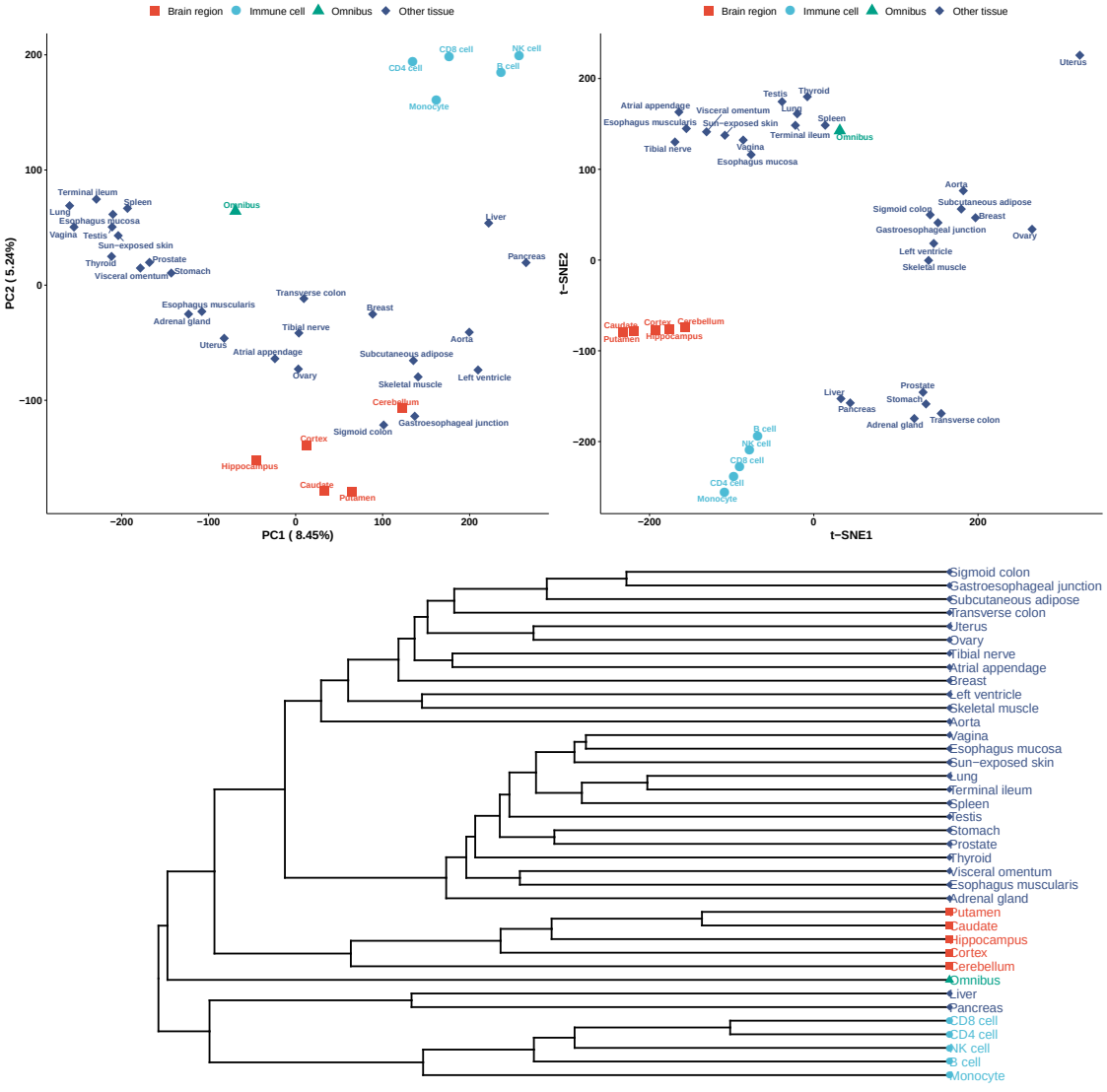

Panel **b** Here the input data matrix has 605 rows (TFs) and 38 columns (networks), where the (i, j)-th entry is 1 if TF i belongs to network j, and it is 0 otherwise.

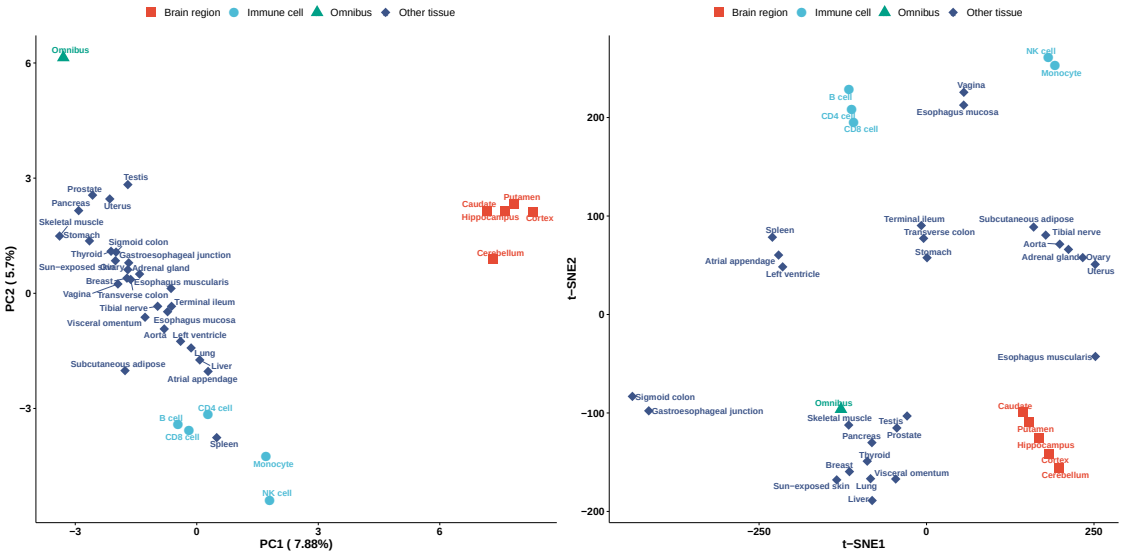

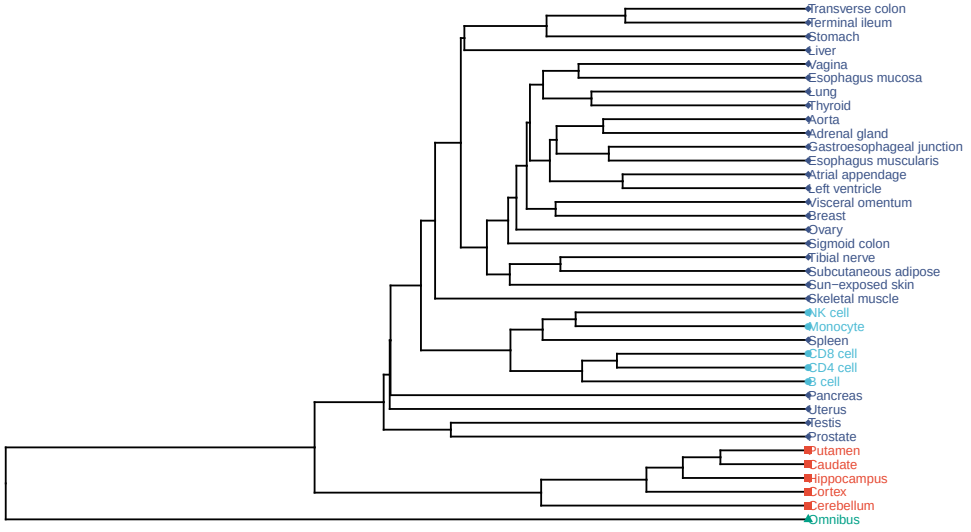

Panel **c** Here the input data matrix has 12,963 rows (TGs) and 38 columns (networks), where the (i, j)-th entry is 1 if TG i belongs to network j, and it is 0 otherwise.

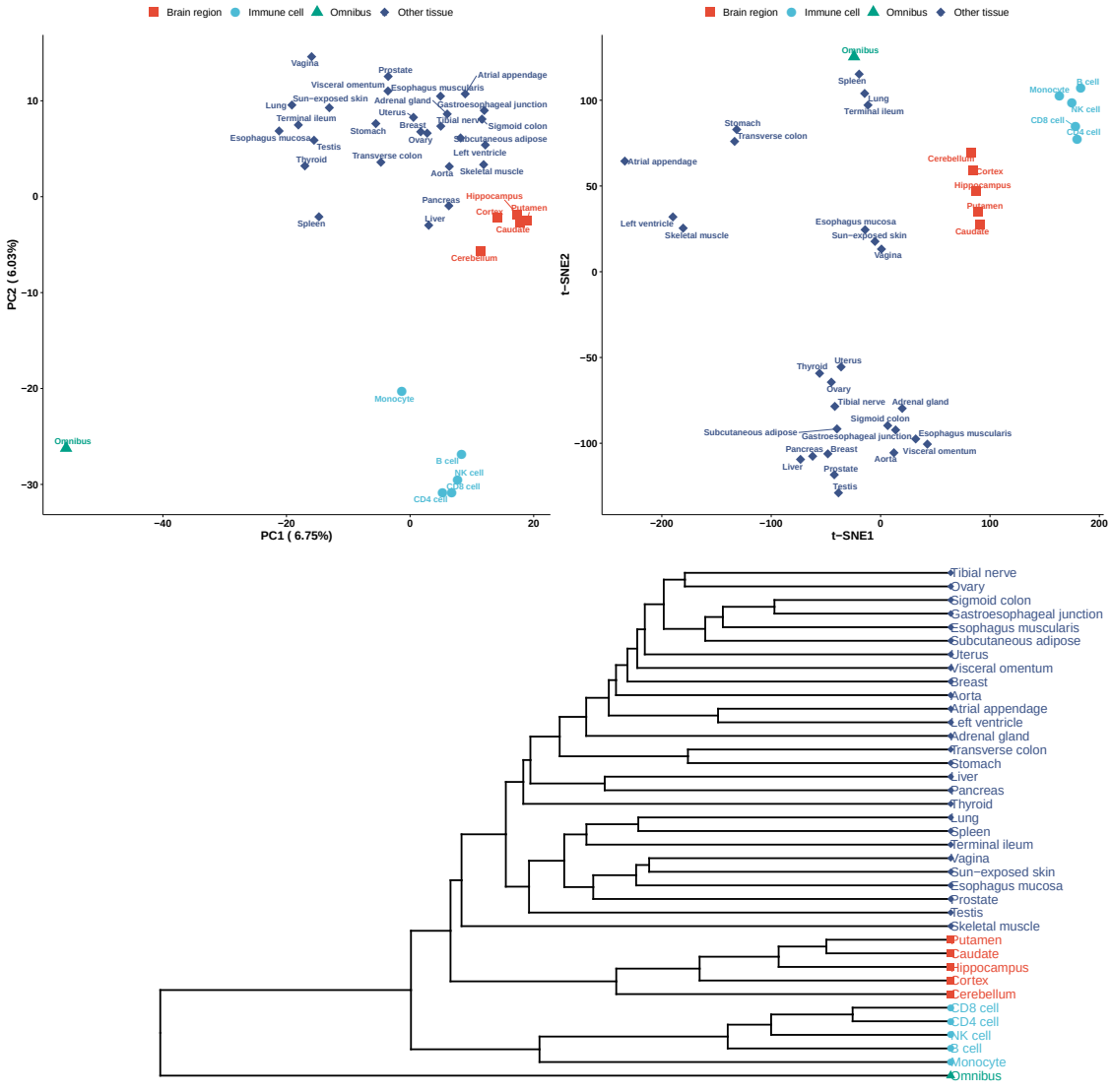

Panel **d** Here the input data matrix has 880,777 rows (TF-TG edges) and 38 columns (networks), where the (i,j)-th entry is the weight of TF-TG edge i in network j, and it is 0 if TF-TG edge i is not available in network j.

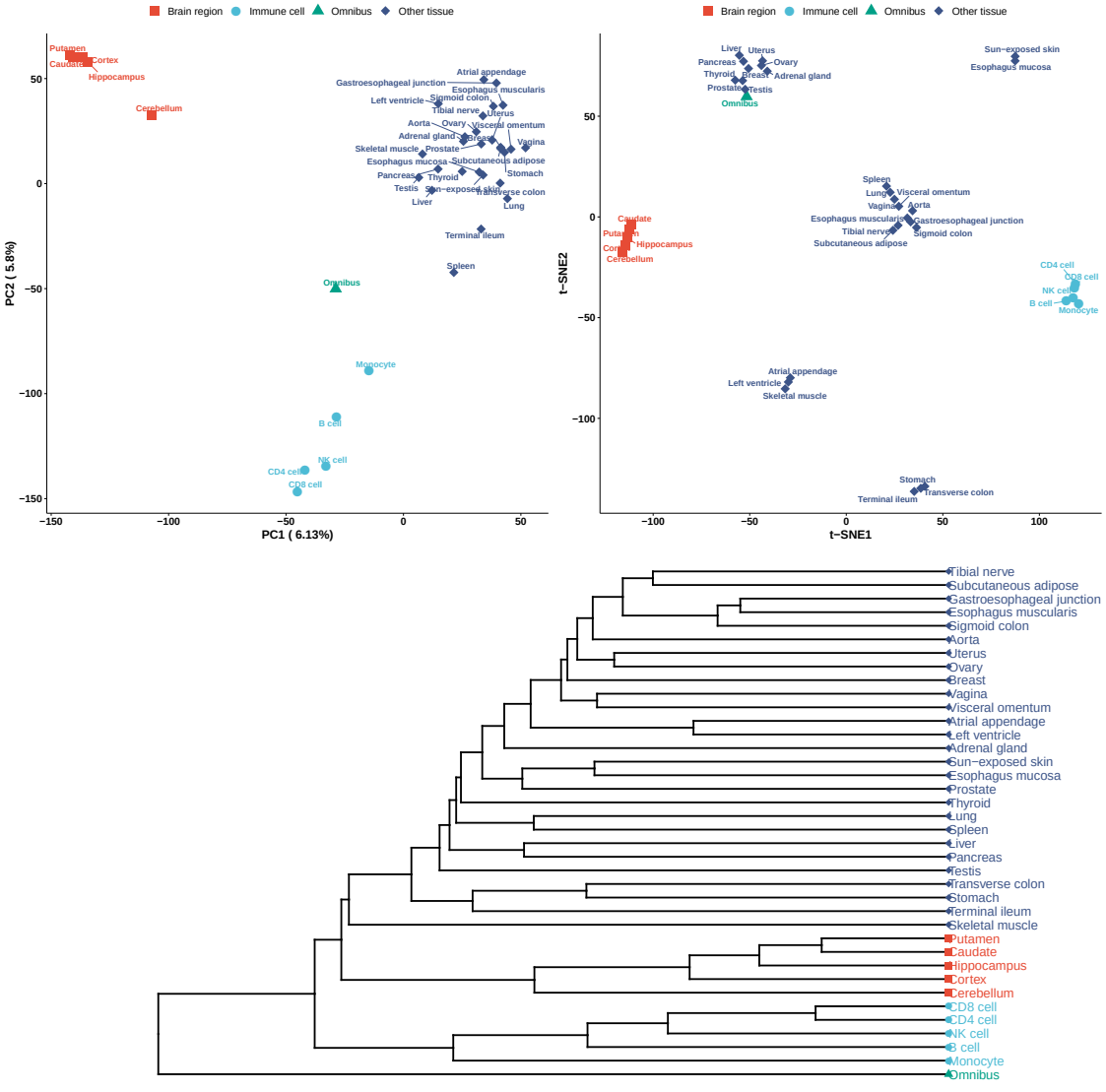

Panel **e** Here the input data matrix is obtained by concatenating the previous 4 data matrices vertically, with a total of 2,184,131 rows and 38 columns (networks).

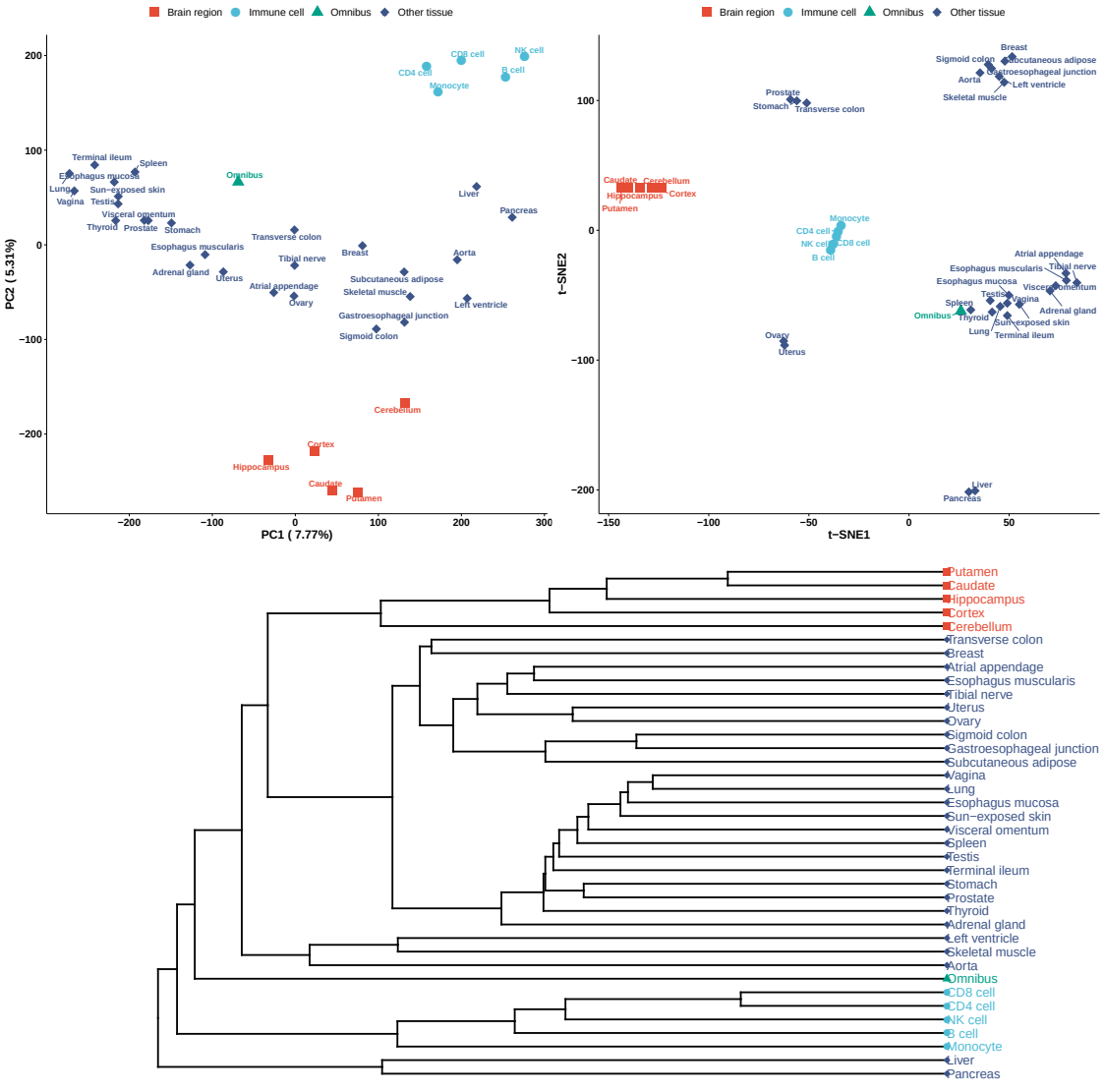

Supplementary Figure 12

Additional results for Figure 5(b). Each panel below shows the node and edge similarities between a given cell type- or tissue-specific PECA-based network (panel caption: cell type or tissue) and CAGE-based networks for 394 cell types and tissues (Marbach et al. 2016) inferred from independent CAGE data (Andersson et al. 2014; The FANTOM Consortium and the RIKEN PMI and CLST (DGT) 2014). In each panel, each point represents a context-specific CAGE-based network, where x- and y-axis values indicate its node and edge set similarity with the given PECA network respectively. For both node and edge sets, the similarity is measured by Jaccard index (the size of the intersection divided by the size of the union).

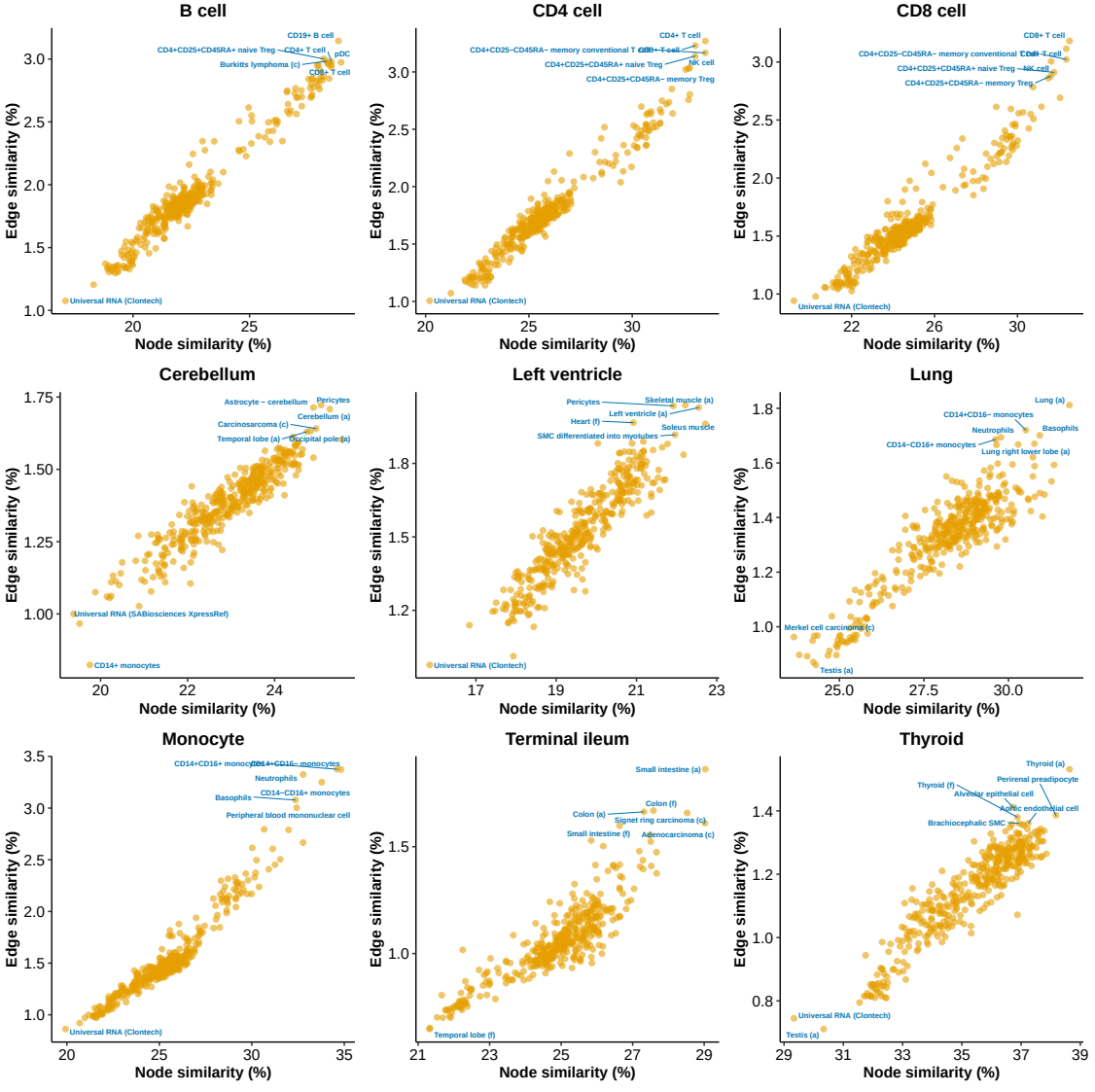

Supplementary Figure 13

RSS-NET results with zero TF-TG edge weights. Here we repeat RSS-NET analyses of 11 GWAS traits on 38 TF-TG regulatory networks by setting all TF-TG edge weights zero (i.e., $v_{gt} = 0$ in main text Equation 5). Each panel below corresponds to one of 11 GWAS traits that pass the near-gene enrichment control for all 38 networks in our original analyses using actual TF-TG edge weights (**Supplementary Table 3**). We remove myocardial infarction since it is a subtype of coronary artery disease. In each panel, each point represents one of the 38 regulatory networks. The x- and y-axis values of each point are log 10 BFs (M_1 against M_0) based on zero and actual edge weights of a network respectively. All diagonal lines have slope 1 and intercept 0. Numerical values are available at https://suwonglab.github.io/rss-net/results.html.

For 10 out 11 traits, BFs based on actual edge weights are unanimously larger than BFs based on zero edge weights across all 38 networks (i.e., all dots above the diagonal line). The only exception is low-density lipoprotein cholesterol, for which BFs based on actual edge weights and BFs based on zero edge weights are not significantly different from zero across 38 networks (Wilcoxon $P = 0.91$).

Of note, setting TF-TG edge weights zero is different from setting the edge enrichment parameter σ^2 zero (see main text Equations 2 and 5-6). Setting edge weights zero induces the following effect size distribution: $\beta_j \sim \pi_j \cdot \mathcal{N}(\sum_{g \in \mathbf{G}_j} c_{jg} \cdot \gamma_{jg},\ \sigma_0^2) + (1-\pi_j) \cdot \delta_0,\ \gamma_{jg} \sim \mathcal{N}(0,\ \sigma^2)$. where $\{\mathbf{G}_j, c_{jg}, \gamma_{jg}\}$ are defined in main text Equations 5-6. Setting $\sigma^2 = 0$ induces a different effect size distribution: $\beta_j \sim \pi_j \cdot \mathcal{N}(0,\ \sigma_0^2) + (1-\pi_j) \cdot \delta_0$.

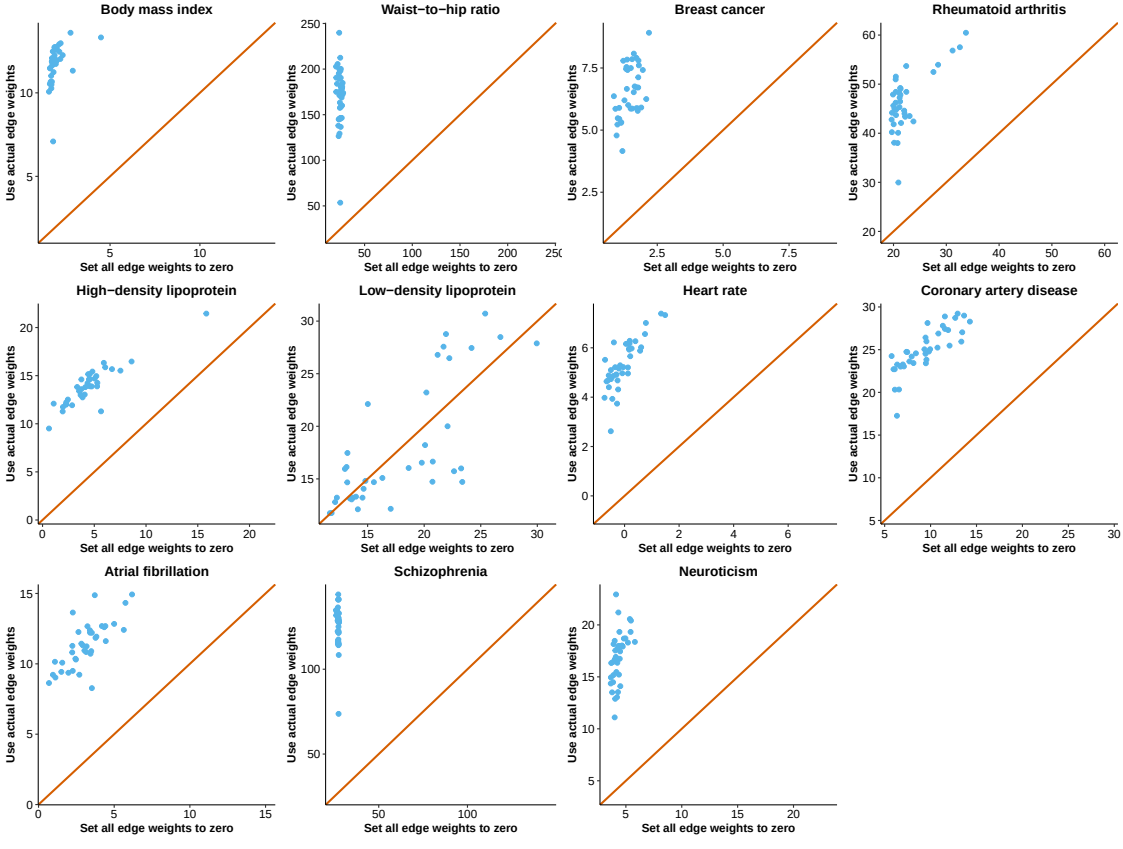

Supplementary Figure 14

Additional results for Figure 5(d). Each panel below shows the comparison of PECA- and CAGE-based network enrichments on the same cell types or tissues (labels) and the same GWAS data (caption). In each panel, each point represents a context (cell type or tissue), where x- and y-axis show the RSS-NET log 10 enrichment BFs for the CAGE- and PECA-based networks in this context respectively. Given a context, the analyzed CAGE- and PECA-based networks have the same TF-TG edge counts, and their edge weights are on the same scale (see main text Methods section). The RSS-NET analyses of CAGE- and PECA-based networks use the same hyper-parameter grids (**Supplementary Table 19**). All dashed lines have slope 1 and intercept 0. Numerical values are available at https://suwonglab.github.io/rss-net/results.html.

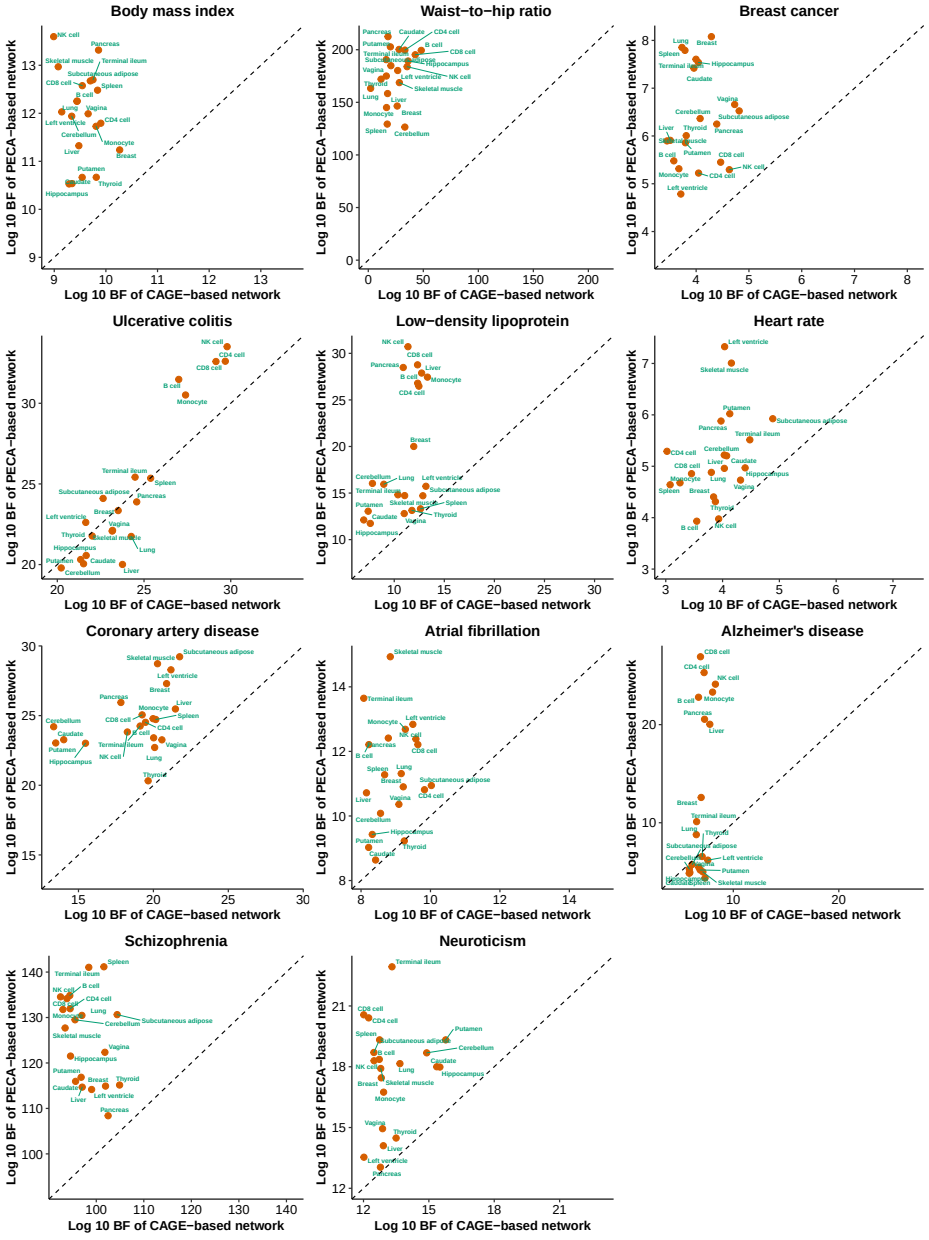

Supplementary Figure 15

Overlap between RSS-NET prioritized genes and genes from external databases. In each panel, each point represents a pair of GWAS trait and knockout mouse phenotype (left) or human Mendelian disorder (right). For each point, the log odds ratio (OR) is produced by running R built-in function `fisher.test` on the following 2 by 2 table:

	Query genes	Other genes
Genes with $P_1^{\text{bma}} \geq 0.9$		
Genes with $P_1^{\text{bma}} < 0.9$		

For the left panel, "query genes" correspond to genes that are implicated in one of 27 categories of knockout mouse phenotypes (Bult et al. 2019), and "other genes" correspond to genes that are not implicated in any mouse phenotype. For the right panel, "query genes" correspond to genes that are implicated in one of 19 categories of Mendelian disorders (Freund et al. 2018; Amberger et al. 2019), and "other genes" correspond to genes that are not implicated in any Mendelian disorder. For all points, the log ORs shown on the x-axis are estimated from all genes, and the log ORs shown on the y-axis are estimated after excluding genes that are implicated in GWAS of the same trait at the time of analysis (**Supplementary Table 10**). The OR values and associated P-values are available in **Supplementary Tables 12-13**. The diagonal lines have slope 1 and intercept 0.

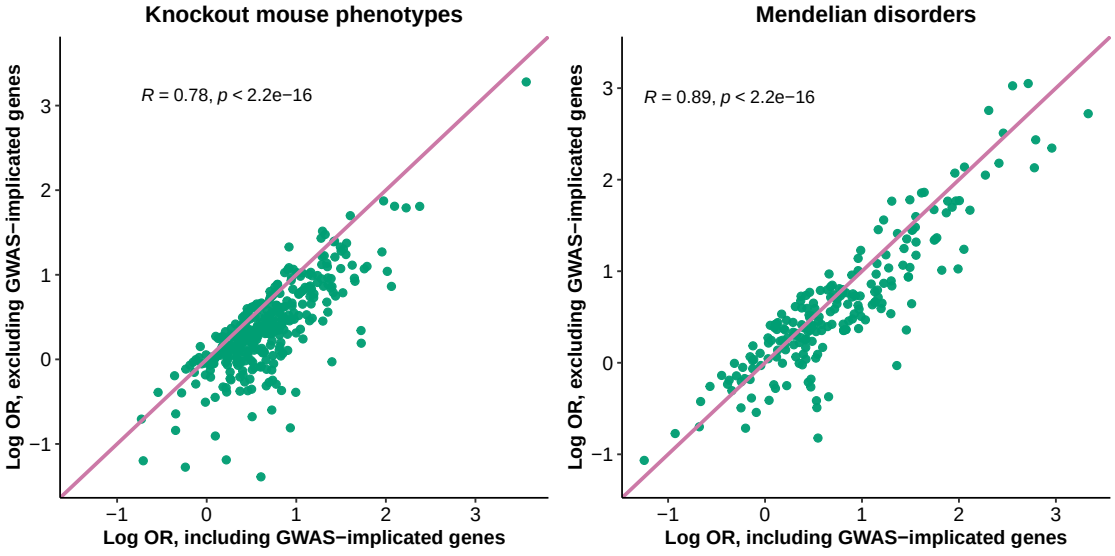

Supplementary Figure 16

Posterior estimation of $\{\sigma,\theta\}$ in simulations. Similar to our calculation of P_1 (20), we estimate the posterior means of $\{\sigma,\theta\}$ as:

$$\mathrm{E}(\sigma \mid \mathbf{D}) \approx \sum_{s=1}^{n_1} \sigma^{(s)} \cdot \omega^{\star}(\theta_0^{(s)},\theta^{(s)},\sigma_0^{(s)},\sigma^{(s)}),$$
$$\mathrm{E}(\theta \mid \mathbf{D}) \approx \sum_{s=1}^{n_1} \theta^{(s)} \cdot \omega^{\star}(\theta_0^{(s)},\theta^{(s)},\sigma_0^{(s)},\sigma^{(s)}),$$

where $\omega^{\star}(\theta_0,\theta,\sigma_0,\sigma)$ is a discrete approximation to the joint posterior of hyper-parameters $\{\theta_0,\theta,\sigma_0,\sigma\}$; see (16). The x-axis indicates the simulation scenarios (true hyper-parameter values of the positive datasets and the target network); see **Supplementary Figures 1-2**. Each box contains results of 200 independent positive datasets for a given scenario. Horizontal dashed lines indicate true values of $\{\sigma,\theta\}$.

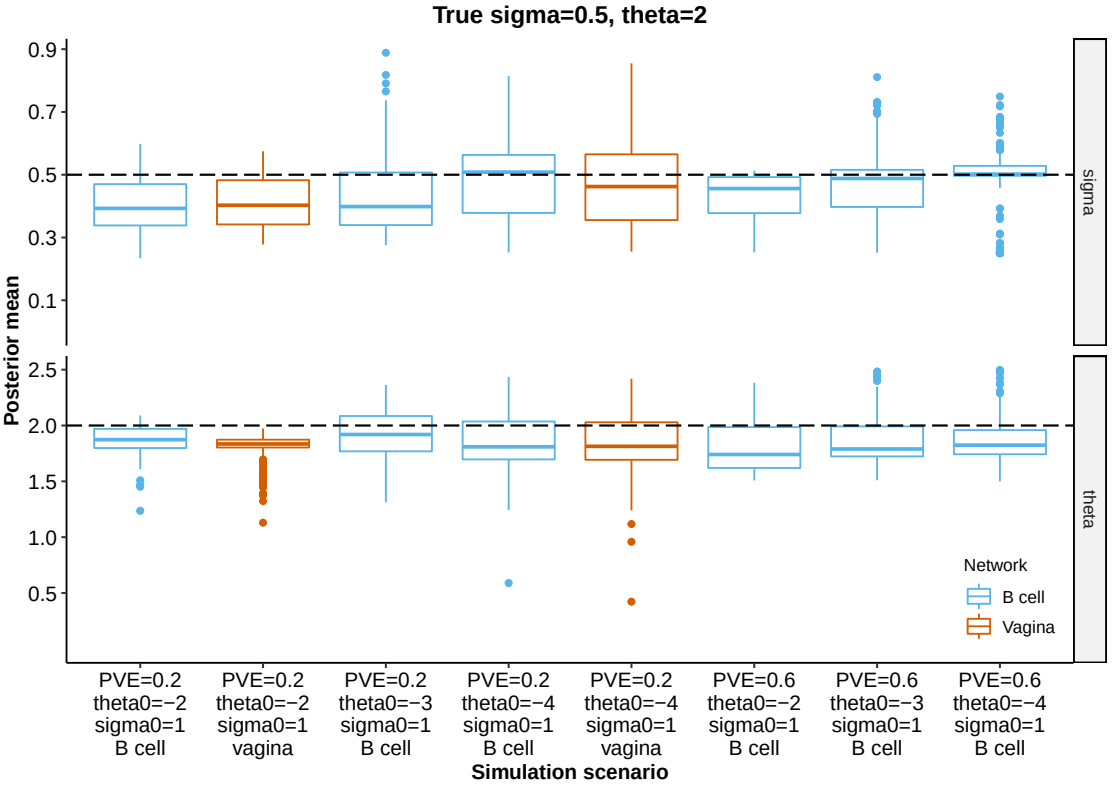

Supplementary Figure 17

Robustness of RSS-NET to σ specification in simulations. Here we repeat RSS-NET analyses of simulated datasets with a fixed value of $\sigma \in \{0.25, 0.5, 0.75, 1\}$. In our original analyses we use a model averaging approach (18) to account for the uncertainty of hyper-parameters.

Panel **a** The simulated negative and positive GWAS summary data are the same as those from **Supplementary Figures 1-2**. The caption of each plot shows the true hyper-parameter values of positive datasets and the target network for enrichment testing.

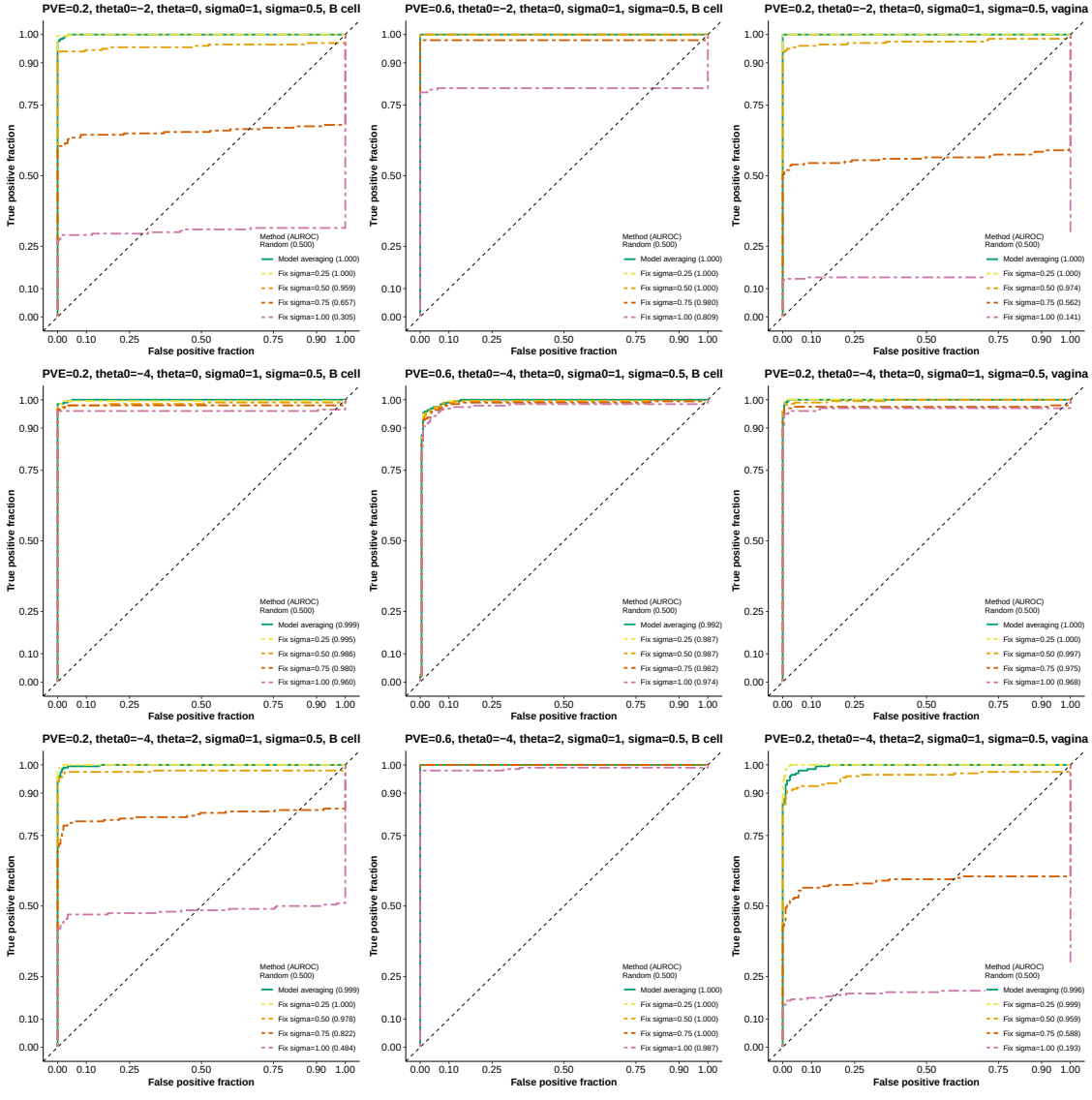

Panel **b** Each plot corresponds to a positive simulation scenario with 200 independent datasets, and its caption indicates the true hyper-parameter values and the target network. In each plot, each point represent a simulated positive dataset. The y-axis value of each point is the log 10 enrichment BF when the value of σ is fixed as 0.5 (ground truth). The x-axis value of each point is the log 10 BF under other σ specifications (differentiated by point shape and color). The dashed lines have slope 1 and intercept 0. The number "$(a$ / $200 - a)$" in each legend indicates that BFs based on $\sigma = 0.5$ are higher than BFs based on other σ specifications in a simulated datasets for this scenario.

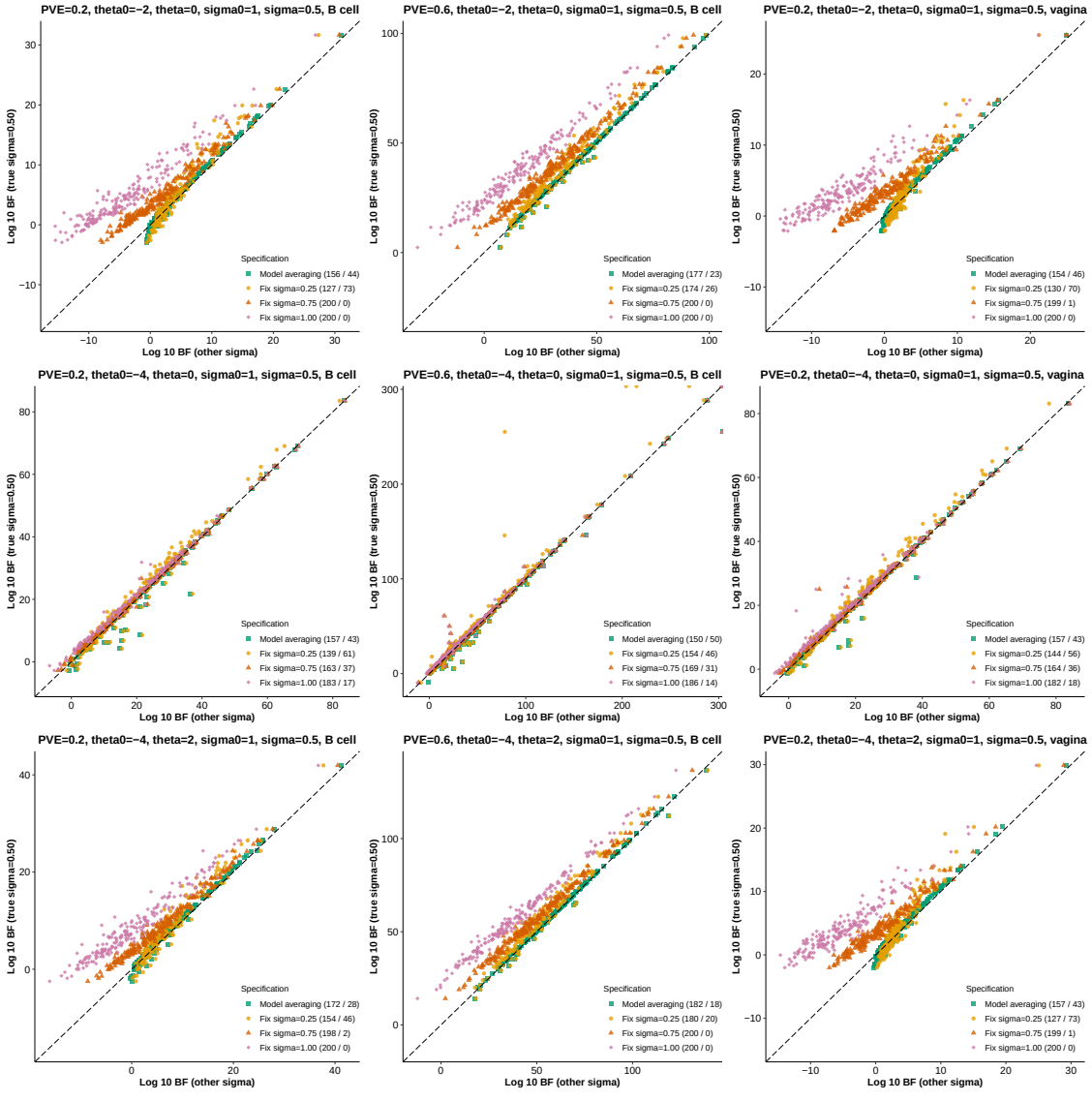

Concluding Remark: Apart from hyper-parameters, RSS-NET uses approximations in the likelihood function (Zhu and Stephens 2017) and the variational inference (Zhu and Stephens 2018). Hence, setting σ as ground truth does not guarantee the optimal outcome in some simulated datasets. Instead we recommend the model averaging approach (18) as used in our main analyses.

Supplementary Figure 18

Robustness of RSS-NET to hyper-parameter grid choice in real data. For three GWAS datasets, we run RSS-NET on 38 networks with two different hyper-parameter grids (grid 1: coarse; grid 2: focused), and then compare results of network enrichments (BF, top panels) and gene associations (P_1^{net}, bottom panels). In each enrichment comparison plot, each point represents a network. In each association comparison plot, each point represent a gene-network pair. All diagonal lines have slope 1 and intercept 0.

Panel **a** Alzheimer's disease (Lambert et al. 2013). In grid 1, $\theta \in (0 : 0.5 : 4)$. In grid 2, $\theta \in (0 : 0.25 : 1)$. For both grids, $\eta = 0.6$, $\rho \in (0 : 0.2 : 0.8)$ and $\theta_0 \in (-5.25 : 0.1 : -4.75)$. Panel **b** low-density lipoprotein (Teslovich et al. 2010). In grid 1, $\theta \in (0 : 0.5 : 3)$. In grid 2, $\theta \in (0 : 0.25 : 1)$. For both grids, $\eta = 0.3$, $\rho \in (0 : 0.2 : 0.8)$ and $\theta_0 \in (-3.75 : 0.05 : -3.5)$. Panel **c** inflammatory bowel disease (Liu et al. 2015). In grid 1, $\theta \in (0 : 0.5 : 3)$. In grid 2, $\theta \in (0 : 0.25 : 1)$. For both grids, $\eta = 0.3$, $\rho \in (0 : 0.2 : 0.8)$ and $\theta_0 \in (-3 : 0.05 : -2.8)$.

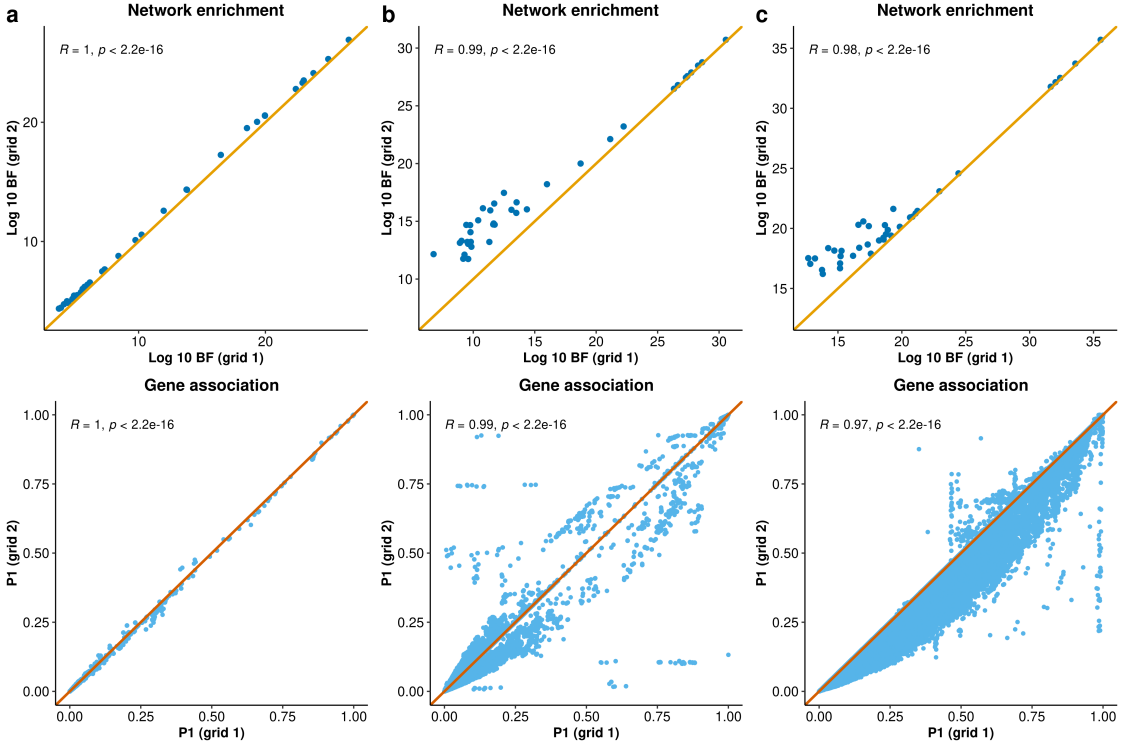

Supplementary Figure 19

Comparison of two LDSC output statistics in simulations. On each simulated dataset two LDSC methods, LDSC-baseline (Finucane et al. 2015) and LDSC-baselineLD (Gazal et al. 2017), are used to test network enrichments. Each LDSC method produces two statistics, enrichment P-value (denoted as `Enrichment_p` in the software) and enrichment coefficient Z-score (`Coefficient_z-score`), both of which can be used to rank the significance of enrichments. In each panel, each point represent a simulation scenario that contains 200 positive and 200 negative independent datasets (**Supplementary Figures 1-6 and 9**). The x- and y-axis of each point show AUROC values evaluated on the basis of enrichment P-value and coefficient Z-score respectively. In total there are 89 simulation scenarios of assessing network enrichments in this study, and thus each panel below consists of 89 points. The diagonal lines in both panels have slope 1 and intercept 0.

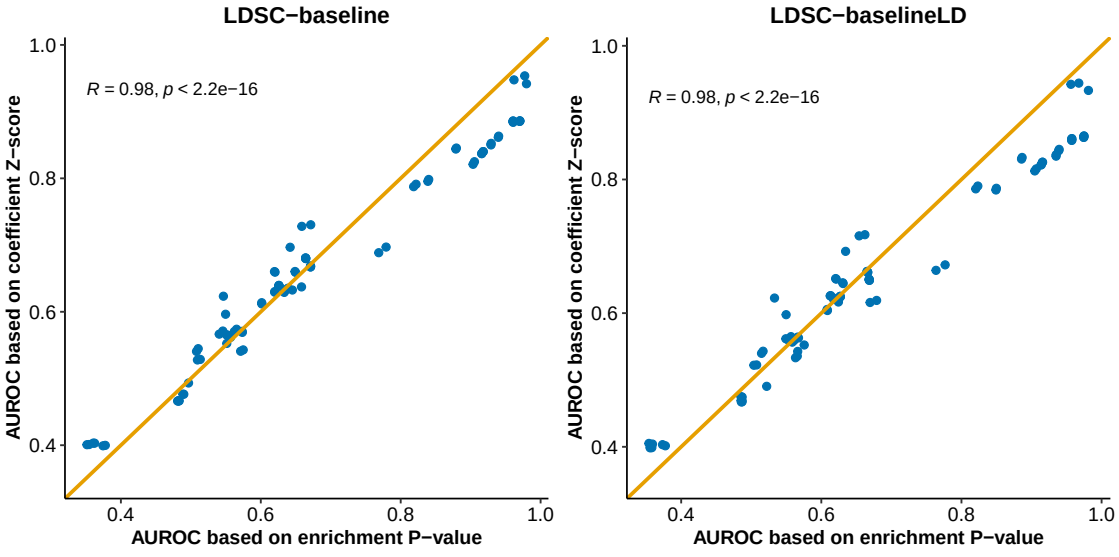

Supplementary Tables

Supplementary Table 1

Paired high-throughput sequencing data of gene expression and chromatin accessibility from 207 biosamples that are used to construct 38 TF-TG regulatory networks.

ID	Cell type or tissue	Expression ID	Accessibility ID	Network
1	Hematopoietic MPP cell	ENCSR000CUA	ENCSR115YPI	Omnibus
2	G-CSF-mobilized HSC	GSM909310	GSM530657	Omnibus
3	Fetal adrenal gland	GSM1220584	GSM530653	Omnibus
4	CD4 primary cell	GSM1059487	GSM665839	CD4 cell; Omnibus
5	CD8 primary cell	GSM1060237	GSM665838	CD8 cell; Omnibus
6	Primary monocyte	GSM1220575	GSM701541	Monocyte; Omnibus
7	Primary B cell	GSM1220576	GSM701507	B cell; Omnibus
8	Primary T cell	GSM1220574	GSM701516	Omnibus
9	CD4 primary cell	GSM1060238	GSM701539	CD4 cell; Omnibus
10	Primary NK cell	GSM1220577	GSM701508	NK cell; Omnibus
11	CD8 primary cell	GSM1060239	GSM701540	CD8 cell; Omnibus
12	Fetal intestine large	GSM1059485	GSM701495	Omnibus
13	Fetal intestine large	GSM1059509	GSM701531	Omnibus
14	Fetal intestine small	GSM1059486	GSM701496	Omnibus
15	Fetal intestine small	GSM1059508	GSM701530	Omnibus
16	Fetal kidney	GSM1059512	GSM701515	Omnibus
17	Fetal renal cortex	GSM1059496	GSM701529	Omnibus
18	Fetal renal cortex	GSM1059515	GSM701532	Omnibus
19	Fetal renal cortex, right	GSM1059498	GSM701517	Omnibus
20	Fetal renal pelvis, left	GSM1059514	GSM701520	Omnibus
21	Fetal renal pelvis, right	GSM1059500	GSM701518	Omnibus
22	Fetal lung, left	GSM1101684	GSM701524	Omnibus
23	Fetal lung, left	GSM1101685	GSM701527	Omnibus
24	Fetal lung, left	GSM1101687	GSM701534	Omnibus
25	Fetal lung, right	GSM1101683	GSM701523	Omnibus
26	Fetal muscle, arm	GSM1101689	GSM701535	Omnibus
27	Fetal muscle, back	GSM1101690	GSM701536	Omnibus
28	Fetal muscle trunk	GSM1101688	GSM701533	Omnibus
29	Fetal muscle, upper limb	GSM1101686	GSM701522	Omnibus
30	Fetal spleen	GSM1220588	GSM701509	Omnibus
31	Fetal stomach	GSM1220587	GSM701521	Omnibus
32	Fetal stomach	GSM1220583	GSM701538	Omnibus
33	Fetal stomach	GSM1220594	GSM701538	Omnibus
34	Fetal thymus	GSM1220591	GSM701497	Omnibus
35	Fetal thymus	GSM1220593	GSM701537	Omnibus
36	Fetal thymus	GSM1220593	GSM774230	Omnibus
37	Fetal intestine large	GSM1059516	GSM774213	Omnibus
38	Fetal intestine large	GSM1059518	GSM774220	Omnibus
39	Fetal intestine large	GSM1059520	GSM774228	Omnibus
40	Treg primary cell	GSM1059522	GSM774233	Omnibus
41	Treg primary cell	GSM1059507	GSM774216	Omnibus
42	Fetal renal pelvis	GSM1059524	GSM774222	Omnibus
43	Fetal lung, right	GSM1101691	GSM774227	Omnibus
44	Fetal lung, right	GSM1101692	GSM774231	Omnibus
45	Fetal muscle, arm	GSM1101694	GSM774226	Omnibus

(continued)

ID	Cell type or tissue	Expression ID	Accessibility ID	Network
46	Fetal muscle, arm	GSM1101695	GSM774234	Omnibus
47	Fetal muscle, arm	GSM1101682	GSM774239	Omnibus
48	Fetal muscle, back	GSM1220596	GSM774224	Omnibus
49	Fetal muscle, back	GSM1101696	GSM774235	Omnibus
50	Fetal muscle leg	GSM1101698	GSM774242	Omnibus
51	Fetal muscle, lower limb	GSM1101697	GSM774238	Omnibus
52	Treg primary cell	GSM1220590	GSM774212	Omnibus
53	Treg primary cell	GSM1220597	GSM774232	Omnibus
54	FK primary cell	GSM941745	GSM817196	Omnibus
55	FK primary cell	GSM941745	GSM817197	Omnibus
56	FF primary cell	GSM941744	GSM817169	Omnibus
57	FF primary cell	GSM941744	GSM817170	Omnibus
58	Melanocyte	GSM941743	GSM1027307	Omnibus
59	Melanocyte	GSM941743	GSM1027312	Omnibus
60	Fetal adrenal gland	GSM1059505	GSM817165	Omnibus
61	Fetal adrenal gland	GSM1059525	GSM817167	Omnibus
62	Fetal heart	GSM1059495	GSM817220	Omnibus
63	Fetal kidney	GSM1059510	GSM817159	Omnibus
64	Fetal kidney, left	GSM1059526	GSM817181	Omnibus
65	Fetal renal cortex, left	GSM1059528	GSM817190	Omnibus
66	Fetal renal cortex, left	GSM1059489	GSM817203	Omnibus
67	Fetal renal cortex, left	GSM1059492	GSM817211	Omnibus
68	Fetal renal cortex, right	GSM1059488	GSM817202	Omnibus
69	Fetal renal cortex, right	GSM1059499	GSM817210	Omnibus
70	Treg primary cell	GSM1059493	GSM817218	Omnibus
71	Fetal renal pelvis, left	GSM1059491	GSM817193	Omnibus
72	Fetal renal pelvis, left	GSM1059504	GSM817205	Omnibus
73	Fetal renal pelvis, left	GSM1059503	GSM817209	Omnibus
74	Fetal renal pelvis, right	GSM1059490	GSM817192	Omnibus
75	Fetal renal pelvis, right	GSM1059502	GSM817204	Omnibus
76	Fetal renal pelvis, right	GSM1059501	GSM817208	Omnibus
77	Fetal lung, left	GSM1101693	GSM817168	Omnibus
78	Fetal lung, left	GSM1101699	GSM817175	Omnibus
79	Fetal lung, left	GSM1101708	GSM817185	Omnibus
80	Fetal lung, right	GSM1101707	GSM817174	Omnibus
81	Fetal lung, right	GSM1101709	GSM817186	Omnibus
82	Fetal muscle, arm	GSM1101701	GSM817178	Omnibus
83	Fetal muscle, arm	GSM1101710	GSM817191	Omnibus
84	Fetal muscle, arm	GSM1101674	GSM817214	Omnibus
85	Fetal muscle, arm	GSM1101675	GSM817216	Omnibus
86	Fetal muscle, back	GSM1101703	GSM817171	Omnibus
87	Fetal muscle, back	GSM1101704	GSM817182	Omnibus
88	Fetal muscle, back	GSM1101661	GSM817200	Omnibus
89	Fetal muscle, back	GSM1101663	GSM817207	Omnibus
90	Fetal muscle, back	GSM1101677	GSM817217	Omnibus
91	Fetal muscle leg	GSM1101705	GSM817179	Omnibus
92	Fetal muscle leg	GSM1101706	GSM817183	Omnibus
93	Fetal muscle leg	GSM1101664	GSM817206	Omnibus
94	Fetal muscle leg	GSM1101671	GSM817213	Omnibus
95	Fetal muscle, back	GSM1101676	GSM817212	Omnibus

(continued)

ID	Cell type or tissue	Expression ID	Accessibility ID	Network
96	Fetal spinal cord	GSM1101711	GSM817189	Omnibus
97	Treg primary cell	GSM1220598	GSM817173	Omnibus
98	Treg primary cell	GSM1220600	GSM817199	Omnibus
99	Fetal thymus	GSM1220599	GSM817172	Omnibus
100	Fibroblasts, fetal skin	GSM1101681	GSM878635	Omnibus
101	Fibroblasts, fetal skin	GSM1101666	GSM878623	Omnibus
102	Fibroblasts, fetal skin	GSM1101667	GSM878634	Omnibus
103	Fibroblasts, fetal skin	GSM1101668	GSM878633	Omnibus
104	Fetal heart	GSM1059494	GSM878630	Omnibus
105	Fetal renal cortex	GSM1059497	GSM878629	Omnibus
106	Fetal muscle, arm	GSM1101700	GSM878610	Omnibus
107	Fetal muscle, arm	GSM1101673	GSM878625	Omnibus
108	Fetal muscle, back	GSM1101678	GSM878632	Omnibus
109	Fetal muscle leg	GSM1101670	GSM878626	Omnibus
110	Fetal muscle leg	GSM1101672	GSM878631	Omnibus
111	Fetal muscle leg	GSM1220579	GSM878653	Omnibus
112	Fetal muscle trunk	GSM1220582	GSM878654	Omnibus
113	Treg primary cell	GSM1220581	GSM878659	Omnibus
114	Fetal spinal cord	GSM1220580	GSM878661	Omnibus
115	Fetal thymus	GSM1220578	GSM878657	Omnibus
116	Pancreas	GSM1010966	GSM1027326	Omnibus
117	Gastric	GSM1010960	GSM1027325	Omnibus
118	Ovary	GSM1010948	GSM1027334	Omnibus
119	Gastric	GSM1120306	GSM1027320	Omnibus
120	Psoas Muscle	GSM1120310	GSM1027321	Omnibus
121	Pancreas	GSM1120309	GSM1027335	Omnibus
122	Fetal adrenal gland	GSM1060240	GSM1027310	Omnibus
123	Fetal adrenal gland	GSM1060241	GSM1027311	Omnibus
124	Fetal ovary	GSM1101662	GSM1027306	Omnibus
125	Fetal spinal cord	GSM1101679	GSM1027308	Omnibus
126	Fetal kidney	GSM1059523	GSM774221	Omnibus
127	BE2C	ENCSR000BYK	ENCFF001CNX	Omnibus
128	BJ	ENCSR000COP	ENCFF001COH	Omnibus
129	GM12878	ENCSR000AEE	ENCFF000SKV	Omnibus
130	H1 BMP4-derived TB cell	ENCSR762CJN	ENCFF983HYM	Omnibus
131	H1-hESC	ENCSR000COU	ENCFF876IHU	Omnibus
132	H7-hESC	ENCSR490SQH	ENCFF000SOL	Omnibus
133	HeLa-S3	ENCSR552EGO	ENCFF000SPR	Omnibus
134	HepG2	ENCSR931WGT	ENCFF000SQJ	Omnibus
135	Jurkat	ENCSR000BXX	ENCFF001DOT	Omnibus
136	K562	ENCSR000CPH	ENCFF000SWS	Omnibus
137	MCF-7	ENCSR000CPT	ENCFF000SYX	Omnibus
138	Panc1	ENCSR000BYM	ENCFF001EDO	Omnibus
139	T47D	ENCSR000BYF	ENCFF000TET	Omnibus
140	Testis	ENCFF673KOG	ENCFF048IOT	Testis; Omnibus
141	Testis	ENCFF438ZIY	ENCFF066TTB	Testis; Omnibus
142	Stomach	ENCFF155AGD	ENCFF025QEQ	Stomach; Omnibus
143	Stomach	ENCFF930JZC	ENCFF184XKI	Stomach; Omnibus
144	Stomach	ENCFF535HFG	ENCFF758MDE	Stomach; Omnibus
145	Ovary	ENCFF232UER	ENCFF420ECZ	Ovary; Omnibus

(continued)

ID	Cell type or tissue	Expression ID	Accessibility ID	Network
146	Ovary	ENCFF957VSL	ENCFF247HQX	Ovary; Omnibus
147	Uterus	ENCFF624VKT	ENCFF678QTC	Uterus; Omnibus
148	Vagina	ENCFF855LJY	ENCFF243NYB	Vagina; Omnibus
149	Liver	ENCFF347TXW	ENCFF244IRQ	Liver; Omnibus
150	Pancreas	ENCFF204BZU	ENCFF011ZXN	Pancreas; Omnibus
151	Pancreas	ENCFF368OME	ENCFF646IYT	Pancreas; Omnibus
152	Transverse colon	ENCFF874CRV	ENCFF629OKO	Transverse colon; Omnibus
153	Transverse colon	ENCFF505DGK	ENCFF159DOO	Transverse colon; Omnibus
154	Transverse colon	ENCFF332OML	ENCFF746GDH	Transverse colon; Omnibus
155	Transverse colon	ENCFF014IOZ	ENCFF715LGJ	Transverse colon; Omnibus
156	Sigmoid colon	ENCFF934VJV	ENCFF482HAC	Sigmoid colon; Omnibus
157	Sigmoid colon	ENCFF192TOO	ENCFF387OFS	Sigmoid colon; Omnibus
158	Sigmoid colon	ENCFF179AVF	ENCFF692DLP	Sigmoid colon; Omnibus
159	Sigmoid colon	ENCFF146ISW	ENCFF754DCA	Sigmoid colon; Omnibus
160	Terminal ileum	ENCFF336EQS	ENCFF748WZP	Terminal ileum; Omnibus
161	Terminal ileum	ENCFF187NLN	ENCFF474HAC	Terminal ileum; Omnibus
162	Terminal ileum	ENCFF715EVL	ENCFF603CAV	Terminal ileum; Omnibus
163	Tibial nerve	ENCFF904FEZ	ENCFF226ZCG	Tibial nerve; Omnibus
164	Tibial nerve	ENCFF241VXT	ENCFF372VAD	Tibial nerve; Omnibus
165	Aorta	ENCFF127YOW	ENCFF984OPE	Aorta; Omnibus
166	Thyroid	ENCFF625QLJ	ENCFF942YPH	Thyroid; Omnibus
167	Thyroid	ENCFF376HXE	ENCFF743DWF	Thyroid; Omnibus
168	Thyroid	ENCFF194VCC	ENCFF611LJR	Thyroid; Omnibus
169	Thyroid	ENCFF509HKT	ENCFF530YPZ	Thyroid; Omnibus
170	Left ventricle	ENCFF470AAE	ENCFF702IJE	Left ventricle; Omnibus
171	Left ventricle	ENCFF870BQB	ENCFF906UQF	Left ventricle; Omnibus
172	Spleen	ENCFF087VIO	ENCFF294ZCT	Spleen; Omnibus
173	Spleen	ENCFF916TWO	ENCFF183HFJ	Spleen; Omnibus
174	Subcutaneous adipose	ENCFF967YNU	ENCFF159RKV	Subcutaneous adipose; Omnibus
175	Prostate	ENCFF454GAP	ENCFF007NTA	Prostate; Omnibus
176	Prostate	ENCFF110THT	ENCFF670GFY	Prostate; Omnibus
177	Adrenal gland	ENCFF254VJQ	ENCFF970LXV	Adrenal gland; Omnibus
178	Adrenal gland	ENCFF250FNI	ENCFF374OSU	Adrenal gland; Omnibus
179	Adrenal gland	ENCFF587WDK	ENCFF279GVQ	Adrenal gland; Omnibus
180	Adrenal gland	ENCFF036ERC	ENCFF430AHU	Adrenal gland; Omnibus
181	Sun-exposed skin	ENCFF153NMV	ENCFF238BRB	Sun-exposed skin; Omnibus
182	Gastroesophageal junction	ENCFF338HIM	ENCFF293BRN	Gastroesophageal junction; Omnibus
183	Gastroesophageal junction	ENCFF749AJA	ENCFF765DRX	Gastroesophageal junction; Omnibus
184	Esophagus muscularis	ENCFF660MOE	ENCFF208ILP	Esophagus muscularis; Omnibus
185	Esophagus muscularis	ENCFF650KLZ	ENCFF762MNF	Esophagus muscularis; Omnibus
186	Atrial appendage	ENCFF406YAV	ENCFF513LVE	Atrial appendage; Omnibus
187	Atrial appendage	ENCFF701KTC	ENCFF939RTU	Atrial appendage; Omnibus
188	Esophagus mucosa	ENCFF560ZBX	ENCFF846JID	Esophagus mucosa; Omnibus
189	Esophagus mucosa	ENCFF301YAH	ENCFF542ZZY	Esophagus mucosa; Omnibus
190	Breast	ENCFF557XAK	ENCFF589ACB	Breast; Omnibus
191	Breast	ENCFF912TDO	ENCFF585YAB	Breast; Omnibus
192	Lung	ENCFF049ETK	ENCFF022PJN	Lung; Omnibus
193	Lung	ENCFF841RGX	ENCFF985OXZ	Lung; Omnibus
194	Lung	ENCFF360GZR	ENCFF803ZER	Lung; Omnibus
195	Visceral omentum	ENCFF324LPM	ENCFF519QGD	Visceral omentum; Omnibus

(continued)

ID	Cell type or tissue	Expression ID	Accessibility ID	Network
196	Visceral omentum	ENCFF766ECG	ENCFF880CAD	Visceral omentum; Omnibus
197	Skeletal muscle	ENCFF342MON	ENCFF508WVY	Skeletal muscle; Omnibus
198	Skeletal muscle	ENCFF728KWY	ENCFF086TID	Skeletal muscle; Omnibus
199	Skeletal muscle	ENCFF092VEZ	ENCFF461GFF	Skeletal muscle; Omnibus
200	Skeletal muscle	ENCFF151LCI	ENCFF858PLS	Skeletal muscle; Omnibus
201	Skeletal muscle	ENCFF149OTO	ENCFF478ARL	Skeletal muscle; Omnibus
202	Cortex	GTEx V7	ENCSR000EIY	Cortex
203	Cortex	GTEx V7	ENCSR000EIK	Cortex
204	Cerebellum	GTEx V7	ENCSR000EIJ	Cerebellum
205	Caudate	GTEx V7	ENCSR015BGH	Caudate
206	Putamen	GTEx V7	ENCSR493VDS	Putamen
207	Hippocampus	GTEx V7	ENCSR584LUZ	Hippocampus

Supplementary Table 2

GWAS publications, total sample sizes and numbers of genetic variants analyzed by RSS-NET for 18 human traits. Click blue links to view publications online.

Trait (abbreviation)	PMID	# of SNPs (analyzed)	Sample size (cases+controls)
Alzheimer's disease (LOAD)	24162737	1,136,997	17,008+37,154
Neuroticism (NEU)	27089181	1,119,108	170,911
Schizophrenia (SCZ)	25056061	1,113,442	152,805
Body mass index (BMI)	25673413	1,012,465	234,069
Height (HEIGHT)	25282103	1,064,575	253,288
Waist-to-hip ratio (WAIST)	25673412	1,008,898	142,762
Crohn's disease (CD)	26192919	1,064,533	5,956+14,927
Inflammatory bowel disease (IBD)	26192919	1,081,481	12,882+21,770
Rheumatoid arthritis (RA)	24390342	1,158,064	14,361+43,923
Ulcerative colitis (UC)	26192919	1,092,170	6,968+20,464
Breast cancer (BC)	23535729	1,188,902	15,863+40,022
Atrial fibrillation (AF)	28416818	1,175,059	17,931+115,142
Coronary artery disease (CAD)	26343387	1,121,322	60,801+123,504
High-density lipoprotein (HDL)	20686565	1,032,214	99,900
Heart rate (HR)	23583979	1,066,168	92,355
Low-density lipoprotein (LDL)	20686565	1,030,397	95,454
Myocardial infarction (MI)	26343387	1,111,568	42,561+123,504
Type 2 diabetes (T2D)	22885922	1,047,618	12,171+56,862

Supplementary Table 3

To confirm that RSS-NET network enrichment results are unlikely to be driven by generic regulatory enrichments harbored in the vicinity of genes, we perform a "near-gene" control analysis. Specifically, we create a "near-gene" control network with 18,334 protein-coding autosomal genes as nodes and no edges, and then analyze this control with RSS-NET on the same GWAS data for 18 traits. The near-gene control analysis is formalized as:

$$\begin{aligned}
\widehat{\boldsymbol{\beta}} &\sim \mathcal{N}(\widehat{\mathbf{S}}\widehat{\mathbf{R}}\widehat{\mathbf{S}}^{-1}\boldsymbol{\beta},\ \widehat{\mathbf{S}}\widehat{\mathbf{R}}\widehat{\mathbf{S}}),\\
\beta_j &\sim \pi_j \cdot \mathcal{N}(\mu_j,\ \sigma_0^2) + (1-\pi_j)\cdot\delta_0,\\
\pi_j &= 1\ /\ [1+10^{-(\theta_0+a_j\theta)}],\\
\mu_j &= \textstyle\sum_{g\in G_j} c_{jg}\cdot\gamma_{jg},\\
\gamma_{jg} &\sim \mathcal{N}(0,\ \sigma^2),
\end{aligned}$$

where $a_j = 1$ if SNP j is within 100 kb of transcribed region of any protein-coding autosomal gene and $a_j = 0$ otherwise, G_j denotes the set of all protein-coding genes within 1 Mb window of SNP j, and c_{jg} measures the relative impact of SNP j on gene g (derived from eQTLGen *cis*-eQTL results; see **Supplementary Notes**).

Panel **a** Using the same GWAS data of each trait and the same hyper-parameter grid, we compare BFs between each network and the near-gene control under four enrichment models: (1) M_{11}: $\theta > 0$ and $\sigma^2 = 0$; (2) M_{12}: $\theta = 0$ and $\sigma^2 > 0$; (3) M_{13}: $\theta > 0$ and $\sigma^2 > 0$; (4) M_1: $\theta > 0$ or $\sigma^2 > 0$. For all 38 networks and the near-gene control, BF computations are based on the same baseline model (M_0: $\theta = 0$ and $\sigma^2 = 0$). Each row below reports the number of networks with BFs greater than near-gene control BF for each trait and each enrichment model. Trait abbreviations are defined in **Supplementary Table 2**.

	# of networks			
Trait	M_{11}	M_{12}	M_{13}	M_1
AF	32	38	38	38
BC	33	38	38	38
BMI	9	38	38	38
CAD	38	38	38	38
HDL	38	38	38	38
HR	32	38	38	38
LDL	38	38	38	38
MI	38	38	38	38
NEU	33	38	38	38
RA	38	38	38	38
SCZ	9	38	38	38
WAIST	38	38	38	38
UC	38	22	34	34
LOAD	38	13	11	11
IBD	38	0	6	6
T2D	2	0	21	5
CD	38	0	5	0
HEIGHT	38	0	0	0

Panel **b** Using the same GWAS data of each trait and the external methods (LDSC, Pascal), we compare enrichment P-values between each network and the near-gene control. Each row below reports the number of networks with enrichment P-value smaller than near-gene control enrichment P-value for each trait and each external method. Numerical values of LDSC and Pascal analyses are available at https://suwonglab.github.io/rss-net/results.html.

	# of networks					
	LDSC methods		Pascal methods			
Trait	baseline	baselineLD	max-chi	max-emp	sum-chi	sum-emp
RA	38	38	0	0	2	0
IBD	36	37	0	0	0	0
UC	37	37	1	0	1	0
HR	31	36	0	0	0	0
WAIST	37	36	1	0	27	24
CD	32	34	0	0	0	0
BC	28	32	0	2	1	0
MI	31	30	0	0	15	15
CAD	23	23	0	0	8	0
T2D	25	22	0	0	5	6
LDL	24	18	0	0	1	0
NEU	18	16	0	0	0	0
HEIGHT	6	11	0	0	0	0
HDL	6	10	0	0	1	0
AF	5	5	0	0	7	0
LOAD	1	2	0	0	1	1
SCZ	2	2	0	0	0	0
BMI	0	0	0	0	0	0

Supplementary Table 4

We compute Pearson correlations between five network features and log 10 enrichment BFs, either across 512 trait-network pairs that pass the near-gene control (**Supplementary Table 3**), or across all 684 trait-network pairs (18 traits and 38 networks). We use R built-in function `cor.test` for all correlation analyses. All tests are two-sided.

	Pearson R (P-value)	
Network feature	512 pairs	684 pairs
% of SNPs in a network	-0.0304 (0.4925)	-0.0403 (0.2924)
# of TF-TG edges	-0.0092 (0.8353)	0.0025 (0.9479)
# of nodes (TF or TG)	-0.0535 (0.2272)	-0.0422 (0.2702)
# of TGs	-0.0531 (0.2308)	-0.0424 (0.2686)
# of TFs	-0.0403 (0.3625)	-0.0184 (0.6312)

Supplementary Table 5

We compute Pearson correlations between 73 binnary functional annotations in LDSC baselineLD v2.1 (Gazal et al. 2017) and log 10 enrichment BFs, either across 512 trait-network pairs that pass the near-gene control (**Supplementary Table 3**), or across all 684 trait-network pairs (18 traits and 38 networks). Specifically, for a given functional annotation, we estimate the correlation between log 10 BFs and proportion of SNPs falling into both a network and this functional category, across all trait-network pairs. Rows are ranked by Pearson P-values based on 512 trait-network pairs. The Bonferroni cutoff is $0.05/73 = 6.8 \times 10^{-4}$. The rest is the same as **Supplementary Table 4**.

	Pearson R (- log 10 P-value)	
Functional annotation	512 pairs	684 pairs
BivFlnk	-0.1295 (2.4786)	-0.1252 (2.9849)
TSS_Hoffman	-0.1256 (2.3543)	-0.1547 (4.3146)
BivFlnk_500	-0.1195 (2.1668)	-0.1166 (2.6468)
TSS_Hoffman_500	-0.1178 (2.1193)	-0.1465 (3.9183)
H3K9ac_peaks_Trynka	-0.0795 (1.1410)	-0.1041 (2.1907)
Promoter_UCSC_500	-0.0777 (1.1022)	-0.1137 (2.5363)
Promoter_UCSC	-0.0772 (1.0926)	-0.1134 (2.5254)
PromoterFlanking_Hoffman_500	-0.0742 (1.0296)	-0.1125 (2.4941)
Enhancer_Hoffman	-0.0707 (0.9579)	-0.0907 (1.7518)
H3K9ac_Trynka	-0.0704 (0.9521)	-0.0939 (1.8543)
PromoterFlanking_Hoffman	-0.0696 (0.9357)	-0.1144 (2.5616)
H3K4me3_peaks_Trynka	-0.0681 (0.9063)	-0.0941 (1.8597)
Enhancer_Hoffman_500	-0.0671 (0.8879)	-0.0891 (1.7044)
H3K4me3_Trynka	-0.0647 (0.8428)	-0.0903 (1.7393)
WeakEnhancer_Hoffman	-0.0641 (0.8313)	-0.0798 (1.4331)
H3K9ac_Trynka_500	-0.0606 (0.7666)	-0.0852 (1.5871)
SuperEnhancer_Hnisz_500	-0.0596 (0.7490)	-0.0806 (1.4540)
SuperEnhancer_Hnisz	-0.0595 (0.7481)	-0.0804 (1.4496)
Enhancer_Andersson	-0.0590 (0.7386)	-0.0747 (1.2932)
WeakEnhancer_Hoffman_500	-0.0564 (0.6929)	-0.0750 (1.3024)
UTR_5_UCSC_500	-0.0562 (0.6897)	-0.0933 (1.8339)
Enhancer_Andersson_500	-0.0557 (0.6807)	-0.0701 (1.1735)
H3K4me3_Trynka_500	-0.0536 (0.6465)	-0.0796 (1.4284)
TFBS_ENCODE	-0.0522 (0.6230)	-0.0767 (1.3473)
UTR_5_UCSC	-0.0497 (0.5823)	-0.0787 (1.4009)
UTR_3_UCSC_500	-0.0480 (0.5559)	-0.0813 (1.4738)
MAFbin1	-0.0474 (0.5461)	-0.0508 (0.7331)
H3K4me1_peaks_Trynka	-0.0460 (0.5249)	-0.0704 (1.1819)
H3K27ac_PGC2	-0.0453 (0.5144)	-0.0712 (1.2030)
CTCF_Hoffman_500	-0.0447 (0.5043)	-0.0655 (1.0606)
DGF_ENCODE	-0.0432 (0.4828)	-0.0676 (1.1124)
H3K27ac_PGC2_500	-0.0429 (0.4775)	-0.0692 (1.1512)
Coding_UCSC_500	-0.0424 (0.4710)	-0.0753 (1.3093)

(continued)

Functional annotation	Pearson R (- log 10 P-value) 512 pairs	684 pairs
CTCF_Hoffman	-0.0421 (0.4667)	-0.0618 (0.9732)
MAFbin2	-0.0420 (0.4642)	-0.0530 (0.7797)
H3K27ac_Hnisz	-0.0412 (0.4531)	-0.0665 (1.0860)
TFBS_ENCODE_500	-0.0408 (0.4474)	-0.0659 (1.0700)
H3K27ac_Hnisz_500	-0.0402 (0.4386)	-0.0658 (1.0682)
H3K4me1_Trynka	-0.0377 (0.4040)	-0.0643 (1.0314)
FetalDHS_Trynka	-0.0375 (0.4013)	-0.0615 (0.9672)
DHS_peaks_Trynka	-0.0365 (0.3869)	-0.0610 (0.9557)
Transcr_Hoffman	-0.0359 (0.3794)	-0.0728 (1.2426)
MAFbin3	-0.0353 (0.3710)	-0.0557 (0.8365)
DGF_ENCODE_500	-0.0350 (0.3675)	-0.0609 (0.9532)
FetalDHS_Trynka_500	-0.0347 (0.3635)	-0.0589 (0.9067)
DHS_Trynka	-0.0347 (0.3629)	-0.0594 (0.9191)
H3K4me1_Trynka_500	-0.0336 (0.3491)	-0.0606 (0.9464)
Intron_UCSC_500	-0.0330 (0.3412)	-0.0661 (1.0752)
Intron_UCSC	-0.0330 (0.3408)	-0.0662 (1.0768)
non_synonymous	-0.0323 (0.3313)	-0.0639 (1.0221)
DHS_Trynka_500	-0.0318 (0.3259)	-0.0575 (0.8757)
MAFbin4	-0.0310 (0.3156)	-0.0557 (0.8374)
Vertebrate_phastCons46way_500	-0.0309 (0.3136)	-0.0583 (0.8935)
Mammal_phastCons46way_500	-0.0305 (0.3084)	-0.0577 (0.8810)
Transcr_Hoffman_500	-0.0297 (0.2992)	-0.0602 (0.9356)
LindbladToh_500	-0.0296 (0.2972)	-0.0554 (0.8312)
Primate_phastCons46way_500	-0.0293 (0.2933)	-0.0565 (0.8541)
Vertebrate_phastCons46way	-0.0285 (0.2838)	-0.0529 (0.7776)
MAFbin5	-0.0268 (0.2635)	-0.0561 (0.8447)
Mammal_phastCons46way	-0.0267 (0.2618)	-0.0511 (0.7392)
MAFbin6	-0.0263 (0.2581)	-0.0576 (0.8780)
LindbladToh	-0.0248 (0.2402)	-0.0482 (0.6828)
MAFbin9	-0.0244 (0.2348)	-0.0580 (0.8876)
Primate_phastCons46way	-0.0244 (0.2348)	-0.0498 (0.7131)
MAFbin8	-0.0241 (0.2314)	-0.0580 (0.8862)
MAFbin7	-0.0241 (0.2313)	-0.0558 (0.8396)
MAFbin10	-0.0237 (0.2267)	-0.0567 (0.8579)
Coding_UCSC	-0.0236 (0.2266)	-0.0542 (0.8045)
GERP.RSsup4	-0.0227 (0.2163)	-0.0461 (0.6402)
UTR_3_UCSC	-0.0220 (0.2079)	-0.0531 (0.7807)
Repressed_Hoffman_500	-0.0176 (0.1599)	-0.0429 (0.5803)
Repressed_Hoffman	-0.0158 (0.1418)	-0.0411 (0.5472)
synonymous	-0.0135 (0.1191)	-0.0425 (0.5734)

Supplementary Table 6

For 512 network-trait pairs passing the near-gene enrichment control (**Supplementary Table 3**), we compute BFs comparing the baseline model (M_0: $\theta = 0$ and $\sigma^2 = 0$) against three disjoint enrichment models: (1) M_{11}: $\theta > 0$ and $\sigma^2 = 0$; (2) M_{12}: $\theta = 0$ and $\sigma^2 > 0$; (3) M_{13}: $\theta > 0$ and $\sigma^2 > 0$. For each network-trait pair, we compare BFs based on M_{11}, M_{12} and M_{13}, and define the "best" enrichment model as the one with the largest BF. Each row below shows, for each trait, the number of networks with M_{11}, M_{12} and M_{13} being the "best" model, respectively. Trait abbreviations are defined in **Supplementary Table 2**. **Figure 5(c)** is based on the table below.

	# of networks			
Trait	M_{11}	M_{12}	M_{13}	Total
AF	0	0	38	38
BC	0	10	28	38
BMI	0	14	24	38
CAD	0	0	38	38
HDL	0	0	38	38
HR	0	0	38	38
LDL	0	0	38	38
MI	0	0	38	38
NEU	0	0	38	38
RA	0	0	38	38
SCZ	0	38	0	38
WAIST	0	37	1	38
UC	0	0	34	34
LOAD	0	0	11	11
IBD	0	0	6	6
T2D	2	0	3	5
Total	2	99	411	512

Supplementary Table 7

Correlations of RSS-NET enrichment log 10 BFs between 18 traits are computed over all 38 networks. Rows are ranked by Pearson P-values. The Bonferroni cutoff is $0.05/153 = 3.3 \times 10^{-4}$. Trait abbreviations are defined in **Supplementary Table 2**. Genetic correlations computed on the same GWAS summary data are retrieved from Watanabe et al. (2019), `gwasATLAS_v20191115_GC.txt.gz` (https://atlas.ctglab.nl/, accessed June 8, 2020).

		Estimate (- log 10 P-value)	
Trait 1	Trait 2	Log 10 BF correlation	Genetic correlation
CD	IBD	0.9551 (19.8723)	0.9058 (Inf)
IBD	UC	0.9204 (15.5240)	0.9017 (Inf)
LDL	LOAD	0.8969 (13.5933)	0.0682 (0.7100)
CAD	MI	0.8954 (13.4826)	NA (NA)
CD	UC	0.8342 (10.1112)	0.6166 (31.1960)
CD	LDL	0.7969 (8.6674)	-0.0706 (1.3799)
RA	UC	0.7853 (8.2783)	0.0550 (0.4411)
CD	LOAD	0.7791 (8.0795)	-0.1196 (0.7964)
RA	SCZ	0.7676 (7.7266)	-0.0430 (0.7792)
IBD	LOAD	0.7548 (7.3575)	-0.1240 (0.8598)
CAD	HR	0.7526 (7.2965)	-0.0116 (0.0980)
NEU	SCZ	0.7335 (6.7908)	0.1936 (6.5036)
BMI	SCZ	0.7289 (6.6741)	-0.0789 (3.9818)
IBD	LDL	0.7237 (6.5469)	-0.0552 (1.0600)
BMI	MI	0.7131 (6.2964)	NA (NA)
IBD	RA	0.7014 (6.0293)	0.0522 (0.4496)
BMI	CAD	0.6858 (5.6952)	0.2046 (12.4028)
AF	BMI	0.6827 (5.6303)	0.2008 (18.0579)
HR	MI	0.6743 (5.4617)	NA (NA)
BMI	RA	0.6671 (5.3205)	0.0500 (1.2590)
CD	RA	0.6562 (5.1122)	0.0393 (0.2860)
AF	CAD	0.6520 (5.0354)	0.1773 (7.4074)
AF	MI	0.6491 (4.9826)	NA (NA)
CAD	HEIGHT	0.6390 (4.8016)	-0.0963 (4.5005)
HEIGHT	MI	0.6269 (4.5958)	NA (NA)
HDL	LDL	0.6244 (4.5539)	-0.0375 (0.4878)
NEU	RA	0.6050 (4.2420)	-0.0303 (0.2968)
LOAD	UC	0.5880 (3.9847)	-0.1587 (1.0109)
LDL	UC	0.5587 (3.5744)	-0.0548 (0.8752)
AF	HEIGHT	0.5499 (3.4575)	0.2466 (33.5271)
AF	RA	0.5291 (3.1956)	0.0864 (1.9809)
LDL	RA	0.5131 (3.0062)	0.0002 (0.0021)
BMI	HR	0.4912 (2.7597)	-0.0548 (1.1392)
CAD	SCZ	0.4684 (2.5202)	-0.0250 (0.4286)
BMI	NEU	0.4586 (2.4222)	-0.0059 (0.0742)

(continued)

		Estimate (- log 10 *P*-value)	
Trait 1	Trait 2	Log 10 BF correlation	Genetic correlation
HDL	MI	0.4563 (2.3999)	NA (NA)
MI	SCZ	0.4541 (2.3784)	NA (NA)
AF	SCZ	0.4516 (2.3544)	-0.0131 (0.2132)
SCZ	UC	0.4371 (2.2164)	0.1122 (2.5792)
BC	IBD	-0.4332 (2.1810)	0.2826 (2.6405)
AF	HR	0.4170 (2.0364)	-0.0823 (1.0538)
BMI	LDL	0.4158 (2.0256)	0.0215 (0.3918)
LDL	MI	0.4149 (2.0181)	NA (NA)
NEU	UC	0.4034 (1.9198)	0.0998 (1.0578)
BMI	HDL	0.4029 (1.9161)	-0.2589 (18.2255)
HEIGHT	HR	0.4012 (1.9018)	-0.0962 (2.6964)
HDL	LOAD	0.4008 (1.8985)	0.1559 (1.7379)
CAD	HDL	0.3992 (1.8848)	-0.2526 (14.6796)
LOAD	RA	0.3956 (1.8554)	-0.1284 (0.7667)
CD	BC	-0.3949 (1.8495)	0.1349 (0.8437)
BMI	WAIST	0.3773 (1.7091)	-0.0776 (2.5595)
BMI	UC	0.3739 (1.6832)	-0.1015 (2.2981)
CD	HDL	0.3616 (1.5904)	-0.0542 (0.8791)
BC	SCZ	0.3603 (1.5807)	-0.0501 (0.4057)
BMI	HEIGHT	0.3542 (1.5359)	-0.0615 (2.9427)
HR	WAIST	0.3500 (1.5051)	0.0601 (0.8069)
MI	RA	0.3476 (1.4883)	NA (NA)
HR	SCZ	0.3396 (1.4321)	0.0623 (1.0736)
SCZ	WAIST	0.3370 (1.4140)	-0.0044 (0.0574)
BMI	IBD	0.3311 (1.3735)	-0.0424 (0.8890)
CD	MI	0.3303 (1.3683)	NA (NA)
AF	UC	0.3275 (1.3496)	-0.0244 (0.2665)
MI	WAIST	0.3259 (1.3389)	NA (NA)
AF	IBD	0.3241 (1.3270)	0.0035 (0.0341)
BMI	CD	0.3204 (1.3025)	0.0089 (0.1156)
IBD	MI	0.3115 (1.2443)	NA (NA)
BC	LOAD	-0.3000 (1.1721)	0.1410 (0.4095)
NEU	WAIST	0.2963 (1.1493)	0.1167 (3.4213)
BC	HR	0.2956 (1.1455)	-0.0508 (0.2254)
HDL	IBD	0.2956 (1.1450)	-0.0274 (0.3364)
HDL	HEIGHT	0.2921 (1.1240)	-0.0095 (0.1868)
BC	UC	-0.2857 (1.0859)	0.3221 (2.5085)
CAD	WAIST	0.2847 (1.0801)	0.2011 (8.1403)
IBD	SCZ	0.2804 (1.0545)	0.1115 (3.3010)
CAD	T2D	-0.2705 (0.9982)	0.3372 (9.7169)
HEIGHT	LDL	0.2692 (0.9905)	-0.0770 (3.2569)

(continued)

		Estimate (- log 10 *P*-value)	
Trait 1	Trait 2	Log 10 BF correlation	Genetic correlation
HDL	RA	0.2680 (0.9841)	0.0085 (0.1005)
IBD	NEU	0.2674 (0.9804)	0.0633 (0.8834)
MI	UC	0.2648 (0.9661)	NA (NA)
HR	LOAD	-0.2619 (0.9500)	0.0794 (0.4073)
AF	NEU	0.2586 (0.9320)	0.0152 (0.1957)
HR	UC	-0.2579 (0.9284)	0.1382 (1.5419)
HR	IBD	-0.2560 (0.9178)	0.0722 (0.7780)
AF	CD	0.2526 (0.8997)	0.0165 (0.1688)
AF	LDL	0.2501 (0.8865)	-0.0171 (0.2734)
CD	NEU	0.2468 (0.8687)	-0.0002 (0.0013)
AF	HDL	0.2466 (0.8680)	-0.0949 (3.7918)
CD	SCZ	0.2461 (0.8653)	0.0924 (2.2076)
RA	WAIST	0.2434 (0.8511)	-0.0367 (0.4518)
CAD	BC	0.2379 (0.8228)	0.0699 (0.4598)
CAD	NEU	0.2361 (0.8139)	0.0782 (1.5651)
CAD	RA	0.2355 (0.8107)	0.0779 (1.4365)
MI	T2D	-0.2351 (0.8089)	NA (NA)
BC	NEU	0.2308 (0.7868)	0.0186 (0.1021)
BMI	BC	0.2249 (0.7578)	-0.0182 (0.1336)
HEIGHT	NEU	-0.2242 (0.7544)	-0.0524 (1.5010)
BC	LDL	-0.2177 (0.7230)	0.0712 (0.6930)
MI	NEU	0.2138 (0.7046)	NA (NA)
LOAD	MI	0.2129 (0.7003)	NA (NA)
CD	HR	-0.2046 (0.6620)	0.0069 (0.0481)
AF	WAIST	0.2024 (0.6517)	-0.0459 (0.9825)
LDL	SCZ	0.2008 (0.6445)	-0.0170 (0.3287)
HEIGHT	LOAD	0.1980 (0.6317)	-0.1321 (1.9932)
HDL	SCZ	0.1973 (0.6289)	0.0336 (0.8680)
CD	WAIST	0.1951 (0.6190)	-0.0349 (0.3788)
BC	HDL	-0.1847 (0.5735)	0.0398 (0.3261)
HDL	HR	0.1833 (0.5674)	-0.0277 (0.3379)
HR	T2D	-0.1819 (0.5615)	0.0508 (0.4013)
HDL	T2D	-0.1722 (0.5211)	-0.3058 (12.5307)
CAD	LDL	0.1717 (0.5191)	0.2115 (7.1408)
LDL	WAIST	0.1622 (0.4805)	0.1095 (3.5518)
LDL	T2D	-0.1611 (0.4764)	0.0505 (0.6992)
BC	WAIST	0.1553 (0.4536)	-0.0291 (0.1636)
LOAD	T2D	-0.1488 (0.4289)	0.0509 (0.1909)
UC	WAIST	0.1412 (0.4003)	-0.0487 (0.5153)
HEIGHT	WAIST	-0.1389 (0.3919)	-0.0209 (0.3626)
HDL	UC	0.1318 (0.3662)	0.0264 (0.2749)
SCZ	T2D	-0.1309 (0.3631)	-0.0092 (0.0871)

(continued)

		Estimate (- log 10 *P*-value)	
Trait 1	Trait 2	Log 10 BF correlation	Genetic correlation
AF	LOAD	0.1305 (0.3618)	-0.0636 (0.5952)
HEIGHT	T2D	-0.1298 (0.3591)	-0.0100 (0.1005)
HR	NEU	0.1289 (0.3560)	0.0577 (0.8406)
IBD	WAIST	0.1254 (0.3438)	-0.0418 (0.5297)
HEIGHT	IBD	0.1239 (0.3386)	0.0690 (1.3587)
BMI	LOAD	0.1200 (0.3251)	-0.0294 (0.2396)
AF	BC	0.1062 (0.2793)	-0.0153 (0.0882)
BC	MI	0.0984 (0.2543)	NA (NA)
HEIGHT	RA	0.0973 (0.2509)	0.0477 (1.0714)
CD	HEIGHT	0.0949 (0.2434)	0.0494 (0.8913)
HEIGHT	SCZ	0.0869 (0.2190)	0.0055 (0.1102)
BMI	T2D	-0.0833 (0.2082)	0.3267 (15.5429)
T2D	WAIST	0.0793 (0.1965)	0.2340 (5.6054)
CAD	LOAD	-0.0752 (0.1846)	-0.0374 (0.2298)
AF	T2D	0.0708 (0.1722)	0.1023 (1.7296)
BC	T2D	-0.0689 (0.1669)	-0.2116 (1.2632)
NEU	T2D	-0.0648 (0.1554)	-0.0468 (0.4010)
HEIGHT	UC	0.0626 (0.1495)	0.0579 (0.8229)
BC	RA	-0.0485 (0.1121)	0.0442 (0.2305)
HR	LDL	-0.0477 (0.1101)	0.0849 (1.6197)
HR	RA	-0.0457 (0.1051)	0.0373 (0.3053)
HDL	NEU	0.0456 (0.1048)	-0.0061 (0.0888)
T2D	UC	0.0447 (0.1024)	0.0520 (0.3240)
RA	T2D	0.0391 (0.0885)	-0.0477 (0.4284)
LOAD	NEU	-0.0390 (0.0881)	0.0789 (0.4814)
IBD	T2D	0.0251 (0.0549)	-0.0021 (0.0144)
HDL	WAIST	-0.0236 (0.0515)	-0.2476 (13.2806)
LOAD	SCZ	0.0212 (0.0460)	0.0336 (0.2694)
LDL	NEU	0.0210 (0.0455)	0.0088 (0.1071)
CD	T2D	-0.0159 (0.0341)	-0.0162 (0.1260)
CAD	CD	0.0112 (0.0238)	0.0497 (0.5809)
BC	HEIGHT	0.0099 (0.0209)	0.0051 (0.0354)
CAD	IBD	0.0055 (0.0116)	0.0435 (0.4331)
CAD	UC	0.0050 (0.0103)	0.0090 (0.0617)
LOAD	WAIST	0.0001 (0.0002)	0.0254 (0.1522)

Supplementary Table 8

For each trait or trait-network pair, we compute the proportion of genes with higher enrichment P_1 estimates (P_1^{bma} or P_1^{net}) than reference estimates (P_1^{base} or P_1^{near}), among genes with reference P_1 estimates higher than a given cutoff.

Panel **a** Median proportion of genes with P_1^{bma} higher than reference estimates (P_1^{base} or P_1^{near}), among genes with reference estimates higher than a given cutoff. Medians shown below are across 16 traits that have multiple networks more enriched than the near-gene enrichment control (**Supplementary Table 3**). **Figure 5(e)** is based on this panel.

	All genes		Only TFs		Only TGs	
Cutoff	P_1^{base}	P_1^{near}	P_1^{base}	P_1^{near}	P_1^{base}	P_1^{near}
0	0.9828	0.9401	0.9556	0.8829	0.9842	0.9423
0.1	0.9531	0.8811	0.9837	0.8593	0.9499	0.8920
0.2	0.9180	0.8590	0.9514	0.8333	0.9166	0.8707
0.3	0.8856	0.8342	0.9564	0.8000	0.8898	0.8360
0.4	0.8754	0.8061	0.9667	0.7500	0.8784	0.8084
0.5	0.8695	0.7871	0.9444	0.7321	0.8771	0.7979
0.6	0.8499	0.7815	0.9348	0.7321	0.8607	0.7872
0.7	0.8647	0.7795	0.9583	0.7321	0.8624	0.7831
0.8	0.8399	0.7578	1.0000	0.6667	0.8521	0.7657
0.9	0.8167	0.7443	1.0000	0.6870	0.8259	0.7245

Panel **b** Median proportion of genes with P_1^{net} higher than reference estimates (P_1^{base} or P_1^{near}), among genes with reference estimates higher than a given cutoff. Medians shown below are across 512 network-trait pairs passing the near-gene enrichment control (**Supplementary Table 3**).

	All genes		Only TFs		Only TGs	
Cutoff	P_1^{base}	P_1^{near}	P_1^{base}	P_1^{near}	P_1^{base}	P_1^{near}
0	0.9637	0.9046	0.8926	0.7058	0.9730	0.9325
0.1	0.9203	0.8613	0.8549	0.6667	0.9340	0.8898
0.2	0.9081	0.8494	0.8571	0.6667	0.9114	0.8696
0.3	0.8623	0.8276	0.8313	0.6667	0.8745	0.8537
0.4	0.8622	0.7971	0.8000	0.6000	0.8750	0.8225
0.5	0.8756	0.7891	0.7656	0.6079	0.8827	0.8053
0.6	0.8707	0.7895	0.7895	0.6154	0.8757	0.8000
0.7	0.8750	0.7906	0.7895	0.6206	0.8788	0.8077
0.8	0.8462	0.7679	0.7471	0.5862	0.8583	0.7863
0.9	0.8333	0.7500	0.7230	0.5000	0.8468	0.7619

Supplementary Table 9

For each trait we compute the correlation between RSS-NET enrichment statistic (log10 BF) and the percentage of network genes with P_1^{net} higher than the reference estimates (P_1^{base} or P_1^{near}), across all networks. Here we only consider 12 traits where all 38 networks show stronger enrichment than the near-gene control (**Supplementary Table 3**). Rows are ranked by Pearson P-values. The Bonferroni cutoff is $0.05/12 = 4.2 \times 10^{-3}$. Trait abbreviations are defined in **Supplementary Table 2**.

Panel **a** The reference P_1 is P_1^{base}.

	Pearson R (- log 10 P-value)		
Trait	All genes	Only TFs	Only TGs
LDL	0.8992 (13.7584)	0.9419 (17.9148)	0.8947 (13.4362)
HR	0.8166 (9.3903)	0.7301 (6.7046)	0.8090 (9.0992)
BMI	0.6810 (5.5959)	0.6628 (5.2378)	0.7271 (6.6306)
AF	0.6687 (5.3518)	0.7041 (6.0910)	0.6492 (4.9850)
MI	0.5851 (3.9420)	0.5452 (3.3972)	0.6125 (4.3594)
SCZ	0.5722 (3.7584)	0.6440 (4.8916)	0.6173 (4.4368)
BC	0.5579 (3.5637)	0.6122 (4.3543)	0.5412 (3.3468)
RA	0.3848 (1.7679)	0.3427 (1.4540)	0.4013 (1.9022)
WAIST	0.3672 (1.6316)	0.4298 (2.1496)	0.3946 (1.8468)
HDL	0.2629 (0.9555)	0.4662 (2.4981)	0.2658 (0.9714)
CAD	0.1948 (0.6175)	0.0261 (0.0574)	0.3409 (1.4413)
NEU	0.1461 (0.4184)	0.0523 (0.1219)	0.2634 (0.9581)

Panel **b** The reference P_1 is P_1^{near}. This panel is reported in the main text.

	Pearson R (- log 10 P-value)		
Trait	All genes	Only TFs	Only TGs
LDL	0.9100 (14.6053)	0.9432 (18.0902)	0.9086 (14.4901)
HR	0.8392 (10.3326)	0.8105 (9.1548)	0.8323 (10.0295)
BMI	0.7247 (6.5719)	0.7711 (7.8321)	0.7873 (8.3440)
MI	0.7079 (6.1755)	0.7797 (8.0986)	0.7372 (6.8854)
AF	0.7069 (6.1523)	0.7894 (8.4116)	0.6956 (5.9022)
NEU	0.5618 (3.6150)	0.6441 (4.8921)	0.6092 (4.3072)
CAD	0.5268 (3.1675)	0.5975 (4.1260)	0.6206 (4.4905)
SCZ	0.5218 (3.1084)	0.6433 (4.8791)	0.5812 (3.8855)
BC	0.5124 (2.9978)	0.5914 (4.0355)	0.4724 (2.5613)
RA	0.5110 (2.9809)	0.5191 (3.0761)	0.5098 (2.9673)
WAIST	0.2877 (1.0977)	0.4315 (2.1654)	0.3785 (1.7184)
HDL	0.2831 (1.0705)	0.4966 (2.8189)	0.3151 (1.2679)

Supplementary Table 10

Here we quantify overlap between RSS-NET prioritized genes ($P_1^{\text{bma}} \geq 0.9$) and genes implicated in the GWAS Catalog (Buniello et al. 2019), for each of 16 traits that pass the near-gene enrichment control (**Supplementary Table 3**). The "Same GWAS" column reports the overlap between RSS-NET prioritized genes and genes implicated in the same GWAS. The "Later GWAS" column reports the overlap between RSS-NET prioritized genes and genes implicated in a later GWAS of the same trait with increased sample size. The "No GWAS" column reports the number of RSS-NET prioritized genes that were not reported in either the same or the later GWAS at the time of analysis. For example, there are 38 genome-wide significant genes in GWAS Catalog for the same GWAS of HDL (Teslovich et al. 2010) that are analyzed by RSS-NET, and 32 of them have $P_1^{\text{bma}} \geq 0.9$; there are 20 new genome-wide significant genes in GWAS Catalog for a later GWAS of HDL (Global Lipids Genetics Consortium 2013), and 3 of them have $P_1^{\text{bma}} \geq 0.9$ based on RSS-NET analysis of previous GWAS (Teslovich et al. 2010); there are 142 genes with $P_1^{\text{bma}} \geq 0.9$ that are not reported in either the same or the later GWAS of HDL. All P-values are generated by R built-in function `fisher.test`. Rows are sorted by P-values in the "Same GWAS" column, then P-values in the "Later GWAS" column. Trait abbreviations are defined in **Supplementary Table 2**.

It is important to note that some published GWAS hits are not necessarily genome-wide significant in the corresponding summary data files. For example, rs34856868 shows $P = 9.80 \times 10^{-9}$ for association with IBD in Table 2 of Liu et al. (2015); however, the P-value of the same SNP is 0.27 in the corresponding summary data file (`EUR.IBD.gwas.assoc.gz`). For this SNP, the result in Table 2 of Liu et al. (2015) was indeed obtained from a combined analysis of data on both GWAS and Immunochip arrays, whereas the result in the summary data file was only based on GWAS arrays. Because of this type of potential discrepancy between summary data files and corresponding publications, the overlap fractions shown in the "Same GWAS" column are not very high for certain traits.

	Fraction (- log 10 P-value)		
Trait	Same GWAS	Later GWAS	No GWAS
RA	44 / 61 (63.75)	4 / 7 (5.79)	190
HDL	32 / 38 (54.66)	3 / 20 (2.87)	142
LDL	26 / 27 (48.62)	1 / 18 (0.75)	141
SCZ	47 / 58 (45.93)	138 / 330 (82.51)	638
AF	16 / 18 (36.05)	10 / 83 (12.79)	35
CAD	18 / 20 (35.64)	21 / 140 (21.75)	72
IBD	33 / 80 (35.50)	4 / 12 (4.60)	101
WAIST	16 / 33 (29.73)	5 / 233 (3.11)	36
HR	10 / 15 (22.08)	2 / 43 (2.33)	29
BC	8 / 9 (21.03)	4 / 107 (4.82)	15
BMI	13 / 59 (19.61)	4 / 461 (1.39)	33
MI	8 / 9 (17.45)	NA	61
T2D	6 / 16 (12.26)	5 / 110 (6.29)	8
LOAD	6 / 18 (11.12)	11 / 29 (22.14)	18
UC	6 / 17 (7.92)	2 / 5 (3.02)	126
NEU	3 / 5 (6.58)	9 / 122 (10.40)	28

Supplementary Table 11

Examples of RSS-NET highlighted genes that were reported in GWAS of the same data. The "mouse trait" column is based on the Mouse Genome Informatics (Bult et al. 2019). The "therapeutic/clinical evidence" column is based on the Online Mendelian Inheritance in Man (Amberger et al. 2019) and Therapeutic Target Database (Wang et al. 2020). Click blue links to view details online. Drugs are highlighted in yellow. CS: cardiovascular system; Metab.: metabolism; NS: nervous system.

Trait	Gene (Role)	P_1^{base}	P_1^{near}	P_1^{bma}	P_1^{net} (Network, BF)	Mouse trait	Therapeutic/clinical evidence
BMI	*ADCY3* (TG)	1.00	1.00	1.00	1.00 (Ileum, 4.99×10^{12})	Growth	Severe obesity
	NPC1 (TG)	0.72	0.93	0.97	0.97 (Colon, 5.49×10^{12})	Growth	Niemann-Pick disease
	RPL27A (TG)	0.66	0.70	0.86	0.90 (Pancreas, 2.07×10^{13})	Growth	
WAIST	*PIGC* (TG)	1.00	1.00	1.00	1.00 (Esophagus, 6.78×10^{239})		GPIBD16
	TBX15 (TF)	1.00	1.00	1.00	1.00 (Pancreas, 2.72×10^{212})	Growth	Cousin syndrome
	PPARG (TF)	0.94	0.94	0.96	0.96 (Esophagus, 6.78×10^{239})	Metab.	Insulin resistance, Obesity
BC	*FGFR2* (TG)	1.00	1.00	1.00	1.00 (Lung, 7.14×10^{7})	Growth	Pfeiffer syndrome
	PTHLH (TG)	1.00	1.00	1.00	1.00 (Aorta, 8.27×10^{8})	Growth	Brachydactyly E2
	MKL1 (TG)	0.80	0.80	0.91	0.92 (Spleen, 6.19×10^{7})		AMKL
RA	*CD40* (TG)	1.00	1.00	1.00	1.00 (B cell, 3.31×10^{57})	Immune	HIGM3
	CTLA4 (TG)	1.00	1.00	1.00	1.00 (CD8, 6.96×10^{56})	Immune	ALPS5
	ICOS (TG)	1.00	1.00	1.00	1.00 (CD8, 6.96×10^{56})	Immune	Immunodeficiency CV1
	IL2RA (TG)	1.00	1.00	1.00	1.00 (NK cell, 2.95×10^{60})	Immune	Immunodeficiency 41
	IL6R (TG)	1.00	1.00	1.00	1.00 (Monocyte, 8.91×10^{53})	Immune	
	RASGRP1 (TG)	1.00	1.00	1.00	1.00 (NK cell, 2.95×10^{60})	Immune	Immunodeficiency 64
	STAT4 (TF)	1.00	1.00	1.00	1.00 (NK cell, 2.95×10^{60})	Immune	
	TYK2 (TG)	1.00	1.00	1.00	1.00 (NK cell, 2.95×10^{60})	Immune	Immunodeficiency 35
IBD	*ATG16L1* (TG)	1.00	1.00	1.00	1.00 (NK cell, 5.07×10^{35})	Immune	
	BACH2 (TF)	1.00	1.00	1.00	1.00 (NK cell, 5.07×10^{35})	Immune	Immunodeficiency 60
	FCGR2A (TG)	1.00	1.00	1.00	1.00 (Monocyte, 6.28×10^{31})	Immune	Lupus nephritis
	JAK2 (TG)	1.00	1.00	1.00	1.00 (Monocyte, 6.28×10^{31})	Immune	Baricitinib
	STAT3 (TF)	1.00	1.00	1.00	1.00 (NK cell, 5.07×10^{35})	Immune	ADMIO1
	TYK2 (TG)	0.96	0.98	0.98	0.98 (NK cell, 5.07×10^{35})	Immune	Immunodeficiency 35
	STAT4 (TF)	0.77	0.82	0.91	0.91 (NK cell, 5.07×10^{35})	Immune	Susceptibility to SLE
HDL	*ABCA1* (TG)	1.00	1.00	1.00	1.00 (Liver, 2.81×10^{21})	Metab.	Tangier disease, Probucol
	APOB (TG)	1.00	1.00	1.00	1.00 (Liver, 2.81×10^{21})	Metab.	FCHL2, FHBL1, Mipomersen
	GALNT2 (TG)	1.00	1.00	1.00	1.00 (Liver, 2.81×10^{21})	Metab.	
	LIPG (TG)	1.00	1.00	1.00	1.00 (Liver, 2.81×10^{21})	Metab.	GSK-264220A
	LPL (TG)	1.00	1.00	1.00	1.00 (Omentum, 8.70×10^{13})	Metab.	Clofibrate Gemfibrozil
	SCARB1 (TG)	1.00	1.00	1.00	1.00 (Liver, 2.81×10^{21})	Metab.	
LDL	*APOB* (TG)	1.00	1.00	1.00	1.00 (Liver, 7.66×10^{27})	Metab.	FCHL2, FHBL1, Mipomersen
	HMGCR (TG)	1.00	1.00	1.00	1.00 (CD8, 5.86×10^{28})	Metab.	
	HNF1A (TF)	1.00	1.00	1.00	1.00 (CD8, 5.86×10^{28})	Metab.	MODY3, Hepatic adenomas
	LDLR (TG)	1.00	1.00	1.00	1.00 (Pancreas, 3.04×10^{28})	Metab.	FHCL1
	NPC1L1 (TG)	1.00	1.00	1.00	1.00 (Liver, 7.66×10^{27})	Metab.	Response to ezetimibe
T2D	*TCF7L2* (TF)	1.00	1.00	1.00	1.00 (NK cell, 1.49×10^{77})	Metab.	Susceptibility to T2D
	IGF2BP2 (TG)	0.99	1.00	1.00	1.00 (Ileum, 4.52×10^{62})	Metab.	Susceptibility to T2D
	PPARG (TF)	0.98	1.00	1.00	1.00 (Prostate, 5.64×10^{66})	Metab.	Insulin resistance, Obesity
	PROX1 (TG)	0.32	0.92	0.92	0.92 (Thyroid, 3.61×10^{61})	CS, Metab.	
HR	*MYH6* (TG)	1.00	1.00	1.00	1.00 (Heart, 2.12×10^{7})	CS, Muscle	Cardiomyopathy D1EE, H14
	GJA1 (TG)	1.00	1.00	1.00	1.00 (Uterus, 1.51×10^{6})	CS, Muscle	AVSD3, HLHS1
	EPHB4 (TG)	1.00	1.00	1.00	1.00 (Aorta, 2.43×10^{7})	CS, Muscle	CMAVM2, LMPHM7
	TTN (TG)	1.00	1.00	1.00	1.00 (Aorta, 2.43×10^{7})	CS, Muscle	Cardiomyopathy D1G, H9
	GNB4 (TG)	0.55	0.64	0.91	0.91 (Aorta, 2.43×10^{7})	CS	CMTDIF
CAD	*SMAD3* (TF)	0.99	1.00	1.00	1.00 (Adipose, 1.67×10^{29})	CS, Blood	Loeys-Dietz syndrome 3
	APOB (TG)	0.94	0.98	0.99	0.99 (Liver, 2.99×10^{25})	CS, Metab.	FCHL2, FHBL1, Mipomersen
	ATP2B1 (TG)	0.91	0.96	0.98	0.99 (Heart, 1.93×10^{28})	CS, Muscle	
	MRAS (TG)	0.89	0.96	0.98	0.98 (Adipose, 1.67×10^{29})	Immune	Noonan syndrome 11
	APOE (TG)	0.80	0.92	0.96	0.96 (Adipose, 1.67×10^{29})	CS, Metab.	Hyperlipoproteinemia 3
	ABHD2 (TG)	0.81	0.92	0.95	0.95 (Adipose, 1.67×10^{29})	CS	
	IL6R (TG)	0.77	0.91	0.93	0.94 (Heart, 1.93×10^{28})	Immune	Serum level of IL6
	FURIN (TG)	0.69	0.86	0.93	0.95 (Heart, 1.93×10^{28})	CS	
AF	*TBX5* (TF)	1.00	1.00	1.00	1.00 (Heart, 2.15×10^{14})	CS, Muscle	Holt-Oram syndrome
	PITX2 (TF)	1.00	1.00	1.00	1.00 (Muscle, 8.55×10^{14})	CS, Muscle	
	CAV1 (TG)	1.00	1.00	1.00	1.00 (Muscle, 8.55×10^{14})	CS, Muscle	PP hypertension 3
	SH3PXD2A (TG)	1.00	1.00	1.00	1.00 (Muscle, 8.55×10^{14})	CS, Muscle	

(continued)

Trait	Gene (Role)	P_1^{base}	P_1^{near}	P_1^{bma}	P_1^{net} (Network, BF)	Mouse trait	Therapeutic/clinical evidence
	ASAH1 (TG)	1.00	1.00	1.00	1.00 (Muscle, 8.55×10^{14})	Metab.	Farber lipogranulomatosis
	TTN (TG)	0.95	0.97	0.99	0.99 (Muscle, 8.55×10^{14})	CS, Muscle	Cardiomyopathy D1G, H9
LOAD	*APOE* (TG)	1.00	1.00	1.00	1.00 (Liver, 1.09×10^{20})	Liver, NS	Hyperlipoproteinemia 3
	BIN1 (TG)	1.00	1.00	1.00	1.00 (CD8, 8.31×10^{26})	Muscle	Centronuclear myopathy 2
	CLU (TG)	1.00	1.00	1.00	1.00 (Aorta, 3.24×10^{23})	CS, Muscle	
	EPHA1 (TG)	0.99	1.00	1.00	1.00 (CD8, 8.31×10^{26})	Immune	
	CD2AP (TG)	0.70	0.95	0.98	0.98 (Pancreas, 3.53×10^{20})	Metab.	FSGS3
SCZ	*CACNA1C* (TG)	1.00	1.00	1.00	1.00 (Spleen, 1.44×10^{141})	Immune, NS	Timothy syndrome
	TCF4 (TF)	1.00	1.00	1.00	1.00 (Colon, 1.20×10^{144})	Immune, NS	Pitt-Hopkins syndrome
	DPYD (TG)	1.00	1.00	1.00	1.00 (Spleen, 1.44×10^{141})	Neuron	DPD deficiency
NEU	*LINGO1* (TG)	0.99	1.00	1.00	1.00 (Putamen, 2.12×10^{19})	NS	Mental retardation
	SBF2 (TG)	0.94	0.97	0.99	0.99 (Lung, 1.42×10^{18})	Neuron, NS	CMT4B2
	PAFAH1B1 (TG)	0.77	0.93	1.00	1.00 (Cerebellum, 4.85×10^{18})	Neuron, NS	Lissencephaly

Supplementary Table 12

For each of 14 GWAS traits, we quantify overlap between RSS-NET prioritized genes ($P_1^{bma} \geq 0.9$) and genes implicated in 27 categories of knockout mouse phenotypes (Bult et al. 2019). These 14 traits are obtained by removing 2 disease subtypes (MI for CAD, UC for IBD) from the 16 traits that pass the near-gene control (**Supplementary Table 3**). Analysis details are provided in **Supplementary Figure 15**. Within a trait, rows are sorted by P-values and then odds ratios from the analysis of all genes (the 4th column). Trait abbreviations are defined in **Supplementary Table 2**. We use the 1st row "41 / 184 (19.17)" to explain the meaning of "GWAS overlap" (the 3rd column): 184 genes are implicated by GWAS of AF (Buniello et al. 2019) at the time of analysis, 41 of them belong to the "Muscle" category, and the $-\log 10$ Fisher exact test P-value is 19.17.

			Odds ratio (- log 10 P-value)	
Trait	Category	GWAS overlap	All genes	Non-GWAS genes
AF	Muscle	41 / 184 (19.17)	3.88 (3.36)	2.42 (1.12)
AF	Skeleton	29 / 184 (7.65)	3.17 (2.74)	2.10 (0.88)
AF	Cardiovascular system	44 / 184 (12.68)	2.92 (2.65)	1.92 (0.79)
AF	Neoplasm	10 / 184 (4.00)	4.11 (2.30)	2.20 (0.72)
AF	Respiratory system	26 / 184 (10.80)	3.25 (2.25)	1.63 (0.48)
AF	Renal/urinary system	10 / 184 (2.41)	3.05 (1.96)	1.69 (0.50)
AF	Growth/size/body region	53 / 184 (10.57)	2.35 (1.93)	1.66 (0.65)
AF	Craniofacial	20 / 184 (8.13)	3.00 (1.79)	2.34 (0.79)
AF	Nervous system	36 / 184 (7.15)	2.33 (1.79)	1.62 (0.58)
AF	Behavior/neurological	45 / 184 (9.40)	2.25 (1.71)	1.33 (0.30)
AF	Reproductive system	29 / 184 (8.19)	2.29 (1.40)	1.04 (-0.00)
AF	Endocrine/exocrine gland	27 / 184 (6.82)	2.26 (1.34)	1.65 (0.52)
AF	Liver/biliary system	19 / 184 (6.73)	2.57 (1.34)	1.61 (0.30)
AF	Digestive/alimentary	17 / 184 (5.52)	2.52 (1.32)	1.58 (0.30)
AF	Mortality/aging	61 / 184 (10.74)	1.92 (1.30)	1.36 (0.26)
AF	Homeostasis/metabolism	63 / 184 (11.65)	1.90 (1.18)	1.08 (-0.00)
AF	Embryo	20 / 184 (5.16)	2.08 (1.06)	1.44 (0.25)
AF	Hematopoietic system	27 / 184 (4.09)	1.86 (1.06)	1.55 (0.43)
AF	Integument	23 / 184 (6.23)	1.97 (0.84)	1.37 (0.25)
AF	Immune system	28 / 184 (4.32)	1.73 (0.77)	1.39 (0.31)

(continued)

Trait	Category	GWAS overlap	Odds ratio (- log 10 P-value)	
			All genes	Non-GWAS genes
AF	Limbs/digits/tail	11 / 184 (3.51)	2.09 (0.74)	1.05 (-0.00)
AF	Vision/eye	13 / 184 (2.26)	1.86 (0.69)	1.45 (0.25)
AF	Adipose tissue	15 / 184 (5.13)	1.83 (0.66)	0.91 (-0.00)
AF	Taste/olfaction	1 / 184 (0.56)	3.64 (0.60)	4.55 (0.67)
AF	Cellular	48 / 184 (9.38)	1.58 (0.59)	1.06 (-0.00)
AF	Hearing/vestibular/ear	8 / 184 (2.91)	1.79 (0.38)	0.00 (0.21)
AF	Pigmentation	1 / 184 (-0.00)	0.93 (-0.00)	1.16 (0.23)
BC	Cardiovascular system	39 / 364 (3.37)	4.60 (2.80)	3.68 (1.54)
BC	Skeleton	41 / 364 (5.33)	4.19 (2.20)	3.35 (1.36)
BC	Renal/urinary system	27 / 364 (5.66)	5.07 (2.12)	3.05 (0.88)
BC	Limbs/digits/tail	21 / 364 (4.41)	5.24 (1.96)	2.52 (0.61)
BC	Neoplasm	21 / 364 (6.37)	5.85 (1.85)	0.00 (-0.00)
BC	Integument	37 / 364 (5.56)	3.82 (1.77)	1.97 (0.40)
BC	Adipose tissue	28 / 364 (6.58)	4.57 (1.75)	2.20 (0.53)
BC	Mortality/aging	83 / 364 (6.67)	2.92 (1.61)	2.25 (0.75)
BC	Respiratory system	22 / 364 (3.19)	4.05 (1.57)	0.97 (-0.00)
BC	Muscle	32 / 364 (6.26)	3.44 (1.34)	2.48 (0.72)
BC	Hearing/vestibular/ear	8 / 364 (0.81)	4.49 (1.27)	3.60 (0.82)
BC	Vision/eye	29 / 364 (3.50)	2.90 (1.12)	2.79 (0.92)
BC	Liver/biliary system	22 / 364 (3.23)	3.21 (1.11)	1.92 (0.46)
BC	Immune system	44 / 364 (2.75)	2.47 (1.02)	1.11 (-0.00)
BC	Growth/size/body region	72 / 364 (6.83)	2.29 (0.93)	1.22 (0.13)
BC	Homeostasis/metabolism	67 / 364 (3.96)	2.16 (0.86)	1.56 (0.26)
BC	Craniofacial	21 / 364 (3.60)	2.80 (0.84)	0.00 (0.00)
BC	Nervous system	45 / 364 (3.09)	2.26 (0.83)	1.16 (-0.00)
BC	Hematopoietic system	45 / 364 (3.07)	2.17 (0.80)	0.75 (-0.00)
BC	Behavior/neurological	60 / 364 (5.64)	2.37 (0.80)	1.42 (0.14)
BC	Cellular	57 / 364 (3.97)	2.11 (0.75)	0.95 (0.00)
BC	Digestive/alimentary	18 / 364 (1.81)	2.36 (0.70)	0.00 (0.23)
BC	Embryo	28 / 364 (3.07)	2.31 (0.61)	0.69 (-0.00)
BC	Reproductive system	38 / 364 (5.07)	2.07 (0.57)	1.24 (0.17)
BC	Endocrine/exocrine gland	39 / 364 (4.84)	1.88 (0.52)	0.00 (0.47)
BC	Pigmentation	7 / 364 (1.40)	2.33 (0.42)	0.00 (-0.00)
BC	Taste/olfaction	4 / 364 (1.95)	0.00 (-0.00)	0.00 (-0.00)
BMI	Renal/urinary system	65 / 889 (6.26)	4.77 (4.16)	3.95 (2.70)
BMI	Liver/biliary system	79 / 889 (9.66)	3.87 (3.05)	2.62 (1.19)
BMI	Embryo	114 / 889 (12.90)	3.24 (2.60)	2.68 (1.65)
BMI	Vision/eye	105 / 889 (10.35)	2.79 (2.01)	2.16 (0.96)
BMI	Growth/size/body region	270 / 889 (24.06)	2.24 (1.76)	1.42 (0.38)
BMI	Adipose tissue	74 / 889 (10.18)	2.93 (1.75)	1.27 (0.14)
BMI	Reproductive system	107 / 889 (7.57)	2.50 (1.65)	1.69 (0.53)

(continued)

Trait	Category	GWAS overlap	Odds ratio (- log 10 P-value)	
			All genes	Non-GWAS genes
BMI	Mortality/aging	301 / 889 (21.97)	2.00 (1.45)	1.35 (0.35)
BMI	Taste/olfaction	8 / 889 (1.84)	7.36 (1.43)	0.00 (-0.00)
BMI	Respiratory system	85 / 889 (11.32)	2.59 (1.35)	1.88 (0.67)
BMI	Homeostasis/metabolism	255 / 889 (13.97)	1.90 (1.18)	1.50 (0.47)
BMI	Endocrine/exocrine gland	134 / 889 (13.01)	2.07 (1.14)	1.75 (0.66)
BMI	Nervous system	220 / 889 (22.42)	1.94 (1.09)	1.50 (0.42)
BMI	Behavior/neurological	238 / 889 (22.82)	1.90 (1.04)	1.10 (0.08)
BMI	Hematopoietic system	178 / 889 (12.03)	1.74 (0.77)	1.44 (0.41)
BMI	Cardiovascular system	154 / 889 (13.34)	1.68 (0.70)	1.24 (0.20)
BMI	Integument	107 / 889 (9.73)	1.75 (0.66)	1.26 (0.23)
BMI	Cellular	224 / 889 (15.69)	1.58 (0.59)	1.10 (0.08)
BMI	Pigmentation	27 / 889 (3.92)	1.87 (0.50)	1.08 (0.21)
BMI	Immune system	170 / 889 (10.05)	1.48 (0.50)	1.28 (0.18)
BMI	Limbs/digits/tail	64 / 889 (8.95)	1.67 (0.49)	0.97 (-0.00)
BMI	Digestive/alimentary	72 / 889 (7.07)	1.57 (0.42)	1.82 (0.65)
BMI	Hearing/vestibular/ear	40 / 889 (4.98)	1.79 (0.38)	1.39 (0.18)
BMI	Craniofacial	76 / 889 (11.06)	1.49 (0.29)	1.30 (0.14)
BMI	Skeleton	140 / 889 (14.46)	1.30 (0.20)	0.86 (-0.00)
BMI	Muscle	87 / 889 (9.77)	1.10 (0.11)	0.64 (0.12)
BMI	Neoplasm	45 / 889 (6.29)	0.58 (-0.00)	0.68 (-0.00)
CAD	Cardiovascular system	70 / 308 (18.88)	2.45 (3.65)	1.59 (0.99)
CAD	Liver/biliary system	36 / 308 (13.08)	2.71 (2.86)	1.37 (0.39)
CAD	Mortality/aging	101 / 308 (16.94)	1.85 (2.24)	1.14 (0.22)
CAD	Embryo	43 / 308 (12.48)	2.15 (2.07)	1.41 (0.55)
CAD	Renal/urinary system	26 / 308 (8.03)	2.25 (1.93)	1.12 (0.08)
CAD	Hematopoietic system	61 / 308 (11.49)	1.81 (1.70)	1.11 (0.11)
CAD	Cellular	68 / 308 (10.97)	1.73 (1.57)	1.14 (0.17)
CAD	Respiratory system	33 / 308 (11.21)	2.01 (1.47)	0.76 (0.08)
CAD	Limbs/digits/tail	22 / 308 (7.33)	2.04 (1.32)	1.18 (0.19)
CAD	Integument	42 / 308 (11.43)	1.84 (1.31)	0.93 (-0.00)
CAD	Digestive/alimentary	33 / 308 (11.13)	1.95 (1.27)	0.89 (-0.00)
CAD	Immune system	54 / 308 (8.90)	1.64 (1.19)	0.99 (-0.00)
CAD	Neoplasm	18 / 308 (6.99)	2.07 (1.15)	0.55 (0.24)
CAD	Growth/size/body region	79 / 308 (13.82)	1.53 (1.08)	0.77 (0.34)
CAD	Endocrine/exocrine gland	40 / 308 (8.64)	1.66 (1.07)	0.88 (0.07)
CAD	Muscle	40 / 308 (13.81)	1.70 (1.00)	0.91 (-0.00)
CAD	Reproductive system	40 / 308 (9.30)	1.65 (0.99)	1.27 (0.31)
CAD	Nervous system	51 / 308 (8.19)	1.54 (0.99)	1.03 (0.05)
CAD	Homeostasis/metabolism	87 / 308 (13.23)	1.45 (0.91)	0.81 (0.31)
CAD	Vision/eye	33 / 308 (7.91)	1.54 (0.77)	0.98 (-0.00)
CAD	Pigmentation	7 / 308 (2.26)	2.07 (0.74)	0.88 (-0.00)
CAD	Craniofacial	29 / 308 (10.32)	1.65 (0.70)	0.70 (0.19)

(continued)

Trait	Category	GWAS overlap	Odds ratio (- log 10 P-value)	
			All genes	Non-GWAS genes
CAD	Adipose tissue	28 / 308 (9.67)	1.45 (0.53)	0.69 (0.19)
CAD	Skeleton	47 / 308 (11.49)	1.31 (0.38)	0.78 (0.22)
CAD	Taste/olfaction	1 / 308 (0.38)	1.60 (0.32)	0.00 (-0.00)
CAD	Behavior/neurological	44 / 308 (5.13)	1.20 (0.31)	0.72 (0.45)
CAD	Hearing/vestibular/ear	7 / 308 (1.35)	0.79 (0.00)	0.28 (0.60)
HDL	Liver/biliary system	12 / 104 (3.13)	2.23 (2.89)	1.74 (1.38)
HDL	Digestive/alimentary	13 / 104 (3.51)	2.18 (2.83)	1.89 (1.71)
HDL	Homeostasis/metabolism	35 / 104 (3.83)	1.72 (2.76)	1.43 (1.17)
HDL	Embryo	17 / 104 (3.88)	1.77 (1.84)	1.32 (0.49)
HDL	Cardiovascular system	24 / 104 (4.49)	1.64 (1.79)	1.22 (0.40)
HDL	Immune system	17 / 104 (1.33)	1.51 (1.39)	1.37 (0.82)
HDL	Hematopoietic system	17 / 104 (1.33)	1.49 (1.29)	1.30 (0.65)
HDL	Respiratory system	9 / 104 (1.82)	1.65 (1.16)	1.38 (0.59)
HDL	Mortality/aging	31 / 104 (2.83)	1.38 (1.08)	1.11 (0.21)
HDL	Vision/eye	13 / 104 (2.26)	1.54 (1.06)	1.25 (0.40)
HDL	Endocrine/exocrine gland	10 / 104 (0.73)	1.49 (1.04)	1.34 (0.61)
HDL	Reproductive system	10 / 104 (0.93)	1.43 (0.89)	1.18 (0.23)
HDL	Cellular	20 / 104 (1.36)	1.35 (0.86)	1.14 (0.23)
HDL	Adipose tissue	5 / 104 (0.63)	1.49 (0.82)	1.45 (0.63)
HDL	Growth/size/body region	20 / 104 (1.33)	1.30 (0.70)	1.18 (0.34)
HDL	Renal/urinary system	11 / 104 (2.86)	1.38 (0.57)	1.25 (0.30)
HDL	Limbs/digits/tail	7 / 104 (1.60)	1.38 (0.52)	1.30 (0.33)
HDL	Muscle	9 / 104 (1.46)	1.26 (0.41)	0.94 (-0.00)
HDL	Behavior/neurological	13 / 104 (0.45)	1.17 (0.34)	1.11 (0.19)
HDL	Integument	10 / 104 (1.19)	1.17 (0.23)	1.05 (0.05)
HDL	Hearing/vestibular/ear	1 / 104 (-0.00)	0.76 (0.17)	0.67 (0.18)
HDL	Neoplasm	3 / 104 (0.36)	1.19 (0.17)	1.15 (0.17)
HDL	Skeleton	12 / 104 (1.27)	1.09 (0.15)	1.00 (-0.00)
HDL	Nervous system	15 / 104 (1.01)	1.08 (0.13)	0.95 (0.04)
HDL	Pigmentation	3 / 104 (0.92)	0.71 (0.10)	0.52 (0.23)
HDL	Craniofacial	6 / 104 (0.89)	0.95 (-0.00)	0.95 (-0.00)
HDL	Taste/olfaction	0 / 104 (-0.00)	0.92 (-0.00)	1.02 (0.00)
HR	Endocrine/exocrine gland	13 / 123 (1.81)	4.45 (2.73)	3.78 (1.87)
HR	Muscle	18 / 123 (5.89)	4.73 (2.45)	3.45 (1.34)
HR	Immune system	17 / 123 (1.59)	3.71 (2.34)	3.40 (1.73)
HR	Reproductive system	10 / 123 (1.17)	4.01 (2.21)	2.60 (0.82)
HR	Nervous system	24 / 123 (3.59)	3.61 (2.14)	2.59 (1.05)
HR	Mortality/aging	30 / 123 (3.00)	3.22 (2.12)	2.30 (0.85)
HR	Cardiovascular system	28 / 123 (6.51)	3.61 (2.09)	3.07 (1.40)
HR	Vision/eye	10 / 123 (1.55)	3.99 (2.07)	2.32 (0.61)
HR	Behavior/neurological	24 / 123 (3.15)	3.30 (2.02)	2.07 (0.61)
HR	Cellular	27 / 123 (3.42)	3.17 (1.92)	2.38 (0.95)

(continued)

Trait	Category	GWAS overlap	Odds ratio (- log 10 P-value)	
			All genes	Non-GWAS genes
HR	Respiratory system	10 / 123 (2.45)	4.17 (1.84)	4.05 (1.57)
HR	Hematopoietic system	12 / 123 (0.63)	3.20 (1.84)	2.80 (1.25)
HR	Liver/biliary system	8 / 123 (1.67)	4.13 (1.83)	4.01 (1.55)
HR	Digestive/alimentary	7 / 123 (1.12)	4.05 (1.80)	2.36 (0.70)
HR	Renal/urinary system	5 / 123 (0.66)	3.62 (1.46)	3.38 (1.17)
HR	Homeostasis/metabolism	29 / 123 (2.84)	2.59 (1.34)	1.95 (0.53)
HR	Limbs/digits/tail	5 / 123 (0.76)	3.59 (1.27)	4.19 (1.42)
HR	Growth/size/body region	22 / 123 (1.93)	2.62 (1.24)	2.29 (0.93)
HR	Hearing/vestibular/ear	4 / 123 (1.01)	3.85 (1.15)	2.99 (0.73)
HR	Neoplasm	2 / 123 (0.16)	3.75 (1.13)	4.38 (1.25)
HR	Adipose tissue	3 / 123 (0.13)	3.13 (1.12)	2.74 (0.82)
HR	Integument	16 / 123 (3.62)	2.81 (1.04)	2.19 (0.59)
HR	Skeleton	7 / 123 (0.32)	2.39 (0.92)	2.79 (1.03)
HR	Embryo	13 / 123 (2.39)	2.47 (0.81)	2.89 (1.11)
HR	Craniofacial	5 / 123 (0.70)	2.40 (0.73)	1.87 (0.46)
HR	Pigmentation	2 / 123 (0.54)	2.00 (0.37)	0.00 (-0.00)
HR	Taste/olfaction	0 / 123 (-0.00)	0.00 (0.00)	0.00 (0.00)
IBD	Hematopoietic system	100 / 374 (17.69)	2.35 (4.48)	1.86 (2.07)
IBD	Neoplasm	23 / 374 (6.95)	3.44 (4.41)	2.70 (2.23)
IBD	Immune system	104 / 374 (18.96)	2.27 (4.14)	1.76 (1.68)
IBD	Digestive/alimentary	44 / 374 (12.09)	2.85 (4.13)	2.67 (3.08)
IBD	Homeostasis/metabolism	104 / 374 (10.69)	2.08 (3.47)	1.74 (1.77)
IBD	Adipose tissue	20 / 374 (2.80)	2.74 (3.04)	2.79 (2.87)
IBD	Endocrine/exocrine gland	57 / 374 (10.02)	2.20 (2.95)	1.88 (1.70)
IBD	Cardiovascular system	56 / 374 (7.29)	2.03 (2.64)	1.61 (1.15)
IBD	Nervous system	48 / 374 (3.21)	2.02 (2.61)	1.92 (1.95)
IBD	Renal/urinary system	26 / 374 (4.60)	2.36 (2.37)	1.63 (0.80)
IBD	Cellular	91 / 374 (11.24)	1.74 (1.91)	1.41 (0.77)
IBD	Liver/biliary system	31 / 374 (6.31)	2.02 (1.74)	2.04 (1.57)
IBD	Respiratory system	26 / 374 (4.24)	1.93 (1.56)	1.67 (0.88)
IBD	Behavior/neurological	53 / 374 (3.34)	1.69 (1.53)	1.30 (0.48)
IBD	Limbs/digits/tail	19 / 374 (3.13)	2.08 (1.53)	1.60 (0.57)
IBD	Skeleton	41 / 374 (4.75)	1.74 (1.53)	1.41 (0.55)
IBD	Reproductive system	36 / 374 (3.72)	1.77 (1.42)	1.47 (0.61)
IBD	Mortality/aging	97 / 374 (8.64)	1.56 (1.41)	1.37 (0.70)
IBD	Growth/size/body region	77 / 374 (7.04)	1.54 (1.26)	1.32 (0.51)
IBD	Embryo	37 / 374 (5.41)	1.61 (1.11)	1.40 (0.59)
IBD	Integument	45 / 374 (7.69)	1.57 (0.99)	1.26 (0.30)
IBD	Vision/eye	24 / 374 (1.66)	1.55 (0.91)	1.55 (0.76)
IBD	Muscle	28 / 374 (4.15)	1.61 (0.86)	1.35 (0.44)
IBD	Craniofacial	19 / 374 (2.55)	1.53 (0.72)	1.52 (0.52)

(continued)

Trait	Category	GWAS overlap	Odds ratio (- log 10 P-value)	
			All genes	Non-GWAS genes
IBD	Pigmentation	8 / 374 (1.63)	1.29 (0.26)	1.16 (0.13)
IBD	Hearing/vestibular/ear	6 / 374 (0.19)	1.11 (0.10)	1.31 (0.23)
IBD	Taste/olfaction	3 / 374 (1.18)	0.00 (-0.00)	0.00 (-0.00)
LDL	Liver/biliary system	15 / 92 (3.81)	2.16 (2.75)	1.48 (0.80)
LDL	Digestive/alimentary	9 / 92 (1.33)	1.97 (2.16)	1.79 (1.48)
LDL	Skeleton	10 / 92 (0.38)	0.48 (1.63)	0.49 (1.45)
LDL	Homeostasis/metabolism	30 / 92 (1.75)	1.26 (0.63)	1.04 (0.08)
LDL	Growth/size/body region	21 / 92 (0.91)	1.21 (0.48)	1.15 (0.27)
LDL	Renal/urinary system	7 / 92 (0.74)	1.29 (0.44)	1.18 (0.21)
LDL	Embryo	6 / 92 (0.09)	1.21 (0.36)	1.30 (0.47)
LDL	Respiratory system	5 / 92 (0.22)	1.23 (0.34)	1.39 (0.57)
LDL	Nervous system	15 / 92 (0.52)	1.14 (0.28)	1.07 (0.13)
LDL	Cellular	18 / 92 (0.58)	1.13 (0.26)	1.05 (0.08)
LDL	Cardiovascular system	12 / 92 (0.46)	0.87 (0.19)	0.86 (0.21)
LDL	Hematopoietic system	16 / 92 (0.64)	1.09 (0.17)	1.03 (0.04)
LDL	Behavior/neurological	17 / 92 (0.61)	1.10 (0.17)	1.01 (-0.00)
LDL	Hearing/vestibular/ear	4 / 92 (0.54)	1.14 (0.16)	1.28 (0.28)
LDL	Limbs/digits/tail	5 / 92 (0.43)	0.79 (0.14)	0.89 (-0.00)
LDL	Endocrine/exocrine gland	9 / 92 (0.27)	1.07 (0.09)	0.96 (-0.00)
LDL	Immune system	14 / 92 (0.41)	1.06 (0.08)	1.02 (0.04)
LDL	Neoplasm	1 / 92 (0.14)	0.83 (0.07)	0.93 (-0.00)
LDL	Mortality/aging	20 / 92 (0.35)	1.05 (0.07)	1.03 (0.04)
LDL	Craniofacial	5 / 92 (0.39)	0.89 (0.06)	1.00 (-0.00)
LDL	Adipose tissue	9 / 92 (1.50)	1.04 (0.06)	0.88 (0.06)
LDL	Integument	10 / 92 (0.71)	1.04 (0.05)	0.93 (0.05)
LDL	Muscle	6 / 92 (0.33)	0.98 (0.00)	0.96 (-0.00)
LDL	Vision/eye	8 / 92 (0.43)	0.99 (-0.00)	1.05 (0.05)
LDL	Reproductive system	8 / 92 (0.17)	0.99 (-0.00)	0.83 (0.24)
LDL	Pigmentation	3 / 92 (0.74)	0.89 (-0.00)	0.75 (0.10)
LDL	Taste/olfaction	0 / 92 (-0.00)	0.86 (-0.00)	0.97 (-0.00)
LOAD	Pigmentation	2 / 98 (0.51)	3.82 (1.20)	3.11 (0.78)
LOAD	Muscle	9 / 98 (1.51)	2.54 (1.16)	0.44 (0.16)
LOAD	Homeostasis/metabolism	24 / 98 (1.56)	1.96 (1.06)	1.41 (0.31)
LOAD	Integument	7 / 98 (0.49)	2.34 (1.00)	1.07 (-0.00)
LOAD	Immune system	19 / 98 (1.92)	1.94 (0.89)	0.99 (-0.00)
LOAD	Vision/eye	4 / 98 (0.00)	2.18 (0.82)	1.90 (0.48)
LOAD	Hearing/vestibular/ear	4 / 98 (0.96)	2.45 (0.80)	2.00 (0.52)
LOAD	Renal/urinary system	7 / 98 (1.14)	2.26 (0.77)	0.00 (0.43)
LOAD	Taste/olfaction	4 / 98 (3.44)	5.24 (0.73)	0.00 (-0.00)
LOAD	Cardiovascular system	17 / 98 (2.22)	1.83 (0.65)	0.25 (0.52)
LOAD	Behavior/neurological	13 / 98 (0.46)	1.62 (0.58)	0.79 (0.11)
LOAD	Embryo	7 / 98 (0.50)	0.30 (0.50)	0.00 (0.89)

(continued)

Trait	Category	GWAS overlap	Odds ratio (- log 10 P-value)	
			All genes	Non-GWAS genes
LOAD	Digestive/alimentary	6 / 98 (0.81)	1.67 (0.49)	0.00 (0.42)
LOAD	Liver/biliary system	5 / 98 (0.43)	1.66 (0.48)	0.51 (-0.00)
LOAD	Growth/size/body region	20 / 98 (1.37)	1.50 (0.41)	0.83 (-0.00)
LOAD	Limbs/digits/tail	5 / 98 (0.74)	1.65 (0.36)	1.35 (0.18)
LOAD	Craniofacial	8 / 98 (1.84)	1.49 (0.33)	1.22 (0.17)
LOAD	Skeleton	9 / 98 (0.59)	0.49 (0.27)	0.30 (0.51)
LOAD	Reproductive system	7 / 98 (0.32)	1.40 (0.25)	1.02 (-0.00)
LOAD	Hematopoietic system	17 / 98 (1.55)	1.30 (0.20)	0.80 (0.11)
LOAD	Cellular	20 / 98 (1.57)	1.25 (0.19)	0.68 (0.23)
LOAD	Endocrine/exocrine gland	14 / 98 (1.99)	1.24 (0.11)	0.30 (0.51)
LOAD	Nervous system	10 / 98 (0.26)	0.71 (0.10)	0.43 (0.45)
LOAD	Mortality/aging	18 / 98 (0.62)	1.10 (0.08)	0.40 (0.61)
LOAD	Respiratory system	5 / 98 (0.43)	0.86 (0.00)	0.00 (0.43)
LOAD	Adipose tissue	5 / 98 (0.66)	0.99 (-0.00)	0.60 (-0.00)
LOAD	Neoplasm	2 / 98 (0.16)	0.74 (-0.00)	0.00 (0.21)
NEU	Endocrine/exocrine gland	33 / 376 (3.62)	2.57 (1.37)	2.54 (1.21)
NEU	Mortality/aging	77 / 376 (6.51)	2.05 (1.21)	2.13 (1.10)
NEU	Muscle	23 / 376 (3.38)	2.63 (1.18)	2.90 (1.48)
NEU	Cellular	48 / 376 (2.94)	2.16 (1.17)	2.22 (1.23)
NEU	Growth/size/body region	62 / 376 (5.32)	2.08 (1.15)	2.14 (1.04)
NEU	Reproductive system	32 / 376 (3.78)	2.27 (0.99)	2.18 (0.82)
NEU	Skeleton	39 / 376 (5.44)	2.03 (0.90)	2.23 (0.98)
NEU	Embryo	22 / 376 (1.87)	2.20 (0.82)	2.43 (1.10)
NEU	Respiratory system	22 / 376 (3.70)	2.21 (0.76)	2.43 (0.80)
NEU	Digestive/alimentary	12 / 376 (0.70)	2.14 (0.75)	2.36 (0.79)
NEU	Taste/olfaction	3 / 376 (1.36)	4.97 (0.71)	5.47 (0.74)
NEU	Nervous system	65 / 376 (9.14)	1.76 (0.61)	1.36 (0.21)
NEU	Hematopoietic system	44 / 376 (3.44)	1.69 (0.60)	1.86 (0.78)
NEU	Immune system	36 / 376 (1.77)	1.68 (0.59)	1.85 (0.78)
NEU	Behavior/neurological	65 / 376 (7.69)	1.61 (0.58)	1.42 (0.33)
NEU	Liver/biliary system	14 / 376 (1.18)	1.75 (0.51)	1.92 (0.55)
NEU	Cardiovascular system	32 / 376 (2.35)	1.67 (0.50)	1.84 (0.69)
NEU	Vision/eye	32 / 376 (5.05)	1.58 (0.43)	1.74 (0.46)
NEU	Limbs/digits/tail	14 / 376 (1.87)	1.71 (0.37)	1.88 (0.39)
NEU	Craniofacial	14 / 376 (1.50)	1.53 (0.34)	1.68 (0.36)
NEU	Adipose tissue	23 / 376 (4.94)	1.49 (0.33)	1.64 (0.36)
NEU	Hearing/vestibular/ear	8 / 376 (0.87)	0.00 (0.21)	0.00 (0.21)
NEU	Neoplasm	12 / 376 (2.40)	1.59 (0.20)	1.75 (0.45)
NEU	Renal/urinary system	15 / 376 (1.62)	1.38 (0.15)	1.52 (0.34)
NEU	Integument	28 / 376 (3.38)	1.19 (0.12)	1.31 (0.12)
NEU	Homeostasis/metabolism	59 / 376 (3.30)	1.18 (0.08)	1.29 (0.18)
NEU	Pigmentation	10 / 376 (3.03)	0.00 (0.00)	0.00 (-0.00)

(continued)

Trait	Category	GWAS overlap	Odds ratio (- log 10 P-value)	
			All genes	Non-GWAS genes
RA	Hematopoietic system	44 / 123 (11.12)	2.14 (5.66)	1.40 (1.09)
RA	Immune system	42 / 123 (10.20)	2.05 (5.02)	1.36 (1.00)
RA	Endocrine/exocrine gland	25 / 123 (6.73)	2.14 (4.48)	1.41 (0.95)
RA	Neoplasm	10 / 123 (4.43)	2.87 (4.20)	2.22 (2.22)
RA	Cellular	33 / 123 (5.49)	1.75 (3.19)	1.32 (0.85)
RA	Digestive/alimentary	12 / 123 (3.49)	2.10 (3.11)	1.46 (0.80)
RA	Liver/biliary system	12 / 123 (3.57)	1.95 (2.42)	1.62 (1.30)
RA	Homeostasis/metabolism	38 / 123 (5.32)	1.49 (1.89)	1.15 (0.37)
RA	Respiratory system	10 / 123 (2.58)	1.76 (1.79)	1.49 (0.92)
RA	Cardiovascular system	16 / 123 (2.37)	1.48 (1.42)	1.24 (0.47)
RA	Nervous system	17 / 123 (1.86)	1.45 (1.39)	1.24 (0.57)
RA	Behavior/neurological	18 / 123 (1.76)	1.40 (1.25)	1.19 (0.42)
RA	Skeleton	20 / 123 (4.60)	1.42 (1.07)	0.93 (0.04)
RA	Reproductive system	15 / 123 (2.80)	1.42 (0.94)	1.00 (0.00)
RA	Vision/eye	16 / 123 (4.03)	1.40 (0.90)	0.96 (0.00)
RA	Renal/urinary system	10 / 123 (2.78)	1.42 (0.78)	0.96 (0.00)
RA	Pigmentation	4 / 123 (1.63)	1.69 (0.75)	1.23 (0.20)
RA	Growth/size/body region	26 / 123 (3.21)	1.26 (0.73)	1.00 (-0.00)
RA	Integument	13 / 123 (2.40)	1.31 (0.69)	1.05 (0.09)
RA	Mortality/aging	31 / 123 (3.49)	1.24 (0.67)	0.96 (0.07)
RA	Limbs/digits/tail	4 / 123 (0.54)	1.43 (0.66)	1.09 (0.13)
RA	Muscle	7 / 123 (1.07)	1.27 (0.51)	1.08 (0.11)
RA	Embryo	8 / 123 (0.92)	1.25 (0.47)	1.05 (0.10)
RA	Adipose tissue	9 / 123 (2.48)	1.24 (0.41)	0.72 (0.37)
RA	Hearing/vestibular/ear	3 / 123 (0.66)	1.20 (0.23)	1.17 (0.24)
RA	Taste/olfaction	0 / 123 (0.00)	0.00 (0.19)	0.00 (0.20)
RA	Craniofacial	5 / 123 (0.73)	1.04 (0.05)	0.81 (0.20)
SCZ	Nervous system	121 / 780 (2.38)	2.04 (13.97)	2.08 (12.69)
SCZ	Behavior/neurological	130 / 780 (2.19)	1.90 (11.46)	1.91 (10.08)
SCZ	Growth/size/body region	130 / 780 (0.87)	1.77 (9.89)	1.86 (10.09)
SCZ	Muscle	52 / 780 (1.34)	2.09 (9.12)	2.13 (8.33)
SCZ	Mortality/aging	167 / 780 (1.67)	1.51 (5.61)	1.53 (5.11)
SCZ	Cardiovascular system	95 / 780 (1.79)	1.62 (5.60)	1.61 (4.74)
SCZ	Craniofacial	36 / 780 (0.55)	1.84 (4.98)	1.95 (5.18)
SCZ	Homeostasis/metabolism	151 / 780 (0.85)	1.48 (4.94)	1.49 (4.41)
SCZ	Hematopoietic system	100 / 780 (0.54)	1.48 (4.13)	1.49 (3.64)
SCZ	Skeleton	82 / 780 (1.82)	1.55 (4.10)	1.60 (4.10)
SCZ	Cellular	132 / 780 (1.37)	1.45 (4.09)	1.48 (3.91)
SCZ	Reproductive system	71 / 780 (1.12)	1.55 (3.77)	1.59 (3.72)
SCZ	Hearing/vestibular/ear	22 / 780 (0.41)	1.82 (3.39)	1.93 (3.53)
SCZ	Adipose tissue	37 / 780 (0.62)	1.65 (3.39)	1.85 (4.44)

(continued)

Trait	Category	GWAS overlap	Odds ratio (- log 10 P-value)	
			All genes	Non-GWAS genes
SCZ	Neoplasm	24 / 780 (0.55)	1.81 (3.35)	1.81 (2.97)
SCZ	Endocrine/exocrine gland	68 / 780 (0.47)	1.46 (3.08)	1.49 (2.90)
SCZ	Vision/eye	53 / 780 (0.33)	1.50 (3.03)	1.48 (2.51)
SCZ	Digestive/alimentary	39 / 780 (0.34)	1.55 (2.93)	1.61 (2.96)
SCZ	Respiratory system	42 / 780 (0.70)	1.53 (2.67)	1.61 (2.91)
SCZ	Renal/urinary system	41 / 780 (0.89)	1.54 (2.64)	1.58 (2.64)
SCZ	Embryo	60 / 780 (0.88)	1.42 (2.30)	1.37 (1.72)
SCZ	Immune system	93 / 780 (0.12)	1.32 (2.21)	1.31 (1.86)
SCZ	Taste/olfaction	1 / 780 (0.42)	2.51 (2.08)	2.96 (2.57)
SCZ	Liver/biliary system	42 / 780 (0.71)	1.38 (1.62)	1.33 (1.22)
SCZ	Integument	53 / 780 (0.16)	1.31 (1.54)	1.33 (1.51)
SCZ	Limbs/digits/tail	28 / 780 (0.17)	1.32 (1.05)	1.44 (1.55)
SCZ	Pigmentation	7 / 780 (0.66)	0.70 (0.59)	0.82 (0.23)
T2D	Liver/biliary system	43 / 300 (12.22)	10.78 (3.64)	6.10 (1.25)
T2D	Digestive/alimentary	35 / 300 (8.11)	9.27 (3.04)	5.99 (1.23)
T2D	Integument	49 / 300 (9.70)	7.51 (2.77)	2.83 (0.55)
T2D	Respiratory system	33 / 300 (7.30)	8.14 (2.54)	6.11 (1.25)
T2D	Taste/olfaction	7 / 300 (4.35)	35.42 (2.47)	26.56 (1.26)
T2D	Cardiovascular system	64 / 300 (10.34)	5.81 (2.34)	2.92 (0.46)
T2D	Muscle	50 / 300 (13.97)	7.08 (2.28)	3.56 (0.68)
T2D	Adipose tissue	46 / 300 (15.52)	7.86 (2.24)	2.37 (0.36)
T2D	Growth/size/body region	106 / 300 (15.13)	5.20 (2.16)	2.61 (0.38)
T2D	Renal/urinary system	37 / 300 (9.88)	7.21 (2.10)	6.51 (1.31)
T2D	Endocrine/exocrine gland	68 / 300 (14.73)	5.61 (2.03)	1.21 (-0.00)
T2D	Vision/eye	39 / 300 (6.42)	5.99 (1.99)	3.00 (0.58)
T2D	Embryo	44 / 300 (8.22)	5.60 (1.88)	1.41 (-0.00)
T2D	Mortality/aging	118 / 300 (14.20)	4.21 (1.73)	2.11 (0.36)
T2D	Neoplasm	21 / 300 (6.07)	7.15 (1.55)	0.00 (0.00)
T2D	Homeostasis/metabolism	113 / 300 (13.25)	3.87 (1.33)	1.75 (0.18)
T2D	Behavior/neurological	80 / 300 (10.29)	3.68 (1.27)	2.37 (0.42)
T2D	Immune system	68 / 300 (8.03)	3.66 (1.26)	1.57 (0.19)
T2D	Craniofacial	29 / 300 (6.74)	4.59 (1.12)	0.00 (-0.00)
T2D	Hematopoietic system	65 / 300 (7.43)	3.15 (1.00)	1.58 (0.19)
T2D	Nervous system	61 / 300 (6.41)	2.79 (0.80)	1.68 (0.20)
T2D	Cellular	87 / 300 (10.57)	2.70 (0.74)	0.68 (-0.00)
T2D	Reproductive system	40 / 300 (5.16)	2.85 (0.73)	1.43 (-0.00)
T2D	Skeleton	54 / 300 (9.28)	3.12 (0.68)	2.35 (0.23)
T2D	Hearing/vestibular/ear	15 / 300 (3.35)	2.51 (0.41)	3.78 (0.51)
T2D	Limbs/digits/tail	25 / 300 (5.89)	1.76 (0.30)	0.00 (-0.00)
T2D	Pigmentation	14 / 300 (4.82)	0.00 (0.00)	0.00 (-0.00)
WAIST	Limbs/digits/tail	46 / 391 (16.62)	4.46 (3.63)	2.93 (1.44)
WAIST	Muscle	72 / 391 (24.63)	3.17 (2.41)	2.24 (1.05)

(continued)

Trait	Category	GWAS overlap	Odds ratio (- log 10 P-value)	
			All genes	Non-GWAS genes
WAIST	Embryo	71 / 391 (19.09)	2.66 (1.88)	1.61 (0.39)
WAIST	Vision/eye	52 / 391 (10.74)	2.46 (1.64)	1.35 (0.24)
WAIST	Skeleton	96 / 391 (25.48)	2.30 (1.62)	1.51 (0.35)
WAIST	Integument	64 / 391 (14.99)	2.32 (1.55)	1.52 (0.38)
WAIST	Respiratory system	49 / 391 (14.22)	2.58 (1.50)	2.62 (1.19)
WAIST	Immune system	102 / 391 (17.34)	2.07 (1.46)	1.58 (0.54)
WAIST	Craniofacial	59 / 391 (22.39)	2.64 (1.37)	1.73 (0.51)
WAIST	Pigmentation	19 / 391 (7.64)	3.31 (1.32)	2.17 (0.58)
WAIST	Behavior/neurological	109 / 391 (17.77)	1.99 (1.27)	1.51 (0.40)
WAIST	Mortality/aging	146 / 391 (20.15)	1.77 (1.08)	1.35 (0.35)
WAIST	Growth/size/body region	135 / 391 (22.39)	1.80 (1.04)	1.65 (0.63)
WAIST	Renal/urinary system	42 / 391 (11.60)	2.09 (1.00)	0.78 (-0.00)
WAIST	Nervous system	91 / 391 (14.22)	1.71 (0.86)	1.64 (0.55)
WAIST	Cardiovascular system	94 / 391 (20.34)	1.76 (0.79)	1.42 (0.32)
WAIST	Digestive/alimentary	47 / 391 (13.07)	1.94 (0.77)	0.73 (-0.00)
WAIST	Hematopoietic system	98 / 391 (16.35)	1.64 (0.72)	1.15 (0.09)
WAIST	Neoplasm	26 / 391 (8.32)	2.06 (0.58)	1.35 (0.18)
WAIST	Liver/biliary system	57 / 391 (18.79)	1.70 (0.57)	1.11 (0.13)
WAIST	Cellular	117 / 391 (17.93)	1.49 (0.55)	1.10 (0.08)
WAIST	Reproductive system	62 / 391 (12.15)	1.46 (0.45)	0.96 (0.00)
WAIST	Adipose tissue	50 / 391 (16.85)	1.61 (0.43)	1.27 (0.14)
WAIST	Endocrine/exocrine gland	83 / 391 (19.81)	1.49 (0.43)	0.87 (-0.00)
WAIST	Hearing/vestibular/ear	37 / 391 (15.85)	1.58 (0.35)	0.69 (-0.00)
WAIST	Homeostasis/metabolism	136 / 391 (17.99)	1.22 (0.22)	1.10 (0.08)
WAIST	Taste/olfaction	6 / 391 (3.29)	0.00 (-0.00)	0.00 (-0.00)

Supplementary Table 13

For each GWAS trait we quantify overlap between RSS-NET prioritized genes ($P_1^{\text{bma}} \geq 0.9$) and genes causing 19 categories of Mendelian disorders (Freund et al. 2018; Amberger et al. 2019). The rest is the same as **Supplementary Table 12**.

			Odds ratio (- log 10 P-value)	
Trait	Category	GWAS overlap	All genes	Non-GWAS genes
AF	Arrythmia	16 / 184 (10.78)	8.28 (4.77)	5.29 (2.02)
AF	Cardiovascular	15 / 184 (5.47)	3.31 (2.06)	1.81 (0.60)
AF	Diabetes	3 / 184 (1.10)	3.21 (0.86)	2.04 (0.40)
AF	Positive mood	3 / 184 (2.18)	5.02 (0.73)	6.39 (0.82)
AF	Renal	10 / 184 (1.55)	1.73 (0.64)	0.44 (0.14)
AF	Immune	4 / 184 (0.26)	1.53 (0.34)	1.30 (0.17)
AF	MODY	7 / 184 (1.41)	1.51 (0.34)	1.28 (0.17)
AF	Psychiatric	5 / 184 (1.78)	1.13 (0.23)	1.44 (0.29)
AF	Reproductive	1 / 184 (-0.00)	1.03 (0.20)	1.31 (0.27)
AF	Hematologic	5 / 184 (0.63)	1.04 (0.14)	0.66 (-0.00)
AF	Growth	7 / 184 (0.91)	0.40 (0.14)	0.00 (0.59)
AF	Insulin	8 / 184 (1.60)	0.91 (0.00)	0.58 (-0.00)
AF	Platelet	4 / 184 (0.51)	0.63 (0.00)	0.00 (0.20)
AF	Uric acid	1 / 184 (-0.00)	0.00 (0.00)	0.00 (-0.00)
AF	Neurologic	3 / 184 (0.91)	0.00 (0.00)	0.00 (-0.00)
AF	Development	4 / 184 (0.25)	0.51 (-0.00)	0.65 (-0.00)
AF	Autism	0 / 184 (-0.00)	0.00 (-0.00)	0.00 (-0.00)
AF	Weight	3 / 184 (1.47)	0.00 (-0.00)	0.00 (-0.00)
AF	Microalbumin	0 / 184 (-0.00)	0.00 (-0.00)	0.00 (-0.00)
BC	Insulin	16 / 364 (3.90)	9.71 (4.35)	7.77 (2.41)
BC	Cardiovascular	8 / 364 (0.78)	7.09 (2.77)	7.94 (2.44)
BC	Platelet	10 / 364 (2.32)	5.71 (1.65)	5.33 (1.17)
BC	Renal	22 / 364 (5.16)	4.15 (1.59)	2.90 (0.75)
BC	Hematologic	10 / 364 (1.56)	4.71 (1.45)	4.40 (1.03)
BC	Uric acid	6 / 364 (1.97)	7.48 (1.45)	0.00 (-0.00)
BC	Immune	10 / 364 (1.57)	4.59 (1.42)	4.29 (1.01)
BC	MODY	8 / 364 (0.83)	4.55 (1.41)	4.25 (1.00)
BC	Reproductive	6 / 364 (1.47)	6.23 (1.31)	0.00 (-0.00)
BC	Growth	16 / 364 (3.21)	3.66 (1.19)	1.71 (0.33)
BC	Positive mood	4 / 364 (2.58)	15.10 (1.16)	21.12 (1.29)
BC	Weight	2 / 364 (0.55)	6.40 (0.81)	0.00 (-0.00)
BC	Development	13 / 364 (2.75)	3.10 (0.81)	2.17 (0.41)
BC	Microalbumin	3 / 364 (0.84)	5.64 (0.76)	0.00 (-0.00)
BC	Diabetes	3 / 364 (0.72)	4.80 (0.70)	0.00 (-0.00)
BC	Psychiatric	7 / 364 (2.15)	3.40 (0.57)	4.76 (0.69)
BC	Arrythmia	8 / 364 (2.61)	0.00 (-0.00)	0.00 (-0.00)
BC	Autism	0 / 364 (-0.00)	0.00 (-0.00)	0.00 (-0.00)
BC	Neurologic	6 / 364 (1.95)	0.00 (-0.00)	0.00 (0.00)

(continued)

Trait	Category	GWAS overlap	Odds ratio (- log 10 P-value)	
			All genes	Non-GWAS genes
BMI	Insulin	38 / 889 (2.71)	2.54 (1.22)	2.08 (0.71)
BMI	Weight	10 / 889 (1.59)	4.75 (1.14)	3.24 (0.56)
BMI	Platelet	29 / 889 (2.75)	2.10 (0.73)	1.90 (0.53)
BMI	Psychiatric	19 / 889 (2.42)	2.51 (0.70)	1.71 (0.34)
BMI	Autism	11 / 889 (2.69)	3.00 (0.54)	0.00 (-0.00)
BMI	Renal	48 / 889 (2.77)	1.52 (0.46)	1.04 (0.14)
BMI	Microalbumin	9 / 889 (0.73)	2.07 (0.41)	0.00 (0.00)
BMI	Hematologic	28 / 889 (1.22)	1.73 (0.37)	1.58 (0.42)
BMI	Cardiovascular	26 / 889 (0.58)	1.56 (0.35)	1.41 (0.18)
BMI	Neurologic	14 / 889 (1.39)	1.53 (0.31)	2.09 (0.41)
BMI	Growth	42 / 889 (2.54)	1.35 (0.31)	1.22 (0.17)
BMI	Uric acid	11 / 889 (0.58)	1.37 (0.28)	1.85 (0.37)
BMI	Arrythmia	11 / 889 (0.21)	1.11 (0.22)	1.52 (0.31)
BMI	Development	46 / 889 (5.79)	1.14 (0.16)	1.55 (0.42)
BMI	Immune	30 / 889 (1.59)	1.12 (0.15)	1.53 (0.41)
BMI	MODY	26 / 889 (0.79)	1.11 (0.15)	0.76 (-0.00)
BMI	Reproductive	20 / 889 (2.26)	0.00 (-0.00)	0.00 (-0.00)
BMI	Diabetes	14 / 889 (2.15)	0.00 (-0.00)	0.00 (-0.00)
BMI	Positive mood	7 / 889 (1.96)	0.00 (-0.00)	0.00 (-0.00)
CAD	Cardiovascular	26 / 308 (11.19)	3.70 (4.01)	2.31 (1.37)
CAD	Platelet	17 / 308 (7.00)	3.19 (2.44)	2.21 (1.05)
CAD	Insulin	25 / 308 (10.10)	2.82 (2.44)	1.60 (0.59)
CAD	Uric acid	10 / 308 (5.10)	4.19 (2.35)	3.48 (1.48)
CAD	Hematologic	15 / 308 (4.54)	2.62 (1.93)	1.45 (0.44)
CAD	Neurologic	6 / 308 (2.20)	3.89 (1.92)	0.97 (-0.00)
CAD	Renal	23 / 308 (6.48)	2.31 (1.87)	1.44 (0.35)
CAD	Development	12 / 308 (2.73)	2.30 (1.50)	1.44 (0.27)
CAD	Microalbumin	7 / 308 (3.69)	3.15 (1.11)	2.63 (0.74)
CAD	MODY	17 / 308 (5.62)	1.96 (0.99)	1.75 (0.65)
CAD	Reproductive	8 / 308 (2.81)	2.30 (0.97)	2.15 (0.76)
CAD	Autism	2 / 308 (0.72)	3.02 (0.83)	1.88 (0.38)
CAD	Immune	14 / 308 (4.00)	1.69 (0.74)	1.41 (0.27)
CAD	Growth	10 / 308 (1.15)	1.58 (0.64)	1.68 (0.56)
CAD	Positive mood	2 / 308 (1.05)	2.77 (0.51)	0.00 (-0.00)
CAD	Diabetes	9 / 308 (4.96)	1.77 (0.50)	2.20 (0.62)
CAD	Arrythmia	7 / 308 (2.33)	1.67 (0.36)	0.00 (0.39)
CAD	Weight	4 / 308 (1.83)	1.17 (0.24)	0.00 (-0.00)
CAD	Psychiatric	5 / 308 (1.34)	1.25 (0.17)	0.78 (-0.00)
HDL	Cardiovascular	10 / 104 (4.09)	2.69 (3.24)	1.66 (0.73)
HDL	Diabetes	5 / 104 (3.31)	4.39 (3.07)	2.56 (1.10)
HDL	Insulin	10 / 104 (3.95)	2.46 (2.60)	1.61 (0.72)
HDL	Weight	5 / 104 (4.01)	4.38 (2.44)	2.55 (0.91)

(continued)

Trait	Category	GWAS overlap	Odds ratio (- log 10 P-value)	
			All genes	Non-GWAS genes
HDL	MODY	7 / 104 (2.39)	2.37 (2.22)	1.58 (0.60)
HDL	Microalbumin	2 / 104 (0.99)	3.17 (1.59)	2.96 (1.27)
HDL	Renal	4 / 104 (0.27)	1.49 (0.78)	1.47 (0.59)
HDL	Growth	9 / 104 (2.87)	1.48 (0.72)	1.10 (0.16)
HDL	Hematologic	6 / 104 (1.87)	1.56 (0.70)	0.81 (-0.00)
HDL	Immune	4 / 104 (0.92)	1.52 (0.68)	1.18 (0.19)
HDL	Platelet	5 / 104 (1.70)	1.47 (0.46)	0.98 (0.00)
HDL	Positive mood	0 / 104 (-0.00)	1.65 (0.34)	1.92 (0.38)
HDL	Neurologic	1 / 104 (0.28)	1.37 (0.31)	1.07 (0.15)
HDL	Arrythmia	0 / 104 (-0.00)	1.34 (0.26)	1.55 (0.47)
HDL	Development	3 / 104 (0.35)	1.20 (0.17)	1.00 (-0.00)
HDL	Uric acid	0 / 104 (-0.00)	1.23 (0.13)	1.43 (0.33)
HDL	Autism	0 / 104 (-0.00)	0.89 (-0.00)	1.04 (0.21)
HDL	Psychiatric	1 / 104 (0.23)	0.74 (-0.00)	0.87 (-0.00)
HDL	Reproductive	2 / 104 (0.60)	0.68 (-0.00)	0.79 (-0.00)
HR	Arrythmia	9 / 123 (5.41)	7.16 (2.93)	5.86 (1.72)
HR	Cardiovascular	10 / 123 (3.50)	2.64 (1.10)	1.80 (0.49)
HR	Neurologic	1 / 123 (0.23)	1.94 (0.38)	2.64 (0.49)
HR	Renal	6 / 123 (0.79)	1.45 (0.33)	1.32 (0.18)
HR	Psychiatric	2 / 123 (0.54)	1.58 (0.32)	2.16 (0.42)
HR	Immune	3 / 123 (0.31)	0.00 (0.19)	0.00 (0.21)
HR	MODY	4 / 123 (0.53)	0.00 (0.19)	0.00 (0.21)
HR	Development	1 / 123 (0.14)	1.45 (0.19)	1.97 (0.54)
HR	Growth	3 / 123 (0.12)	0.57 (0.00)	0.77 (-0.00)
HR	Diabetes	1 / 123 (0.28)	0.00 (0.00)	0.00 (-0.00)
HR	Platelet	3 / 123 (0.37)	0.88 (-0.00)	1.20 (0.24)
HR	Hematologic	1 / 123 (0.14)	0.73 (-0.00)	0.99 (-0.00)
HR	Insulin	2 / 123 (-0.00)	0.64 (-0.00)	0.87 (-0.00)
HR	Autism	0 / 123 (-0.00)	0.00 (-0.00)	0.00 (-0.00)
HR	Weight	1 / 123 (0.39)	0.00 (-0.00)	0.00 (-0.00)
HR	Uric acid	0 / 123 (-0.00)	0.00 (-0.00)	0.00 (0.00)
HR	Reproductive	0 / 123 (0.20)	0.00 (-0.00)	0.00 (-0.00)
HR	Microalbumin	1 / 123 (0.32)	0.00 (-0.00)	0.00 (0.00)
HR	Positive mood	3 / 123 (2.52)	0.00 (-0.00)	0.00 (-0.00)
IBD	Immune	27 / 374 (9.51)	4.32 (6.22)	3.87 (4.14)
IBD	MODY	21 / 374 (5.77)	3.92 (4.95)	4.10 (4.40)
IBD	Psychiatric	5 / 374 (0.68)	5.16 (3.80)	6.44 (4.46)
IBD	Uric acid	13 / 374 (5.97)	4.46 (3.06)	2.83 (1.21)
IBD	Renal	15 / 374 (1.25)	2.45 (2.42)	2.05 (1.39)
IBD	Growth	14 / 374 (1.41)	2.45 (2.12)	2.61 (2.18)
IBD	Neurologic	3 / 374 (0.30)	3.48 (1.46)	3.25 (1.13)

(continued)

Trait	Category	GWAS overlap	Odds ratio (- log 10 P-value)	
			All genes	Non-GWAS genes
IBD	Insulin	19 / 374 (4.13)	1.99 (1.18)	1.52 (0.52)
IBD	Development	10 / 374 (0.84)	1.91 (1.07)	1.48 (0.40)
IBD	Arrythmia	6 / 374 (1.14)	2.11 (0.87)	2.01 (0.70)
IBD	Autism	1 / 374 (-0.00)	3.10 (0.83)	1.93 (0.38)
IBD	Cardiovascular	8 / 374 (0.38)	1.75 (0.83)	1.65 (0.56)
IBD	Hematologic	17 / 374 (3.84)	1.72 (0.81)	1.10 (0.10)
IBD	Platelet	12 / 374 (2.47)	1.67 (0.56)	1.81 (0.67)
IBD	Diabetes	5 / 374 (1.35)	1.69 (0.47)	1.05 (0.21)
IBD	Reproductive	2 / 374 (0.11)	1.46 (0.33)	1.82 (0.62)
IBD	Weight	2 / 374 (0.41)	1.25 (0.25)	1.59 (0.32)
IBD	Microalbumin	1 / 374 (-0.00)	0.86 (-0.00)	1.07 (0.21)
IBD	Positive mood	0 / 374 (-0.00)	0.00 (-0.00)	0.00 (-0.00)
LDL	Cardiovascular	10 / 92 (4.51)	3.40 (4.96)	2.38 (1.93)
LDL	MODY	5 / 92 (1.53)	2.35 (2.06)	1.90 (1.01)
LDL	Hematologic	9 / 92 (4.07)	2.24 (1.83)	1.52 (0.62)
LDL	Uric acid	4 / 92 (2.32)	2.67 (1.51)	2.07 (0.86)
LDL	Platelet	3 / 92 (0.83)	2.03 (1.28)	2.10 (1.20)
LDL	Insulin	6 / 92 (1.87)	1.79 (1.17)	1.52 (0.58)
LDL	Renal	10 / 92 (3.36)	1.59 (0.96)	1.43 (0.60)
LDL	Reproductive	2 / 92 (0.68)	0.00 (0.93)	0.00 (0.75)
LDL	Neurologic	0 / 92 (-0.00)	1.97 (0.81)	2.30 (0.97)
LDL	Development	2 / 92 (0.16)	1.65 (0.73)	1.50 (0.47)
LDL	Immune	6 / 92 (2.11)	1.63 (0.72)	1.26 (0.31)
LDL	Microalbumin	3 / 92 (1.90)	2.00 (0.70)	2.33 (0.83)
LDL	Arrythmia	2 / 92 (0.71)	1.43 (0.43)	1.25 (0.13)
LDL	Weight	2 / 92 (1.25)	1.50 (0.41)	0.00 (0.20)
LDL	Diabetes	2 / 92 (0.99)	1.70 (0.37)	0.66 (-0.00)
LDL	Psychiatric	0 / 92 (0.00)	0.40 (0.28)	0.46 (0.14)
LDL	Positive mood	0 / 92 (-0.00)	0.00 (0.00)	0.00 (0.00)
LDL	Autism	0 / 92 (-0.00)	0.95 (-0.00)	1.11 (0.22)
LDL	Growth	4 / 92 (0.55)	0.86 (-0.00)	0.83 (0.08)
LOAD	Immune	6 / 98 (2.30)	7.32 (3.77)	2.79 (0.74)
LOAD	Renal	5 / 98 (1.08)	5.73 (3.49)	3.82 (1.49)
LOAD	Platelet	5 / 98 (2.07)	7.78 (3.48)	3.45 (0.88)
LOAD	MODY	4 / 98 (1.16)	6.19 (2.98)	2.75 (0.73)
LOAD	Cardiovascular	5 / 98 (1.58)	5.79 (2.84)	3.86 (1.25)
LOAD	Arrythmia	1 / 98 (0.28)	6.58 (1.84)	5.85 (1.26)
LOAD	Hematologic	3 / 98 (0.73)	4.30 (1.68)	1.43 (0.29)
LOAD	Microalbumin	2 / 98 (1.16)	7.69 (1.48)	0.00 (-0.00)
LOAD	Insulin	4 / 98 (1.03)	3.67 (1.48)	2.45 (0.66)
LOAD	Neurologic	1 / 98 (0.35)	5.88 (1.28)	3.92 (0.62)
LOAD	Uric acid	2 / 98 (0.92)	5.06 (1.17)	0.00 (-0.00)

(continued)

Trait	Category	GWAS overlap	Odds ratio (- log 10 P-value)	
			All genes	Non-GWAS genes
LOAD	Weight	0 / 98 (0.00)	4.46 (0.68)	5.93 (0.78)
LOAD	Diabetes	0 / 98 (-0.00)	3.21 (0.56)	4.28 (0.66)
LOAD	Psychiatric	2 / 98 (0.80)	2.43 (0.46)	0.00 (-0.00)
LOAD	Growth	3 / 98 (0.35)	1.67 (0.45)	0.00 (-0.00)
LOAD	Development	1 / 98 (-0.00)	1.10 (0.22)	1.47 (0.29)
LOAD	Reproductive	3 / 98 (1.35)	0.00 (0.00)	0.00 (-0.00)
LOAD	Autism	1 / 98 (0.59)	0.00 (-0.00)	0.00 (0.00)
LOAD	Positive mood	0 / 98 (0.00)	0.00 (-0.00)	0.00 (-0.00)
NEU	Arrythmia	4 / 376 (0.49)	4.74 (1.50)	4.94 (1.55)
NEU	Positive mood	4 / 376 (2.40)	7.82 (0.90)	8.48 (0.93)
NEU	Platelet	9 / 376 (1.41)	1.97 (0.55)	2.04 (0.57)
NEU	Development	16 / 376 (3.64)	1.61 (0.43)	0.84 (-0.00)
NEU	Immune	12 / 376 (2.16)	1.58 (0.43)	1.64 (0.44)
NEU	Neurologic	7 / 376 (2.28)	2.15 (0.42)	2.25 (0.43)
NEU	Renal	11 / 376 (0.58)	1.61 (0.36)	1.67 (0.36)
NEU	Psychiatric	3 / 376 (0.13)	1.76 (0.35)	0.00 (-0.00)
NEU	Cardiovascular	4 / 376 (0.08)	1.46 (0.19)	1.52 (0.40)
NEU	Growth	13 / 376 (1.55)	1.26 (0.17)	1.31 (0.18)
NEU	Hematologic	6 / 376 (0.19)	0.81 (0.00)	0.84 (-0.00)
NEU	MODY	10 / 376 (1.34)	0.78 (0.00)	0.81 (-0.00)
NEU	Diabetes	3 / 376 (0.62)	0.00 (0.00)	0.00 (-0.00)
NEU	Insulin	8 / 376 (0.41)	0.71 (-0.00)	0.74 (-0.00)
NEU	Autism	3 / 376 (1.07)	0.00 (-0.00)	0.00 (-0.00)
NEU	Weight	2 / 376 (0.48)	0.00 (-0.00)	0.00 (-0.00)
NEU	Uric acid	2 / 376 (-0.00)	0.00 (-0.00)	0.00 (0.00)
NEU	Reproductive	6 / 376 (1.26)	0.00 (-0.00)	0.00 (-0.00)
NEU	Microalbumin	1 / 376 (-0.00)	0.00 (-0.00)	0.00 (-0.00)
RA	Immune	12 / 123 (5.69)	3.11 (5.04)	1.94 (1.40)
RA	MODY	8 / 123 (2.89)	2.25 (2.47)	1.43 (0.51)
RA	Hematologic	4 / 123 (0.87)	2.05 (1.85)	1.80 (1.18)
RA	Uric acid	1 / 123 (0.27)	2.61 (1.80)	2.74 (1.73)
RA	Platelet	5 / 123 (1.64)	1.81 (1.19)	1.18 (0.19)
RA	Renal	4 / 123 (0.27)	1.61 (1.18)	1.50 (0.75)
RA	Positive mood	0 / 123 (-0.00)	2.61 (0.73)	3.13 (0.85)
RA	Insulin	5 / 123 (1.13)	1.42 (0.66)	0.99 (-0.00)
RA	Psychiatric	0 / 123 (-0.00)	0.29 (0.57)	0.34 (0.27)
RA	Growth	3 / 123 (0.13)	1.37 (0.50)	1.38 (0.56)
RA	Cardiovascular	0 / 123 (0.57)	1.21 (0.32)	1.45 (0.61)
RA	Development	3 / 123 (0.34)	1.20 (0.24)	1.28 (0.27)
RA	Neurologic	0 / 123 (0.00)	1.07 (0.12)	1.28 (0.29)
RA	Arrythmia	0 / 123 (-0.00)	1.04 (0.10)	1.24 (0.24)
RA	Reproductive	0 / 123 (-0.00)	0.79 (0.00)	0.95 (-0.00)

(continued)

Trait	Category	GWAS overlap	Odds ratio (- log 10 P-value)	
			All genes	Non-GWAS genes
RA	Microalbumin	2 / 123 (0.96)	0.96 (-0.00)	0.00 (0.38)
RA	Diabetes	1 / 123 (0.33)	0.82 (-0.00)	0.49 (0.14)
RA	Autism	0 / 123 (-0.00)	0.69 (-0.00)	0.83 (-0.00)
RA	Weight	1 / 123 (0.44)	0.54 (-0.00)	0.00 (0.39)
SCZ	Development	28 / 780 (1.92)	2.23 (6.26)	2.22 (5.35)
SCZ	Psychiatric	17 / 780 (2.63)	2.22 (3.21)	2.14 (2.47)
SCZ	Positive mood	7 / 780 (2.43)	2.25 (1.18)	1.42 (0.32)
SCZ	Autism	5 / 780 (0.60)	1.79 (0.96)	1.42 (0.35)
SCZ	Uric acid	3 / 780 (0.65)	0.51 (0.92)	0.50 (0.87)
SCZ	Arrythmia	4 / 780 (0.70)	1.38 (0.68)	1.36 (0.64)
SCZ	Weight	4 / 780 (0.10)	1.54 (0.65)	1.81 (1.08)
SCZ	Immune	11 / 780 (0.53)	1.24 (0.63)	1.15 (0.35)
SCZ	Reproductive	9 / 780 (0.14)	1.34 (0.59)	1.39 (0.65)
SCZ	Hematologic	19 / 780 (0.36)	1.23 (0.57)	1.23 (0.49)
SCZ	Diabetes	3 / 780 (0.30)	1.38 (0.53)	1.35 (0.46)
SCZ	Platelet	11 / 780 (0.11)	1.17 (0.36)	1.27 (0.55)
SCZ	Insulin	14 / 780 (0.34)	1.14 (0.35)	1.15 (0.32)
SCZ	Renal	19 / 780 (0.41)	1.13 (0.34)	1.07 (0.14)
SCZ	Growth	18 / 780 (0.19)	0.88 (0.23)	0.94 (0.07)
SCZ	Microalbumin	4 / 780 (-0.00)	0.78 (0.15)	0.61 (0.38)
SCZ	MODY	9 / 780 (1.05)	1.03 (0.07)	1.05 (0.08)
SCZ	Neurologic	11 / 780 (1.16)	0.87 (0.06)	0.68 (0.32)
SCZ	Cardiovascular	14 / 780 (0.28)	0.96 (0.03)	0.97 (-0.00)
T2D	Immune	19 / 300 (4.39)	11.17 (4.07)	8.85 (2.03)
T2D	Weight	18 / 300 (13.61)	28.03 (3.49)	15.19 (1.14)
T2D	Diabetes	23 / 300 (16.01)	19.27 (3.03)	10.44 (0.98)
T2D	Neurologic	12 / 300 (4.84)	16.09 (2.81)	8.41 (0.90)
T2D	Psychiatric	8 / 300 (1.91)	11.68 (2.43)	12.29 (1.77)
T2D	MODY	29 / 300 (9.87)	7.42 (2.36)	5.88 (1.20)
T2D	Cardiovascular	26 / 300 (7.49)	6.89 (2.25)	5.47 (1.15)
T2D	Insulin	40 / 300 (16.01)	6.49 (2.16)	5.15 (1.11)
T2D	Microalbumin	9 / 300 (3.95)	12.85 (1.85)	20.60 (2.19)
T2D	Reproductive	11 / 300 (3.20)	8.07 (1.48)	0.00 (-0.00)
T2D	Positive mood	3 / 300 (1.35)	20.43 (1.27)	0.00 (0.00)
T2D	Renal	22 / 300 (3.07)	3.70 (1.17)	5.84 (1.57)
T2D	Platelet	16 / 300 (4.04)	4.75 (1.09)	3.74 (0.59)
T2D	Development	12 / 300 (1.30)	3.58 (0.89)	2.82 (0.48)
T2D	Growth	23 / 300 (4.57)	2.99 (0.77)	2.36 (0.43)
T2D	Uric acid	10 / 300 (3.54)	4.85 (0.70)	0.00 (-0.00)
T2D	Hematologic	18 / 300 (3.90)	1.86 (0.36)	0.00 (-0.00)
T2D	Arrythmia	3 / 300 (0.00)	0.00 (-0.00)	0.00 (-0.00)

(continued)

Trait	Category	GWAS overlap	Odds ratio (- log 10 P-value)	
			All genes	Non-GWAS genes
T2D	Autism	4 / 300 (1.41)	0.00 (-0.00)	0.00 (0.00)
WAIST	Platelet	14 / 391 (2.11)	3.34 (1.64)	1.92 (0.53)
WAIST	Diabetes	8 / 391 (2.26)	5.09 (1.60)	0.00 (-0.00)
WAIST	Cardiovascular	17 / 391 (2.03)	2.47 (1.19)	2.12 (0.73)
WAIST	Renal	30 / 391 (4.75)	2.18 (0.92)	2.08 (0.83)
WAIST	Uric acid	10 / 391 (2.79)	2.61 (0.73)	1.87 (0.37)
WAIST	Insulin	21 / 391 (3.24)	1.93 (0.56)	0.69 (-0.00)
WAIST	Growth	24 / 391 (3.37)	1.71 (0.51)	0.61 (-0.00)
WAIST	Weight	5 / 391 (1.41)	2.23 (0.43)	0.00 (-0.00)
WAIST	Microalbumin	6 / 391 (1.54)	1.97 (0.39)	0.00 (-0.00)
WAIST	Development	15 / 391 (1.45)	0.00 (0.37)	0.00 (0.20)
WAIST	Immune	17 / 391 (2.23)	1.60 (0.36)	0.77 (-0.00)
WAIST	MODY	14 / 391 (1.32)	1.59 (0.35)	0.00 (0.20)
WAIST	Neurologic	6 / 391 (0.84)	1.45 (0.30)	2.07 (0.41)
WAIST	Psychiatric	4 / 391 (0.10)	1.19 (0.24)	1.70 (0.34)
WAIST	Reproductive	12 / 391 (2.89)	1.08 (0.22)	0.00 (0.00)
WAIST	Arrythmia	7 / 391 (0.91)	1.06 (0.21)	1.51 (0.31)
WAIST	Hematologic	13 / 391 (1.00)	1.10 (0.15)	0.79 (-0.00)
WAIST	Autism	0 / 391 (0.38)	0.00 (-0.00)	0.00 (0.00)
WAIST	Positive mood	2 / 391 (0.58)	0.00 (-0.00)	0.00 (-0.00)

Supplementary Table 14

Descriptive statistics of proportion of GWAS SNPs inside a network ($a_j = 1$) over 18 traits for each of 38 regulatory networks. Rows are sorted by the "Median" column.

	Summary of $\sum_{j=1}^{p} a_j/p$				
Network	Min	Q1	Median	Q3	Max
Vagina	0.6400	0.6423	0.6438	0.6481	0.6505
Lung	0.6377	0.6399	0.6414	0.6460	0.6485
Thyroid	0.6287	0.6305	0.6324	0.6368	0.6394
Terminal ileum	0.6145	0.6170	0.6188	0.6230	0.6256
Testis	0.6109	0.6129	0.6149	0.6193	0.6220
Esophagus mucosa	0.6068	0.6090	0.6107	0.6153	0.6180
Sun-exposed skin	0.6014	0.6037	0.6056	0.6101	0.6129
Spleen	0.5965	0.5988	0.6003	0.6056	0.6085
Visceral omentum	0.5875	0.5901	0.5912	0.5963	0.5989
Prostate	0.5738	0.5762	0.5788	0.5828	0.5856
Stomach	0.5632	0.5655	0.5677	0.5725	0.5753
Adrenal gland	0.5576	0.5605	0.5621	0.5673	0.5699
Uterus	0.5508	0.5534	0.5551	0.5602	0.5631
Omnibus	0.5475	0.5494	0.5516	0.5567	0.5597
Esophagus muscularis	0.5442	0.5469	0.5489	0.5535	0.5561
Hippocampus	0.5429	0.5450	0.5463	0.5516	0.5545
Cortex	0.5068	0.5083	0.5101	0.5164	0.5197
Ovary	0.4999	0.5028	0.5049	0.5103	0.5135
Atrial appendage	0.4976	0.5001	0.5017	0.5070	0.5099
Transverse colon	0.4930	0.4956	0.4981	0.5034	0.5067
Caudate	0.4914	0.4930	0.4946	0.5001	0.5033
Tibial nerve	0.4876	0.4900	0.4918	0.4971	0.5002
Putamen	0.4701	0.4721	0.4743	0.4793	0.4824
CD4 cell	0.4468	0.4487	0.4521	0.4578	0.4614
Breast	0.4426	0.4451	0.4477	0.4532	0.4564
Sigmoid colon	0.4397	0.4425	0.4446	0.4501	0.4533
Cerebellum	0.4366	0.4385	0.4405	0.4467	0.4503
CD8 cell	0.4198	0.4213	0.4249	0.4307	0.4345
Subcutaneous adipose	0.4170	0.4193	0.4219	0.4275	0.4309
Gastroesophageal junction	0.4150	0.4180	0.4202	0.4260	0.4294
Skeletal muscle	0.4116	0.4145	0.4169	0.4225	0.4258
Monocyte	0.4093	0.4111	0.4148	0.4202	0.4236
Aorta	0.3766	0.3786	0.3817	0.3869	0.3901
Left ventricle	0.3713	0.3742	0.3768	0.3826	0.3859
B cell	0.3669	0.3691	0.3730	0.3786	0.3822
Liver	0.3611	0.3640	0.3676	0.3730	0.3763
NK cell	0.3494	0.3508	0.3549	0.3605	0.3643
Pancreas	0.3241	0.3262	0.3300	0.3355	0.3390

Supplementary Table 15

Descriptive statistics of 38 regulatory networks. Rows are sorted by "# of TF-TG edges".

Network	# of TF-TG edges	# of TGs	# of TFs
Stomach	96135	3727	450
Omnibus	96008	9317	571
Esophagus mucosa	95797	4891	419
Terminal ileum	95596	3700	408
Pancreas	95446	2941	481
Transverse colon	95446	3696	435
Lung	95361	4123	415
Breast	95355	3260	442
Left ventricle	95030	2546	424
Sun-exposed skin	94988	4144	448
Gastroesophageal junction	94838	2380	443
Atrial appendage	94749	2564	399
Vagina	94592	4325	431
Sigmoid colon	94549	2545	460
Esophagus muscularis	94408	2993	429
Visceral omentum	94334	3701	428
Tibial nerve	94133	3214	431
Subcutaneous adipose	94005	2718	434
Ovary	93822	3659	430
Liver	93706	3398	412
Spleen	93494	4358	397
Aorta	93408	3295	414
Uterus	93057	3569	453
Skeletal muscle	92832	2308	490
NK cell	92399	3105	376
Thyroid	92263	5369	450
CD8 cell	91925	3439	424
B cell	91728	3018	436
Prostate	91722	3165	474
CD4 cell	91569	3643	433
Monocyte	91401	3702	384
Testis	90804	4646	474
Cortex	90579	2972	333
Adrenal gland	90401	2758	434
Caudate	89754	2547	374
Cerebellum	89371	3301	336
Hippocampus	88948	2592	366
Putamen	88634	2380	365

Supplementary Table 16

Descriptive statistics of TF-TG edge weights $\{v_{gt}\}$ over all TF-TG edges available in each of 38 regulatory networks. Rows are sorted by the "Median" column.

	Summary of v_{gt}				
Network	Min	Q1	Median	Q3	Max
Cortex	0.6946	0.7105	0.7315	0.7636	1.0000
Putamen	0.6797	0.6972	0.7201	0.7560	0.9944
Cerebellum	0.6817	0.6970	0.7170	0.7484	1.0000
Caudate	0.6704	0.6880	0.7113	0.7469	1.0000
Hippocampus	0.6678	0.6843	0.7063	0.7403	0.9977
Atrial appendage	0.6489	0.6674	0.6920	0.7314	1.0000
CD8 cell	0.6385	0.6553	0.6775	0.7125	1.0000
Subcutaneous adipose	0.6339	0.6520	0.6769	0.7160	1.0000
Omnibus	0.6278	0.6484	0.6748	0.7143	1.0000
Transverse colon	0.6353	0.6518	0.6740	0.7099	1.0000
Terminal ileum	0.6362	0.6522	0.6736	0.7082	1.0000
Adrenal gland	0.6296	0.6445	0.6650	0.6987	1.0000
CD4 cell	0.6266	0.6430	0.6647	0.6989	1.0000
Gastroesophageal junction	0.6233	0.6413	0.6645	0.7020	1.0000
Stomach	0.6276	0.6431	0.6640	0.6984	1.0000
Skeletal muscle	0.6187	0.6366	0.6609	0.6998	1.0000
Lung	0.6243	0.6393	0.6597	0.6927	1.0000
NK cell	0.6138	0.6324	0.6568	0.6949	1.0000
B cell	0.6101	0.6278	0.6515	0.6885	1.0000
Breast	0.6087	0.6263	0.6497	0.6870	1.0000
Spleen	0.6122	0.6279	0.6492	0.6831	1.0000
Monocyte	0.6088	0.6259	0.6488	0.6844	1.0000
Sigmoid colon	0.6079	0.6250	0.6482	0.6849	1.0000
Prostate	0.6047	0.6210	0.6427	0.6780	1.0000
Left ventricle	0.6006	0.6185	0.6418	0.6788	1.0000
Esophagus muscularis	0.5972	0.6157	0.6405	0.6797	1.0000
Uterus	0.5977	0.6142	0.6369	0.6728	1.0000
Sun-exposed skin	0.5984	0.6149	0.6368	0.6724	1.0000
Ovary	0.5938	0.6122	0.6368	0.6763	1.0000
Tibial nerve	0.5920	0.6104	0.6350	0.6740	1.0000
Liver	0.5867	0.6060	0.6312	0.6707	1.0000
Pancreas	0.5847	0.6046	0.6305	0.6722	1.0000
Vagina	0.5852	0.6010	0.6228	0.6581	1.0000
Visceral omentum	0.5814	0.5977	0.6198	0.6552	1.0000
Aorta	0.5646	0.5826	0.6067	0.6438	1.0000
Esophagus mucosa	0.5643	0.5809	0.6034	0.6400	1.0000
Thyroid	0.5621	0.5766	0.5966	0.6288	0.9587
Testis	0.5512	0.5675	0.5896	0.6252	1.0000

Supplementary Table 17

Descriptive statistics of *cis*-eQTL databases used in this study. Rows are sorted by the "# of SNP-gene pairs" column.

Source of eQTL	# of SNP-gene pairs	# of genes	# of SNPs
Testis, GTEx (V7)	15,759,533	17,366	1,230,746
Prostate, GTEx (V7)	14,585,826	16,085	1,219,002
Terminal ileum, GTEx (V7)	14,546,128	16,041	1,215,324
Lung, GTEx (V7)	14,483,585	15,973	1,214,950
Sun-exposed skin, GTEx (V7)	14,404,353	15,869	1,213,959
Transverse colon, GTEx (V7)	14,402,835	15,875	1,215,596
Breast, GTEx (V7)	14,392,706	15,872	1,212,389
Vagina, GTEx (V7)	14,380,972	15,869	1,217,316
Thyroid, GTEx (V7)	14,336,449	15,810	1,214,645
Tibial nerve, GTEx (V7)	14,288,824	15,761	1,217,709
Cortex, GTEx (V7)	14,261,947	15,745	1,226,087
Hippocampus, GTEx (V7)	14,233,460	15,719	1,224,980
Stomach, GTEx (V7)	14,220,507	15,684	1,213,739
Caudate, GTEx (V7)	14,209,653	15,689	1,226,945
Sigmoid colon, GTEx (V7)	14,202,126	15,668	1,219,231
Cerebellum, GTEx (V7)	14,192,621	15,679	1,224,520
Visceral omentum, GTEx (V7)	14,151,283	15,611	1,210,453
Uterus, GTEx (V7)	14,144,127	15,599	1,208,996
Spleen, GTEx (V7)	14,088,656	15,568	1,203,063
Ovary, GTEx (V7)	14,083,563	15,543	1,211,776
Subcutaneous adipose, GTEx (V7)	14,074,828	15,528	1,213,026
Esophagus mucosa, GTEx (V7)	14,050,266	15,504	1,201,919
Putamen, GTEx (V7)	14,036,948	15,503	1,226,334
Gastroesophageal junction, GTEx (V7)	13,998,654	15,446	1,217,148
Esophagus muscularis, GTEx (V7)	13,940,389	15,390	1,211,409
Adrenal gland, GTEx (V7)	13,918,735	15,368	1,215,183
Aorta, GTEx (V7)	13,913,807	15,356	1,207,409
Pancreas, GTEx (V7)	13,707,801	15,139	1,200,808
Atrial appendage, GTEx (V7)	13,683,429	15,122	1,207,966
Liver, GTEx (V7)	13,481,989	14,908	1,190,839
Left ventricle, GTEx (V7)	13,120,834	14,507	1,195,904
Skeletal muscle, GTEx (V7)	13,077,954	14,458	1,193,409
CD8 cell, DICE (DB1)	12,467,472	18,258	944,172
CD4 cell, DICE (DB1)	12,464,676	18,258	943,869
NK cell, DICE (DB1)	12,379,934	18,258	937,629
Blood, eQTLGen	12,372,754	13,588	1,173,301
B cell, DICE (DB1)	12,344,429	18,258	934,954
Monocyte, DICE (DB1)	12,344,429	18,258	934,954

Supplementary Table 18

Descriptive statistics of relative *cis* impact of SNPs on genes $\{c_{jg}\}$ over all SNP-gene pairs available in *cis*-eQTL databases. Rows are sorted by the "Median" column.

	Summary of $(c_{jg} - 1)$				
Source of eQTL	Min	Q1	Median	Q3	Max
Uterus, GTEx (V7)	0	0.033	0.069	0.118	0.935
Vagina, GTEx (V7)	0	0.032	0.067	0.115	0.932
Putamen, GTEx (V7)	0	0.032	0.067	0.114	0.923
Hippocampus, GTEx (V7)	0	0.031	0.066	0.114	0.912
CD8 cell, DICE (DB1)	0	0.024	0.065	0.118	0.774
CD4 cell, DICE (DB1)	0	0.023	0.064	0.118	0.771
Monocyte, DICE (DB1)	0	0.023	0.064	0.118	0.792
Terminal ileum, GTEx (V7)	0	0.030	0.064	0.109	0.935
NK cell, DICE (DB1)	0	0.023	0.064	0.117	0.762
Ovary, GTEx (V7)	0	0.030	0.063	0.108	0.931
B cell, DICE (DB1)	0	0.021	0.063	0.117	0.777
Cortex, GTEx (V7)	0	0.029	0.061	0.105	0.915
Prostate, GTEx (V7)	0	0.029	0.061	0.104	0.943
Spleen, GTEx (V7)	0	0.028	0.059	0.101	0.942
Caudate, GTEx (V7)	0	0.028	0.059	0.101	0.908
Cerebellum, GTEx (V7)	0	0.027	0.058	0.101	0.952
Liver, GTEx (V7)	0	0.027	0.057	0.098	0.921
Adrenal gland, GTEx (V7)	0	0.026	0.054	0.093	0.945
Sigmoid colon, GTEx (V7)	0	0.024	0.050	0.087	0.942
Gastroesophageal junction, GTEx (V7)	0	0.023	0.049	0.085	0.948
Pancreas, GTEx (V7)	0	0.023	0.049	0.084	0.939
Testis, GTEx (V7)	0	0.023	0.049	0.084	0.927
Stomach, GTEx (V7)	0	0.022	0.046	0.080	0.942
Transverse colon, GTEx (V7)	0	0.022	0.046	0.079	0.943
Breast, GTEx (V7)	0	0.021	0.045	0.078	0.949
Atrial appendage, GTEx (V7)	0	0.021	0.045	0.077	0.943
Aorta, GTEx (V7)	0	0.021	0.045	0.077	0.948
Left ventricle, GTEx (V7)	0	0.021	0.044	0.076	0.943
Visceral omentum, GTEx (V7)	0	0.019	0.041	0.071	0.939
Esophagus muscularis, GTEx (V7)	0	0.019	0.040	0.070	0.955
Tibial nerve, GTEx (V7)	0	0.019	0.040	0.069	0.964
Esophagus mucosa, GTEx (V7)	0	0.018	0.039	0.068	0.938
Subcutaneous adipose, GTEx (V7)	0	0.018	0.038	0.066	0.952
Thyroid, GTEx (V7)	0	0.018	0.038	0.065	0.955
Lung, GTEx (V7)	0	0.018	0.038	0.065	0.928
Sun-exposed skin, GTEx (V7)	0	0.017	0.037	0.064	0.948
Skeletal muscle, GTEx (V7)	0	0.016	0.034	0.058	0.918
Blood, eQTLGen	0	0.003	0.007	0.014	0.855

Supplementary Table 19

RSS-NET hyper-parameter grids used in the present study. For all traits, the grid for θ is $(0 : 0.25 : 1)$ and the grid for ρ is $(0 : 0.2 : 0.8)$. Here $(j : i : k)$ denotes a regularly-spaced vector that starts at j, uses i as the increment, and (roughly) stops at k. RSS-NET analyses of the same trait across different networks use the same hyper-parameter grid specified here. Trait abbreviations are defined in **Supplementary Table 2**.

Trait	θ_0	η
LOAD	$(-5.25 : 0.1 : -4.75)$	0.6
NEU	$(-4.4 : 0.05 : -4)$	0.3
SCZ	$(-2.175 : 0.025 : -2.05)$	0.3
BMI	$(-4.1 : 0.025 : -3.95)$	0.3
HEIGHT	$(-2.05 : 0.05 : -1.95)$	0.3
WAIST	$(-3 : 0.025 : -2.95)$	0.3
CD	$(-3 : 0.05 : -2.9)$	0.3
IBD	$(-3 : 0.05 : -2.8)$	0.3
RA	$(-3.25 : 0.025 : -3.125)$	0.3
UC	$(-3.05 : 0.025 : -2.95)$	0.3
BC	$(-4.25 : 0.05 : -4)$	0.2
AF	$(-4.5 : 0.25 : -4)$	$0.2, 0.3$
CAD	$(-4 : 0.025 : -3.85)$	0.3
HDL	$(-3.575 : 0.025 : -3.45)$	0.3
HR	$(-4.45 : 0.05 : -4.25)$	$0.3, 0.4$
LDL	$(-3.75 : 0.05 : -3.5)$	0.3
MI	$(-4.3 : 0.025 : -4.1)$	0.3
T2D	$(-4.65 : 0.05 : -4.55)$	$0.4, 0.5, 0.6$

Supplementary Table 20

False positive rates of RSS-NET under different log 10 enrichment BF cutoffs across 47 simulation scenarios of negative datasets.

Panel **a** Descriptive statistics of RSS-NET false positive rates across 17 negative scenarios in **Supplementary Figures 1-2 & 9**.

Cutoff	Min	Q1	Median	Q3	Max
0	0.0000	0.0000	0.0200	0.1250	0.3800
1	0.0000	0.0000	0.0000	0.0250	0.1800
2	0.0000	0.0000	0.0000	0.0000	0.1150
3	0.0000	0.0000	0.0000	0.0000	0.0900
4	0.0000	0.0000	0.0000	0.0000	0.0600
5	0.0000	0.0000	0.0000	0.0000	0.0550
6	0.0000	0.0000	0.0000	0.0000	0.0450
7	0.0000	0.0000	0.0000	0.0000	0.0400
8	0.0000	0.0000	0.0000	0.0000	0.0400
9	0.0000	0.0000	0.0000	0.0000	0.0350

Panel **b** Descriptive statistics of RSS-NET false positive rates across 6 negative scenarios in **Supplementary Figure 3**.

Cutoff	Min	Q1	Median	Q3	Max
0	0.0150	0.0438	0.3300	0.6050	0.6300
1	0.0000	0.0000	0.0475	0.1362	0.2000
2	0.0000	0.0000	0.0075	0.0300	0.0750
3	0.0000	0.0000	0.0000	0.0037	0.0150
4	0.0000	0.0000	0.0000	0.0000	0.0050
5	0.0000	0.0000	0.0000	0.0000	0.0050
6	0.0000	0.0000	0.0000	0.0000	0.0000
7	0.0000	0.0000	0.0000	0.0000	0.0000
8	0.0000	0.0000	0.0000	0.0000	0.0000
9	0.0000	0.0000	0.0000	0.0000	0.0000

Panel **c** Descriptive statistics of RSS-NET false positive rates across 6 negative scenarios in **Supplementary Figure 4**.

Cutoff	Min	Q1	Median	Q3	Max
0	0.0200	0.0563	0.4225	0.8337	0.8700
1	0.0000	0.0000	0.1450	0.3013	0.4200
2	0.0000	0.0000	0.0100	0.0650	0.1400
3	0.0000	0.0000	0.0025	0.0125	0.0200
4	0.0000	0.0000	0.0000	0.0000	0.0050
5	0.0000	0.0000	0.0000	0.0000	0.0000
6	0.0000	0.0000	0.0000	0.0000	0.0000
7	0.0000	0.0000	0.0000	0.0000	0.0000
8	0.0000	0.0000	0.0000	0.0000	0.0000
9	0.0000	0.0000	0.0000	0.0000	0.0000

Panel **d** Descriptive statistics of RSS-NET false positive rates across 6 negative scenarios in **Supplementary Figure 5**.

Cutoff	Min	Q1	Median	Q3	Max
0	0.0150	0.0287	0.0950	0.1462	0.2350
1	0.0000	0.0000	0.0125	0.0287	0.0350
2	0.0000	0.0000	0.0000	0.0000	0.0050
3	0.0000	0.0000	0.0000	0.0000	0.0000
4	0.0000	0.0000	0.0000	0.0000	0.0000
5	0.0000	0.0000	0.0000	0.0000	0.0000
6	0.0000	0.0000	0.0000	0.0000	0.0000
7	0.0000	0.0000	0.0000	0.0000	0.0000
8	0.0000	0.0000	0.0000	0.0000	0.0000
9	0.0000	0.0000	0.0000	0.0000	0.0000

Panel **e** Descriptive statistics of RSS-NET false positive rates across 12 negative scenarios in **Supplementary Figure 6**.

Cutoff	Min	Q1	Median	Q3	Max
0	0.2100	0.4625	0.8075	0.9950	1.0000
1	0.0400	0.0900	0.5675	0.9413	1.0000
2	0.0050	0.0138	0.3825	0.8712	1.0000
3	0.0000	0.0050	0.2675	0.7650	0.9900
4	0.0000	0.0050	0.2050	0.6262	0.9800
5	0.0000	0.0050	0.1425	0.4888	0.9700
6	0.0000	0.0050	0.0775	0.3700	0.9550
7	0.0000	0.0000	0.0400	0.2500	0.9250
8	0.0000	0.0000	0.0275	0.1675	0.8900
9	0.0000	0.0000	0.0225	0.1038	0.8550

Panel **f** Descriptive statistics of RSS-NET false positive rates across 47 negative scenarios from Panels **a** to **e** above.

Cutoff	Min	Q1	Median	Q3	Max
0	0.0000	0.0200	0.1350	0.6150	1.0000
1	0.0000	0.0000	0.0300	0.1900	1.0000
2	0.0000	0.0000	0.0000	0.0750	1.0000
3	0.0000	0.0000	0.0000	0.0150	0.9900
4	0.0000	0.0000	0.0000	0.0050	0.9800
5	0.0000	0.0000	0.0000	0.0050	0.9700
6	0.0000	0.0000	0.0000	0.0025	0.9550
7	0.0000	0.0000	0.0000	0.0000	0.9250
8	0.0000	0.0000	0.0000	0.0000	0.8900
9	0.0000	0.0000	0.0000	0.0000	0.8550

Supplementary Table 21

False positive rates of RSS-NET under different P_1 cutoffs across 49 simulation scenarios in **Supplementary Figures 7-9**.

Panel **a** Descriptive statistics of RSS-NET false positive rates across 8 scenarios with $\theta = 0$ and $\sigma^2 = 0$.

Cutoff	Min	Q1	Median	Q3	Max
0.50	1.9158e-05	4.3152e-05	1.3280e-04	3.1445e-02	6.6337e-02
0.55	1.9158e-06	3.9181e-05	1.1041e-04	1.7910e-02	3.7976e-02
0.60	9.5791e-07	3.7196e-05	9.1061e-05	1.0309e-02	2.1019e-02
0.65	7.1843e-07	3.2524e-05	8.2365e-05	5.7166e-03	1.1068e-02
0.70	7.1843e-07	2.8846e-05	7.1198e-05	3.0852e-03	5.6593e-03
0.75	0.0000e+00	2.5692e-05	6.2483e-05	1.5269e-03	2.9909e-03
0.80	0.0000e+00	2.3357e-05	5.5691e-05	6.9265e-04	1.4404e-03
0.85	0.0000e+00	1.9970e-05	5.2003e-05	2.7399e-04	6.2126e-04
0.90	0.0000e+00	1.7868e-05	4.4425e-05	8.9064e-05	1.8040e-04
0.95	0.0000e+00	1.4094e-05	1.5193e-05	2.1983e-05	6.0961e-05

Panel **b** Descriptive statistics of RSS-NET false positive rates across 16 scenarios with $\theta = 0$ and $\sigma^2 > 0$.

Cutoff	Min	Q1	Median	Q3	Max
0.50	3.4568e-05	7.9590e-05	1.8260e-04	3.9777e-02	1.3713e-01
0.55	3.1765e-05	7.3369e-05	1.3957e-04	2.4210e-02	9.0496e-02
0.60	2.8028e-05	6.3212e-05	1.3148e-04	1.4952e-02	5.6791e-02
0.65	2.5926e-05	5.2579e-05	1.2136e-04	8.2891e-03	3.3777e-02
0.70	2.5225e-05	4.7513e-05	1.1207e-04	4.4175e-03	1.8742e-02
0.75	2.4525e-05	4.1115e-05	1.0169e-04	2.1514e-03	9.8169e-03
0.80	2.1722e-05	3.7478e-05	9.0797e-05	9.1384e-04	4.7398e-03
0.85	2.1255e-05	3.2583e-05	7.9758e-05	3.8602e-04	2.0535e-03
0.90	1.9620e-05	2.8757e-05	7.1112e-05	1.4587e-04	6.6205e-04
0.95	1.7518e-05	2.1299e-05	3.8781e-05	8.3458e-05	1.1029e-04

Panel **c** Descriptive statistics of RSS-NET false positive rates across 8 scenarios with $\theta > 0$ and $\sigma^2 = 0$.

Cutoff	Min	Q1	Median	Q3	Max
0.50	3.1391e-04	2.7308e-03	8.4924e-02	1.0921e-01	1.6779e-01
0.55	1.4283e-04	1.3149e-03	6.0600e-02	8.4700e-02	1.3078e-01
0.60	5.7572e-05	6.2062e-04	4.6203e-02	6.5058e-02	9.8028e-02
0.65	2.6867e-05	2.9597e-04	3.4367e-02	4.9285e-02	6.9542e-02
0.70	1.5078e-05	1.3498e-04	2.4858e-02	3.5227e-02	4.6563e-02
0.75	8.2246e-06	5.4906e-05	1.7402e-02	2.3246e-02	2.8511e-02
0.80	3.0157e-06	2.1513e-05	1.1155e-02	1.3445e-02	1.6516e-02
0.85	5.4831e-07	5.1493e-06	6.1871e-03	6.8245e-03	1.0139e-02
0.90	0.0000e+00	1.0088e-06	2.1403e-03	3.0779e-03	4.6428e-03
0.95	0.0000e+00	2.8646e-07	2.5865e-04	8.9441e-04	1.1598e-03

Panel **d** Descriptive statistics of RSS-NET false positive rates across 17 scenarios with $\theta > 0$ and $\sigma^2 > 0$.

Cutoff	Min	Q1	Median	Q3	Max
0.50	3.6369e-03	1.4967e-02	9.4407e-02	1.1433e-01	2.8226e-01
0.55	1.8042e-03	9.9008e-03	7.1041e-02	9.6921e-02	2.4531e-01
0.60	8.8415e-04	6.4193e-03	5.1986e-02	8.7748e-02	2.0722e-01
0.65	4.2384e-04	3.9577e-03	4.0081e-02	6.6512e-02	1.6879e-01
0.70	2.0918e-04	2.2908e-03	3.0449e-02	5.0644e-02	1.3095e-01
0.75	1.1240e-04	1.1916e-03	2.1810e-02	3.5411e-02	9.5022e-02
0.80	6.4700e-05	5.0790e-04	1.4876e-02	2.5534e-02	6.2574e-02
0.85	3.1671e-05	1.8625e-04	8.6225e-03	1.2890e-02	3.6571e-02
0.90	1.7724e-05	9.7325e-05	4.3930e-03	6.0918e-03	2.0671e-02
0.95	1.1623e-05	4.5801e-05	7.0200e-04	1.6252e-03	8.4746e-03

Panel **e** Descriptive statistics of RSS-NET false positive rates across 49 scenarios from Panels **a** to **d** above.

Cutoff	Min	Q1	Median	Q3	Max
0.50	1.9158e-05	1.5303e-04	2.3029e-02	9.9199e-02	2.8226e-01
0.55	1.9158e-06	1.1734e-04	1.3126e-02	7.1041e-02	2.4531e-01
0.60	9.5791e-07	8.9924e-05	7.9050e-03	5.1986e-02	2.0722e-01
0.65	7.1843e-07	7.9649e-05	4.4754e-03	3.7725e-02	1.6879e-01
0.70	7.1843e-07	7.3107e-05	2.5532e-03	2.8071e-02	1.3095e-01
0.75	0.0000e+00	6.8903e-05	1.3102e-03	2.0162e-02	9.5022e-02
0.80	0.0000e+00	4.7177e-05	6.6729e-04	1.2758e-02	6.2574e-02
0.85	0.0000e+00	3.4724e-05	3.1254e-04	6.7839e-03	3.6571e-02
0.90	0.0000e+00	2.6867e-05	1.2389e-04	2.6863e-03	2.0671e-02
0.95	0.0000e+00	1.8642e-05	4.5801e-05	3.8126e-04	8.4746e-03

References

1000 Genomes Project Consortium (2015) A global reference for human genetic variation. *Nature*, **526**, 68–74.

Amberger, J., Bocchini, C., Scott, A. and Hamosh, A. (2019) OMIM.org: leveraging knowledge across phenotype-gene relationships. *Nucleic Acids Research*, **47**, D1038–D1043.

Andersson, R., Gebhard, C., Miguel-Escalada, I., Hoof, I., Bornholdt, J., Boyd, M., Chen, Y., Zhao, X., Schmidl, C., Suzuki, T. et al. (2014) An atlas of active enhancers across human cell types and tissues. *Nature*, **507**, 455–461.

Bult, C. J., Blake, J. A., Smith, C. L., Kadin, J. A. and Richardson, J. E. (2019) Mouse genome database (MGD) 2019. *Nucleic Acids Research*, **47**, D801–D806.

Buniello, A., MacArthur, J., Cerezo, M., Harris, L., Hayhurst, J., Malangone, C., McMahon, A., Morales, J., Mountjoy, E., Sollis, E. et al. (2019) The NHGRI-EBI GWAS Catalog of published genome-wide association studies, targeted arrays and summary statistics 2019. *Nucleic Acids Research*, **47**, D1005–D1012.

Christophersen, I. E., Rienstra, M., Roselli, C., Yin, X., Geelhoed, B., Barnard, J., Lin, H., Arking, D. E., Smith, A. V., Albert, C. M. et al. (2017) Large-scale analyses of common and rare variants identify 12 new loci associated with atrial fibrillation. *Nature Genetics*, **49**, 946.

Den Hoed, M., Eijgelsheim, M., Esko, T., Brundel, B. J., Peal, D. S., Evans, D. M., Nolte, I. M., Segrè, A. V., Holm, H., Handsaker, R. E. et al. (2013) Identification of heart rate-associated loci and their effects on cardiac conduction and rhythm disorders. *Nature Genetics*, **45**, 621–631.

Duren, Z., Chen, X., Jiang, R., Wang, Y. and Wong, W. H. (2017) Modeling gene regulation from paired expression and chromatin accessibility data. *Proceedings of the National Academy of Sciences*, **114**, E4914–E4923.

Finucane, H. K., Bulik-Sullivan, B., Gusev, A., Trynka, G., Reshef, Y., Loh, P.-R., Anttila, V., Xu, H., Zang, C., Farh, K. et al. (2015) Partitioning heritability by functional annotation using genome-wide association summary statistics. *Nature Genetics*, **47**, 1228–1235.

Freund, M. K., Burch, K. S., Shi, H., Mancuso, N., Kichaev, G., Garske, K. M., Pan, D. Z., Miao, Z., Mohlke, K. L., Laakso, M. et al. (2018) Phenotype-specific enrichment of Mendelian disorder genes near GWAS regions across 62 complex traits. *The American Journal of Human Genetics*, **103**, 535–552.

Gazal, S., Finucane, H. K., Furlotte, N. A., Loh, P.-R., Palamara, P. F., Liu, X., Schoech, A., Bulik-Sullivan, B., Neale, B. M., Gusev, A. et al. (2017) Linkage disequilibrium–dependent architecture of human complex traits shows action of negative selection. *Nature Genetics*, **49**, 1421–1427.

Global Lipids Genetics Consortium (2013) Discovery and refinement of loci associated with lipids levels. *Nature Genetics*, **45**, 1274–1283.

Lambert, J.-C., Ibrahim-Verbaas, C. A., Harold, D., Naj, A. C., Sims, R., Bellenguez, C., Jun, G., DeStefano, A. L., Bis, J. C., Beecham, G. W. et al. (2013) Meta-analysis of 74,046 individuals identifies 11 new susceptibility loci for Alzheimer's disease. *Nature Genetics*, **45**, 1452–1458.

Lamparter, D., Marbach, D., Rueedi, R., Kutalik, Z. and Bergmann, S. (2016) Fast and rigorous computation of gene and pathway scores from SNP-based summary statistics. *PLoS Computational Biology*, **12**, e1004714.

Liu, J. Z., van Sommeren, S., Huang, H., Ng, S. C., Alberts, R., Takahashi, A., Ripke, S., Lee, J. C., Jostins, L., Shah, T. et al. (2015) Association analyses identify 38 susceptibility loci for inflammatory bowel disease and highlight shared genetic risk across populations. *Nature Genetics*, **47**, 979–986.

Locke, A. E., Kahali, B., Berndt, S. I., Justice, A. E., Pers, T. H., Day, F. R., Powell, C., Vedantam, S., Buchkovich, M. L., Yang, J. et al. (2015) Genetic studies of body mass index yield new insights for obesity biology. *Nature*, **518**, 197–206.

Luo, Y., Hitz, B. C., Gabdank, I., Hilton, J. A., Kagda, M. S., Lam, B., Myers, Z., Sud, P., Jou, J., Lin, K. et al. (2020) New developments on the Encyclopedia of DNA Elements (ENCODE) data portal. *Nucleic Acids Research*, **48**, D882–D889.

Marbach, D., Lamparter, D., Quon, G., Kellis, M., Kutalik, Z. and Bergmann, S. (2016) Tissue-specific regulatory circuits reveal variable modular perturbations across complex diseases. *Nature Methods*, **13**, 366–370.

Morris, A. P., Voight, B. F., Teslovich, T. M., Ferreira, T., Segre, A. V., Steinthorsdottir, V., Strawbridge, R. J., Khan, H., Grallert, H., Mahajan, A. et al. (2012) Large-scale association analysis provides insights into the genetic architecture and pathophysiology of type 2 diabetes. *Nature Genetics*, **44**, 981–990.

Nikpay, M., Goel, A., Won, H.-H., Hall, L. M., Willenborg, C., Kanoni, S., Saleheen, D., Kyriakou, T., Nelson, C. P., Hopewell, J. C. et al. (2015) A comprehensive 1000 genomes–based genome-wide association meta-analysis of coronary artery disease. *Nature Genetics*, **47**, 1121–1130.

Okada, Y., Wu, D., Trynka, G., Raj, T., Terao, C., Ikari, K., Kochi, Y., Ohmura, K., Suzuki, A., Yoshida, S. et al. (2014) Genetics of rheumatoid arthritis contributes to biology and drug discovery. *Nature*, **506**, 376–381.

Okbay, A., Baselmans, B., De Neve, J., Turley, P., Nivard, M., Fontana, M., Meddens, S., Linnér, R., Rietveld, C., Derringer, J. et al. (2016) Genetic variants associated with subjective well-being, depressive symptoms, and neuroticism identified through genome-wide analyses. *Nature Genetics*, **48**, 624–633.

Ripke, S., Neale, B. M., Corvin, A., Walters, J. T., Farh, K.-H., Holmans, P. A., Lee, P., Bulik-Sullivan, B., Collier, D. A., Huang, H. et al. (2014) Biological insights from 108 schizophrenia-associated genetic loci. *Nature*, **511**, 421–427.

Sachs, M. C. (2017) plotROC: a tool for plotting ROC curves. *Journal of Statistical Software*, **79**, 1–19.

Saito, T. and Rehmsmeier, M. (2017) precrec: fast and accurate precision-recall and ROC curve calculations in R. *Bioinformatics*, **33 (1)**, 145–147.

Shungin, D., Winkler, T. W., Croteau-Chonka, D. C., Ferreira, T., Locke, A. E., Mägi, R., Strawbridge, R. J., Pers, T. H., Fischer, K., Justice, A. E. et al. (2015) New genetic loci link adipose and insulin biology to body fat distribution. *Nature*, **518**, 187–196.

Teslovich, T. M., Musunuru, K., Smith, A. V., Edmondson, A. C., Stylianou, I. M., Koseki, M., Pirruccello, J. P., Ripatti, S., Chasman, D. I., Willer, C. J. et al. (2010) Biological, clinical and population relevance of 95 loci for blood lipids. *Nature*, **466**, 707–713.

The FANTOM Consortium and the RIKEN PMI and CLST (DGT) (2014) A promoter-level mammalian expression atlas. *Nature*, **507**, 462–470.

Wang, Y., Zhang, S., Li, F., Zhou, Y., Zhang, Y., Wang, Z., Zhang, R., Zhu, J., Ren, Y., Tan, Y. et al. (2020) Therapeutic target database 2020: enriched resource for facilitating research and early development of targeted therapeutics. *Nucleic Acids Research*, **48**, D1031–D1041.

Watanabe, K., Stringer, S., Frei, O., Mirkov, M. U., de Leeuw, C., Polderman, T. J., van der Sluis, S., Andreassen, O. A., Neale, B. M. and Posthuma, D. (2019) A global overview of pleiotropy and genetic architecture in complex traits. *Nature Genetics*, **51**, 1339–1348.

Wellcome Trust Case Control Consortium (2007) Genome-wide association study of 14,000 cases of seven common diseases and 3,000 shared controls. *Nature*, **447**, 661–678.

Wood, A. R., Esko, T., Yang, J., Vedantam, S., Pers, T. H., Gustafsson, S., Chu, A. Y., Estrada, K., Luan, J., Kutalik, Z. et al. (2014) Defining the role of common variation in the genomic and biological architecture of adult human height. *Nature Genetics*, **46**, 1173–1186.

Zhu, X. and Stephens, M. (2017) Bayesian large-scale multiple regression with summary statistics from genome-wide association studies. *Annals of Applied Statistics*, **11**, 1561–1592.

— (2018) Large-scale genome-wide enrichment analyses identify new trait-associated genes and pathways across 31 human phenotypes. *Nature Communications*, **9**, 4361.